Addressing impact of climate change on wind and solar energy infrastructures: the case of India

Yasmine ZAKARI

We but mirror the world. All the tendencies present in the outer world are to be found in the world of our body. If we could change ourselves, the tendencies in the world would also change. As a man changes his own nature, so does the attitude of the world change towards him. This is the divine mystery supreme. A wonderful thing it is and the source of our happiness. We need not wait to see what others do.

—

Mahatma Gandhi

A la mémoire de mes grands-parents ...

Acknowledgments

If I could advise my younger self, I would tell her to trust the struggles that life brings her way. My journey as a Ph.D. student has been overwhelming and tough at times. Yet it has been the most extraordinary experience in my life. I feel fortunate to have had the opportunity to pursue this dream and make it come true. I was blessed with crossing paths with several people throughout my studies who influenced the accomplishment of this Ph.D. Although I cannot possibly acknowledge every single person here, I would like to express my gratitude to the cohort of mentors whose influence led me to the day of writing this thesis.

I would like to express my deepest gratitude to my research supervisors, Professor Lehning, for his patient guidance, encouragement, and kindness, and Dr. Francois Vuille for his encouragement and valuable critiques of this research work. I want to express my most profound appreciation to my co-authors colleagues and friends, Dr. Adrien Michel and Dr. Jerome Dujardin, who provided insight and expertise that greatly assisted this research. Many thanks to my colleagues at CRYOS.

This work would not have been possible without the financial support of CLP. Special thanks to Chi Cheung Ngan, Jeanne Chi Yun Ng and Cheuk Wing Lee for valuable discussions regarding wind resource assessment, for sharing the data and for the critical feedback during these past four and a half years.

I thank the World Climate Research Program, the Copernicus Climate Change Service, and NOAA's National Climatic Data Center for producing and making available their model outputs. Thanks should also go to the scientific community that provided the open-source software used to perform the analysis presented in this thesis.

I would like to acknowledge Dr. Anne-Perrine Avrin; I was inspired to take on the academic journey by her example. Todd Davis, who taught me more than I could ever give him credit for here. My dear friend and fellow scientist Gionatta, for his availability and generosity with his time and for the great discussions on ideas.

I could not have started this Ph.D. without the encouragement of my beloved family and my dad, to be more precise. My mom and sisters, Kenza and Ines, have always been there for me

Abstract

Climate change is one of the biggest threats to humanity and is tightly linked to the rising population and increased energy consumption derived from fossil fuels. Available wind and solar resources in India may be subject to significant changes in the future due to global warming. The contributions to the electricity supply from wind and solar are sensitive to climate perturbations, and monsoon variability under future warmer climate conditions could present unprecedented challenges to the energy industry and therefore warrants further investigation.

The ultimate goals of this thesis are to address the impact of climate change on the electricity production of wind and solar energy, and explore tools to render potential investments more robust to the uncertainty of future climate trends.

The approach adopted in this thesis is based on statistical methods to characterize past and future climate trends extracted from high-resolution climate models to understand the long-term characteristics and uncertainty of the climate variables impacting wind and solar production in India. Climate models are combined with reanalysis datasets, local measurements, and real wind and solar farm data of CLP Group assets in India. Climate data, energy estimation, and portfolio methods are applied to build a framework assessing how the combination of wind and solar could strengthen the resilience of the energy system, in particular on the supply side. In addition, a deep-learning model, Wind-Topo, designed to estimate wind flows is tested to investigate its applicability in regions where access to data remains a challenge.

The first part of the thesis analyzes future trends in wind availability in the Indian sub-continent. An additional contribution of this investigation is the suggestion of a decision-making tool enabling the quantification of the spatio-temporal consistency of wind trends using a structure-function. The second part of the thesis considers the impact of climate on the joint exploitation of wind and solar energy resources. It demonstrates that the uncertainty about the energy production of a mixed portfolio can be reduced by optimizing the combination of wind and solar assets in a producer portfolio, thus mitigating the economic impact of climate change. The last part of the thesis investigates the results of machine learning methods to estimate wind flows in an India domain using Wind-Topo, a deep learning model designed to downscale wind in regions with complex topographies. Wind-Topo is trained with a reanalysis dataset and calibrated with meteorological stations in Switzerland.

Abstract

In the first part of this thesis, the comparison of two families of CORDEX regional climate simulations suggests improved performance of the latest version in reproducing the local climate. The results indicate increasing future trends for annual wind speeds in the north-west (0.04 m/s per decade ($\pm 8\%$)), the center (0.03 m/s per decade ($\pm 11\%$)) and the east (0.02 m/s per decade ($\pm 19\%$)) of the Indian sub-continent under the representative concentration pathway scenario RCP 8.5 at the end of the century, with changes occurring more substantially during the last 30 years of the period. Furthermore, future projections also display seasonal wind perturbations occurring during the pre-monsoon, and trends with the highest magnitude concentrating during the monsoon. When combining wind and solar assets in a portfolio, we find that the climate-change induced variability on the energy production ranges from 33% to 50% when compared to the pure wind-only portfolios and from 30% to 96% when compared to pure solar assets. The analysis undertaken in the last part of the thesis demonstrates that the new Wind-Topo improves the estimation at stations located in the Himalayan mountains. Overall, the mean bias error of Wind-Topo output with local data is reduced and the correlation of Wind-Topo output with local data is increased compared to the values obtained with ERA5.

Key words Climate change, CORDEX, renewable energy, wind energy, solar energy, solar PV, future trends, energy portfolio, portfolio analysis, Spatio-temporal complementarity, seasonality, India, monsoon, Wind-Topo, machine learning, wind forecasting

Résumé

Le changement climatique représente l'une des principales menaces pour l'humanité. Les perturbations climatiques sont étroitement liées à la croissance démographique et à l'augmentation de la consommation d'énergie produite à partir de combustibles fossiles. Les ressources éoliennes et solaires disponibles en Inde pourraient subir d'importants changements à l'avenir en raison du réchauffement climatique. Les contributions de l'énergie éolienne et solaire à l'approvisionnement en électricité sont sensibles aux perturbations climatiques, et la variabilité de la mousson dans des conditions climatiques plus chaudes pourrait présenter des défis sans précédent pour l'industrie de l'énergie. Il convient de poursuivre l'étude des effets de cette variabilité.

Les objectifs de cette thèse sont l'étude de l'impact du changement climatique sur la production d'électricité des énergies éolienne et solaire, et l'exploration d'outils permettant de rendre les investissements dans ces énergies plus robustes face à l'incertitude des tendances climatiques futures.

L'approche adoptée dans la présente thèse est fondée sur des méthodes statistiques de caractérisation des tendances climatiques passées et futures.Ces tendances sont extraites de modèles climatiques à haute résolution afin de comprendre les caractéristiques à long terme et analyser l'incertitude des variables climatiques ayant un impact sur la production éolienne et solaire en Inde. Les modèles climatiques sont combinés avec des mesures météorologiques et des données réelles sur les parcs éoliens et solaires appartenant aux actifs du Groupe CLP en Inde. Les données climatiques, l'estimation énergétique et les méthodes d'analyse du portfolio sont appliquées pour construire un cadre évaluant comment la combinaison de l'éolien et du solaire pourrait réduire l'incertitude des tendances futures. En outre, un modèle de machine learning, Wind-Topo, conçu pour estimer les flux de vent, est testé pour étudier son applicabilité dans les régions où l'accès aux données demeure un obstacle.

La première partie de la thèse analyse les perspectives d'avenir des ressources éoliennes du sous-continent indien. Une autre contribution de cette étude est la proposition d'un outil d'aide à la décision afin de quantifier la cohérence spatio-temporelle des tendances éoliennes à l'aide d'une fonction structurale. Le deuxième volet de la thèse examine l'impact du climat sur l'exploitation conjointe des ressources éoliennes et solaires. On y démontre que l'incertitude sur la production d'énergie d'un portefeuille mixte peut être réduite en optimisant la combinaison des actifs éoliens

Résumé

et solaires dans un portefeuille producteur, atténuant ainsi l'impact économique du changement climatique. La dernière partie de la thèse étudie les résultats des méthodes d'apprentissage automatique pour estimer les flux de vent dans un domaine indien en utilisant Wind-Topo, un modèle d'apprentissage profond conçu pour réduire l'éolien dans les régions à topographie complexe. Wind-Topo est entraîné avec un jeu de données de réanalyse et calibré avec des stations météorologiques en Suisse.

Dans la première partie de cette thèse, la comparaison de deux familles CORDEX donne à penser que la dernière version reproduit mieux le climat local. Les résultats indiquent des tendances futures croissantes pour les vitesses annuelles du vent dans le nord-ouest ($0,04$ m/s par décennie ($\pm 8\%$)), le centre ($0,03$ m/s par décennie ($\pm 11\%$)) et l'est ($0,02$ m/s par décennie ($\pm 19\%$)) du sous-continent indien sous le scénario RCP 8.5 à la fin du siècle, les changements se produisant de manière plus importante au cours des 30 dernières années de la période. En outre, les projections futures montrent également des perturbations saisonnières du vent qui se produisent avant la mousson, et des tendances dont l'ampleur la plus élevée se concentre pendant la mousson. En combinant des actifs éoliens et solaires dans un portefeuille, nous constatons que le niveau de réduction de l'incertitude sur la production d'énergie varie de 33 % à 50 % par rapport aux portefeuilles purement éoliens et de 30 % à 96 % par rapport aux actifs purement solaires. L'analyse entreprise dans la dernière partie de la thèse démontre que le nouveau Wind-Topo améliore l'estimation aux stations situées dans les montagnes de l'Himalaya. Globalement, l'erreur moyenne de biais est réduite et la corrélation augmentée.

Mots clés Changement climatique, CORDEX, énergies renouvelables, énergie éolienne, énergie solaire, solaire photovoltaïque, tendances futures, portefeuille énergétique, analyse de portefeuille, Complémentarité spatio-temporelle, saisonnalité, Inde, mousson, Wind-Topo, apprentissage automatique, prédiction du vent

Contents

Contents

Introduction

This introductory chapter sets the background for investigating the risk of climate change on wind and solar energy production. It highlights the state of the art and research gaps that warrant additional examination. The chapter begins with an overview of the state of climate change, the need to shift to renewable energy to achieve the energy transition and the advancements in wind and solar deployment worldwide. After arguing that understanding the importance of the impacts of climate change on renewable energy sources is necessary to build a foundation for developing resilient future energy infrastructures and achieving the decarbonization targets set by policy-makers, I present monsoon-related impacts of climate change on wind and solar infrastructures in India. An overview of climate change impacts on the future availability of wind and sunshine is summarized, followed by a highlight of the central role of climate models in advancing the fight against global warming. The repercussions climate change can have on wind and solar, and my findings regarding their future trends are illustrated. In this context, I propose an overview of the methods proposed by the scientists for energy stakeholders to take climate model information into accounting for decision-making. The issues related to the tools available for successful long-term planning of wind and solar deployment with portfolio methods are also discussed. Finally, I investigate a different perspective of wind assessment using machine learning methods to wind forecasting in complex terrains. In this context, the importance of adopting innovative tools in order to achieve the decarbonization of the power sector is highlighted, specifically in planning new wind installations. Relevant research gaps are identified and summarized in this chapter. The remainder of this thesis will be written in a scientific style with the use of "we" rather than "I".

The state of the climate crisis and the energy transition

The world faces a climate crisis with rising temperatures and the effects of greenhouse gas (GHG) emissions [1]–[3]. Scientists determined that human-induced climate change was causing perturbations to the earth's system and proved that dioxide carbon concentrations affect the GHG effect [4], [5]. The science is well established, as recognized by recent Nobel prize awards on the subject won by Dr. Manabe and Dr. Hasselmann for creating climate models that linked weather and climate while demonstrating how increased carbon dioxide levels warmed the earth's surface, and Dr. Parisi for his discoveries leading to understanding complex systems [6]. Climate change

affects every region globally, with human influence contributing to many observed changes in weather and climate extremes. The World Meteorological Organization and the United Nations formed the Intergovernmental Panel on Climate Change (IPCC) to examine the latest climate science every few years and support governments worldwide in understanding climate change impacts and measures to adapt and mitigate [7]. The IPCC has a central role in the fight against the climate crisis as the entity that keeps the scientific compass on climate issues. The Working Group I contribution to the sixth assessment report on 6 August 2021 established on the "unequivocal" human influence on the warming of the atmosphere, ocean, and land [8]. The report released on February 2022 states that the warming rate in temperatures has been at unprecedented levels, with land-regions warming substantially more than the global mean [9]. Increasing temperatures lead to perturbations to the water cycle with increasing moisture content, more precipitations with higher intensity, and more incidences of floods and droughts in the future [10]. The scientific community assesses the state of the depletion of glaciers [11] and the tendency for rising sea levels as already observed in many parts of the world [12]. The risk of compound events, impacts of different types of events happening simultaneously, at the same or multiple locations, for example, the concurrence of heatwaves and droughts that could emphasize the risk of fire hazard, is also increasing [13], [14]. The emergency of the crisis lies in the fact that GHG emissions are irreversible. Even if carbon emissions were to stop, the anomaly would stay because of the long lifetime of carbon dioxide in the atmosphere. The warming could in principle be mitigated by geoengineering technologies that would enhance outgoing longwave radiation and cool down the Earth [15], [16].

The world has started broadly proclaiming its intent to act against the climate crisis in the past few years. A push to accelerate renewable energy technologies adoption worldwide is critical together with coordinated national policies and actions [17]. The European Union (EU) parliament pledged for a 60% carbon dioxide reduction by 2030 and for net-zero by 2050 [18]. China also pledged to reach carbon neutrality by 2060 [19]. The pledges are a big step in the face of the climate emergency, but no concrete actions nor much progress did follow declarations since 2015. The recent Glasgow climate conference (COP 26) recognizes that the world is not on track with a large gap between 2030 commitments and Paris Agreements Goals, as we are now on a trajectory towards 2.4°C. Efforts by the global scientific community to support technological innovation and foster the green economy shall be encouraged and supported financially and strategically to speed up the trend towards carbon neutrality [20].

The cause of human-induced global warming is the burning of fossil fuels and land use including deforestation. For an energy mix coherent with the Paris Agreement, we must avoid, capture or neutralize carbon emissions. The energy sector is central in the efforts to reduce carbon dioxide emissions. If the usage of coal, oil and gas was to be replaced with renewable energy, the reduction of current carbon dioxide emissions could reach a 90% cut below 1990 levels [21]. Replacing fossil fuels with renewables by the mid-century is only possible if aggressive action is implemented and challenges related to intermittency, location, transportation bottlenecks, environmental impacts, and land availability are tackled [22]. It involves changes in energy supply and consumption and societal and geopolitical transformation across from individuals,

communities, and multinational organizations. Furthermore, a prosperous energy transition can only happen if the trade-off between transition risks and the many physical, economic, and societal risks related to climate change are resolved satisfactorily.

The challenge for society is to take long-term decisions and shift the paradigm by aligning portfolios with climate goals and establishing more scientifically robust and realistic climate goals. Climate change does not operate in isolation from other important crisis events in the world and works in nexus with other crisis [23]. Recent circumstances in Ukraine should push Europe and other nations to decrease their reliance on fossil fuels and turn the status of the energy transition from impossible to inevitable as renewable offers a solution to the dependence to Russian resources.

Research gap 1 The incorporation of climate models knowledge is missing as demonstrated by the misalignment of climate goals with policy goals, and decision makers need tools to understand and act on climate change.

Worldwide advancements of wind and solar energy

The economies of China, United States and India are at the core of environmental solutions because of their maximum contribution to climate change [24]. The trends in carbon dioxide emissions indicate a rise in the future, and curbing carbon dioxide emissions cannot be achieved without a comprehensive shift from fossil to renewable resources in those countries. Renewable supply represents 15% of the global primary energy with less than 2% of sources such as photovoltaic (PV) and wind energy [25]. The recent years marked the reduction in the cost of PV and wind power generation systems and improved efficiency. The global installed capacity of wind turbines grew at about 14% annualized rate during the last two decades [26]. Wind turbines provide 6-7% of the global electricity supply [27]. Scenarios by the World Energy Outlook estimated that, by 2040, renewables might supply 20 to 30% of the world's primary energy, and studies suggest it is theoretically possible to move toward a completely renewable energy system by 2050. The shift to a lower-carbon economy is also happening in Asia where investments in setting up wind, solar and other renewable energy sources are flourishing [28].

In the case of India, energy demand has increased in recent years because of the need to meet the industrialization and infrastructure development [29]. India is the third-largest emitter of carbon dioxide in the world and coal-fired power plants in the country contribute approximately to half of its carbon emissions [30], [31]. India has a great potential for renewables, especially solar and wind, favored by a location in the solar belt and reception of large amounts of annual sunshine. Renewable energy deployment can accomplish up to 63% of the carbon dioxide reduction in 2050 [30], [32]. Therefore, India should further enhance the use of low-carbon sources in the power supply, limit the dependence on coal, and increase the penetration of renewables to mitigate the climate crisis. The Indian government announced the goal of reaching 500 GW of renewable

power capacity by 2030 to accelerate the clean energy transition [33], [34]. The energy transition in the sub-continent is underway to reach its sustainability targets [35], [36]. Before the covid outbreak, India ranked fourth in the cumulative wind capacity installed (after China, the US, Germany, and before Spain[I]) with over 19 GW installed [37]. Wind energy accounts for 8.5% of the total installed capacity in India [29]. India is also home to one of the most extensive solar photovoltaic plant installation programs. After a large scale installation of ground-mounted solar photovoltaic plants, India is moving towards rooftop installations to increase economic viability [38].

Climate change and monsoon trends in India

India is characterized by the diversity of its socioeconomic conditions, geography, and climate, which renders its study and the implementation of uniform policies a challenge [39]. Large-scale weather regimes in India follow an evolution throughout the year dictated by the onset and retreat of the Asian summer monsoon [40]. The monsoon pattern is such that during the northern summer, strong climatological south-westerlies over the Arabian Sea provide moisture [41]. An anomalous anticyclonic circulation influences the Indian monsoon during El Niño, weakening the south-westerly circulation's southern part [42], [43]. This pattern is usually predictable, but the summer monsoon 2020 has been very erratic, with episodes of heavy and devastating rains, landslides, and catastrophic winds over South Asia, and a delay of two weeks in the withdrawal of the summer monsoon in India [44]. Lockdown activities to control the spread of COVID-19 led to reduced aerosols impacting the strength of the incoming solar radiation and enhancing the heat, causing heavy rains over West-Central India [44]. The events in 2020 are a glance of what could happen in the future if the warming intensifies even with more efforts to mitigate air pollution. What can we expect regarding future monsoon patterns? Future monsoon patterns project dryer conditions in the Northeastern parts of India [45], [46]. CMIP5 GCMs indicate a consistent increase in monsoon rainfall and its variability under global warming [47]. Simulations of the Indian monsoon in the historical period by CMIP5 GCMs were not always accurate [48]. Recent GCMs from the CMIP6 family are now available, and scientists are busy evaluating their ability to simulate the Indian monsoon [49]. Climate sensitivity is higher on average in CMIP6 due primarily to strengthened cloud feed-backs [50]. Gusain et al. use CMIP6 models to explore their added skill in representing Indian monsoon characteristics and uncover their improved statistical consistency with observational data compared to the previous CMIP3 and CMIP5. [51].

Review of how climate change impacts wind and solar energy generation

Climate processes fuel renewable power resources. Climate change can strongly affect green energy by modifying future demand and generation [52], [53]. Climate change is expected to influence the long-term mean and variability of the climate variables and alter extremes [54]. Wind and solar energy are inherently uncertain and sensitive to climate change because of the

---

[I]https://gwec.net/global-wind-report-2022/, last accessed on 17/08/2022

natural variability of near-surface wind speed and solar radiation. The demand in energy is impacted by a high probability of lower heating and increased cooling [55]–[57]. In this thesis, we focus solely on the impacts on the supply side. Climate change impacts on wind power are expected to be more substantial than any other renewable technology [25]. Surface wind speeds are sensitive to surface roughness and topography. A long-term reduction in near-surface wind speed has been observed around the globe and described as the stilling effect [58]. With climate change, the risk of extended periods of low winds might worsen in the future. Such changes affect wind power density and impact the cost, planning, future investments, and contribution of wind to the energy mix [59], [60].

Climate change-induced variations in PV-energy potential are linked to changes in temperature and radiation [61]. PV power generation has an opposite relation to cell temperature and a proportional response to total radiation [62]. Sunlight duration determines the amount of effective radiation received by PV panels. Future changes in the cloud cover and air pollution can also result in variations in power generation under changing climate. The cloud cover indirectly impacts PV systems by causing radiation variations, leading to fluctuations in power generation. The decrease in precipitation and cloudiness under climate change could positively impact solar energy production [63]. Surface wind speed and atmospheric aerosol concentrations also influence the efficiency of PV panels. Furthermore, PV modules are highly vulnerable to climate extremes [64].

The central of role of climate models in advancing climate mitigation

State of the art studies on renewable energy production around the world rely on global climate models (GCM) and regional climate models (RCM) with various adaptations. Climate models are built to estimate trends rather than events [65]. The climate modeling community engaged in massive efforts for GCMs and RCMs improvements [66]. Previous results are however not obsolete, as most climate predictions proved accurate until now. Climate models published during the past 50 years proved valid in predicting global warming in the years following publication, mainly when differences between modeled and actual changes in atmospheric carbon dioxide and other climate drivers were accounted for [67]. The demand for quantitative projections of climate evolution [68] led to more research on the topic of uncertainty quantification in climate science [69]. Uncertainties arise because of an incomplete understanding of climate change as well as limitations in models and observations. Techniques for quantifying uncertainties of past climate and future projections also enable to express uncertainties in terms of probabilities and are described in the literature [68]. It is possible to produce quantitative projections of climate change, combining models of varying complexity and observations that measure our current uncertainty in those projections. Efforts to analyze whether the latest models, which presumably represent the climate system better than their predecessors, enable to obtain a more realistic picture of the evolution of climate. Better constraining processes affecting regional climate sensitivity could strongly reduce the uncertainty in the projections of extremes and climate impacts, potentially even more than further refinements of global climate sensitivity [70].

Projections of wind and solar PV generation potential are tainted with uncertainties [52]. In the next two paragraphs, we discuss the trends and findings on future changes in wind and solar under changing climate.

Trends in wind and solar under changing climate

The complexity in understanding climate change stems from the spatial and temporal heterogeneousness of its impacts over the world. Most recent literature review on future wind projections indicates a likely decline in the northern hemisphere and an increasing trend in the south [71]. The assessment of climate change impacts using RCMs in Ontario indicate that wind speed trends are expected to decrease in the energy portfolio mix [63]. In West Africa, the analysis of future change of wind using simulations from Coupled Model Inter-comparison Project version 6 (CMIP6) uncover an increase of 70% in wind power density over the Guinea coast sub-region of West Africa, especially in June–July–August season under global warming [72]. In Greece, projections of the future wind climatology in a changing climate using downscaled GCM with the Weather Research and Forecasting (WRF) detect increases in mainland Greece and the northern parts of Crete, and decreases in the southern part of the Crete [73]. In Russia, changes in wind potential in the subarctic regions are foreseen to vary from -15 to -20% [74]. In the Gulf of Oman, the evaluation of potential of wind energy offshore using the CORDEX wind speed data simulations concludes on promising prospects for wind energy exploitation[75]. Studies evaluating climate change impacts at the wind site level [76]–[78] are less abundant than those at regional level. In summary, the disparity of the impacts described confirms the necessity of conducting regional investigations to better understand local challenges and consequences.

Research gap 2   The consistency of future wind speed trends under changing climate is underexplored. Its relevance is timely in regions where the climate is exacerbating.

Wild et al. pioneered the analysis of climate change impacts on PV trends with a global study using CMIP5 GCMs [79]. This avant-garde study describes decreases in PV in large parts of the world under RCP 8.5 scenarios for the first half of the twenty-first century and positive trends in Europe, the South-east of North America, and southeast China. Since then, various analysis using GCMs and RCMs followed [61]. The evaluation of climate change impacts on solar PV with RCMs finds slight decreases in PV production by the end of the century unlikely to imperil the European PV sector [80]. The examination of projected PV changes using GCMs indicates increases in output in China from 2010 to 2080 and decreases in the US and Saudi Arabia [81]. Increasing temperatures in Africa could lead to reduced PV potential which calls for efforts to reduce the dependency of the performance of PV cells on the ambient temperature [82], [83]. Climate change projections in Burundi predict a huge change in PV power potential by 2050 calling for more investments in energy from solar PV [84]. The estimation of future changes in solar energy potential in Australia under climate change reveals that future changes in PV potential are determined primarily by the increasing temperatures and reduction in radiation[85].

In the case of India, studies on solar energy focus more on the policy perspective and the ambition of India to expand its solar capacity to meet the ever-growing energy demand [86]–[90].

Research gap 3 The analysis of future wind and solar energy patterns under changing climate in India with latest climate models is missing and requires further investigations.

Integrated responses for wind and solar planning

Early work of Archer et al. shows the benefits of interconnecting wind farms in the United States as a way to decrease intermittency [91]. The co-deployment of wind and solar PV could balance diurnal and seasonal variability locally [92]–[94]. Climate change can also exacerbate solar and wind energy contingencies and extend the risk of long periods of wind and solar shortage which could be detrimental in regions with high renewable energy penetration [59]. Low wind and solar periods or high wind events may render a significant part of the capacity in a particular location unproductive over a long period and impact the revenue streams of the projects [59], [95], [96]. Planning must ensure that the deployment of wind and solar accounts for the spatiotemporal complementarity of all resources to offset the local variability and mitigate the effect of long-term variability [97]. Researchers play an active role in evaluating solutions of hybrid power generation with wind and solar [98].

Strategies and actions need to be pursued to move towards climate-resilient renewable energy infrastructures. In some cases, diversification can be an essential element of such strategies. Therefore, we need tools to plan effectively. Modern Portfolio Theory (MPT) is a financial theory that helps to guide investment decision-making in assessing the trade-off between (expected) financial return and risk (represented by the volatility of the return) [99]. It is used to obtain the efficient frontier of portfolios of individual financial assets. From an investor's point of view, the optimal choice is maximizing returns for a given level of risk. DeLlano-Paz et al. provide a review of energy and portfolio theory [100]. Return is usually represented as the (physical) power output and risk as to the output volatility. MPT is recognized as an efficient planning tool in supporting sustainable investment planning and decreasing the risk to environmental benefits [101]. The application of portfolio theory to the investigation of climate change impacts enables to account for evolving inter-dependencies regionally and across sectors, and facilitate strong and early action on the climate-related effects [102]. The use of MPT to analyze the smoothing effect for the future Chinese power system uncovers its effectiveness to develop mitigation strategies reduce integration costs and disperse the deployment of wind and solar over a large area with diverse weather patterns [103].

Research gap 4 The exploration of climate resilient portfolios in studies accounting for the complementarity and balancing of wind and solar is missing in India.

The need for higher resolution data in India

Recently, there has been a growing interest in using artificial intelligence methods, including neural networks for both weather and climate predictions [104]–[106]. Machine learning algorithms have a wide range of applications from wind prediction in complex topography to climate [107]. Neural network can be used for the post-processing of RCMs to assess the impact of climate on wind power resources [108], and the improvement of the predictions [109], [110]. The improvement of long-term wind predictions in regions threatened by climate change offers an additional incentive for wind energy developers to invest in assets. The ability of state-of-the-art climate models to represent mean winds and their seasonality in areas with a complex topography is limited and wind speed biases are persistent over mountainous terrain [111]. With the growing interest in assessing wind energy potential in complex terrains [112], machine learning techniques can play a significant role in improving wind speed predictions. Mortezazadeh et al. use an approach combining computational fluid dynamics and random forest to predict wind potential for a long-term period in a urban area [113]. Biswas et al. investigate the accuracy of the prediction for two types of deep learning methods with daily wind from low resolution reanalysis datasets at the Bay of Bengal and Arabian Sea as inputs [114]. In Wind-Topo, the universal wind-topography interactions discovered by the model were successfully applied at the validation stations and to a high-resolution grid that exhibited most of the expected orographic effects [115].

Research gap 5   Studies on wind energy using machine learning methods in India are characterized by their scarcity, and the research on its application to provide wind energy forecasts is also rare.

Research goals

This thesis aims at understanding the state of climate change impact assessment studies, with a focus on the wind and solar situation in India, scrutinize prospects of wind and solar energy under climate change, and gather insights to enhance the achievement of resilient energy production portfolio. To address the overall goal and fill the identified research gaps, three main objectives are articulated and tackled in three research modules.

The first objective is to work with Coordinated Regional Dynamical Experiment regional climate models in South Asia under different climate change scenarios to investigate climate change impact on future wind resources in India. We provide insights on the consistency of wind speed trends and demonstrate that wind projections increase in India, triggering more enthusiasm for wind development in the northwest. We also propose a decision-making tool in the form of a structure-function to quantify the spatiotemporal consistency of wind trends. This objective is formulated with two main research questions (RQ) addressed in Chapter 1:

- RQ 1.a. What are the patterns of future wind speed trends from climate models projections?

- RQ 1.b. Can we formulate tools to quantify the spatio-temporal consistency of the climate trends?

In the second part of the thesis, we assess the impact of climate change on wind and solar PV in India based on climate models, evaluate the variability in models output, analyze the trends in models' predictions, and use portfolio methods to show how the combination of wind and solar can limit the variability on future trends of expected returns from combined installations. This objective is formulated with the following research question, addressed in Chapter 2:

- RQ 2. Can we use the anti-correlation of solar and wind resources to reduce uncertainty in the estimation of future yield if the combined generation of solar and wind power is considered?

The third objective is to focus on the high-resolution data to present a different perspective on wind prediction. We work on the prediction of surface wind speed and direction while taking into account terrain characteristics in the Indian sub-continent with a new version of a machine learning based model (Wind-Topo). Another objective explored in this work is to provide a scientific basis for the long-term planning of wind energy development and the availability of more reliable and low-cost wind energy forecasts. This objective is formulated with following research question, addressed in Chapter 3:

- RQ 3. Can we improve wind speeds estimation in areas with complex topography by leveraging machine learning methods and available measurements?

Challenges

Predictions from climate models

The literature on climate models contains methods to improve the predictions from raw climate models. There are four main methods; bias correction [116], downscaling to augment the spatial and temporal resolution [117], models' selection to shortlist the number of climate models in the prediction [118], and machine learning techniques [110], [119]. In the preliminary steps of this research, we applied quantile mapping to correct the bias of CORDEX models with the European Centre for Medium-Range Weather Forecasts (ECMWF) reanalysis datasets. We decided not to use this method in this thesis because of the limited availability of "ground truth" observations in the domain studied that would enable us to judge the added value of bias correction. We also tested the "best models" approach selection on World Climate Research Program (WCRP) models from the COordinated Regional Downscaling EXperiments (CORDEX) WAS-44. This approach uses models with a higher ability to reproduce the local climate in the prediction. The rationale behind this is that some models can have more "accurate" parametrization, initialization, more accurate and complete external forcings [120] or can show better performances for a specific application

or a particular variable demonstrated by [121]. In the application of this method, we picked ERA-interim ([122]) as a reference. We defined key performance indicators (KPIs), including the correlation, the difference in the average monthly wind speed, and other statistical metrics, to rank the individual WAS-44 models based on their performance with reference to ERA-interim in the historical period. The sensitivity analysis on the KPIs selected and ranking methods to choose the best models did not lead to the distinction of any robust set. Therefore, we decided not to adopt this approach. However, the pre-screening makes sense where the prediction applies to a feature that has impactful socioeconomic relevance [121] and only models best performing in reproducing the elements characteristic of the region would have to be included. We chose not to select a subset of best models because the multi-model ensemble average approach considering all models enables leverage on error cancellation and removes random errors between the models [123]–[126]. Furthermore, we justify this choice by the fact that multi-model selection enables us to represent better the full range of possibilities and ultimately, by incorporating information from different models, improve the skill of the ensemble prediction [121], [127].

Reliability of existing local measurements in India

In this thesis, we use wind speed measurements at ten meters from the Integrated Surface Database of NCEI NOAA (ISD). The standard resolution of ISD data is from three hours to daily, and five hundred thirty-four stations are accessible across India. While ISD integrates data from more than hundred original data sources for numerous parameters, including data that were key-entered from paper forms, to the best of our knowledge, ISD data do not include metadata on the maintenance or history of the stations. We found that wind speed data are sparse and available only for short periods of time in many stations. Unfortunately, we could only rely on the available information and exclude the data that did not pass the quality check developed by the data provider.

Accomplishments

This thesis builds a collaboration between the climate research community and the renewable energy industry. It contributes to increase the general understanding of the impact of climate change on wind and solar energy and delivers a first-order estimate of the impacts in India. This research provides insights to push the practical use of climate models in investment and planning decisions and supports wind and solar energy stakeholders in anticipating the impact of climate change on their assets. Given that both future investment and existing assets are subject to climate risk, this work provides with a scientific basis to help industry actors prepare for climate change with a risk assessment based on portfolio methods. This method can be applied to existing wind and solar assets and to explore what happens if the climate variables trends are as predicted.

This work provides the climate and energy community with analytical methods and a framework defining data requirements to assess climate change impacts on wind and solar installations in

any region. The trends calculated for surface wind highlight the potential for increasing wind capacity in the regions with promising wind prospects. In other words, resizing the capacity and installing more efficient turbines in existing wind farms is an alternative to installing new farms. In identifying optimal portfolios, we define the results in terms of the spatial distribution of different assets without considering existing capacity. The formulation enables the incorporation of existing capacities by framing them as constraints by the user. Furthermore, the demand profile can be fed to the optimization model by setting a ceiling for the regional maximum installed capacity to derive portfolios embedding characteristics closer to reality.

The methodological tools integrating climate change considerations are flexible and can be applied to any region.

Structure of the thesis

Chapter 1 investigates CORDEX RCMs models and future wind speed projections in the India subcontinent. Chapter 2 presents the assessment of climate change impacts for future wind and solar energy installations in India. Chapter 3 explores the application of a new version of Wind-topo to provide with high-resolution wind flows. The last part of the thesis includes the conclusions and addresses open questions for future work.

This thesis is mainly based on two published and one non-submitted papers [128], [129]. Chapters 1 and 2 are based on published manuscripts. Further details are given as a preamble to each chapter.

1 Future trends in wind resources and their consistency

Background This chapter is adapted from a published manuscript.

Data availability CORDEX model outputs are freely accessible on the Earth System Grid Federation database (ESGF; http://esgf.llnl.gov/). The Modern-Era Retrospective analysis for Research and Applications Version 2 (MERRA2) provides data since 1980 and runs until a few weeks before real time, they are available at https://disc.sci.gsfc.nasa.gov/datasets, which is managed by the NASA Goddard Earth Sciences (GES) Data and Information Services Center (DISC). ERA5 data are available on the European Centre for Medium-Range Weather Forecasts database (ECMWF; http://www.ecmwf.int/en/forecasts/datasets/reanalysis-datasets/era5). NOAA ISD station data are accessible from the NOAA FTP server (NOAA; ftp://ftp.ncdc.noaa.gov/pub/data/noaa/).Unfortunately, it is not allowed to publicly share wind data measurements. The source code developed for the analysis is available upon request.

1.1 Introduction

Regional climate change impacts average atmospheric conditions and affects various elements of the energy system [130]. Wind energy, similarly to other renewable energy sources, is sensitive to changes in climate [131], [132]. Thus, it is becoming increasingly important to assess how climate change influences future wind resources, and future climate projections should inform long-term planning decisions on wind energy projects to reduce risks and utilize opportunities.

India has been leading global wind energy deployment, investing billions in wind power with the aggressive intention to double its wind power fleet in about five years since 2017 [133]. The World Economic Forum Annual meeting in 2020 recognized India as one of the hot spots for renewable energy investors and its emergence as home to one of the world's most extensive clean-energy expansion programs [134]. Energy access and security of supply are critical for India's fast-growing economy and demography and - at the same time - the nation is the third biggest carbon emitter after the United States of America and China [135]. Pryor et al. pioneered climate change impact studies on wind energy [136]. Since then, assessing likely future changes in wind power resources across the globe has been an active research area. The alterations of wind direction and velocity, as a direct or indirect effect of climate change, are limiting factors for wind energy harvesting potential and affecting regional economic and social development [137], [138]. Wind energy deployment is increasingly important in the context of rising global energy demand. Global Climate Models (GCMs) are used to assess future change in wind energy and found decreases near the end of the century across the northern mid-latitudes (independently from the emission scenario) and increases across the tropics and southern hemisphere under the RCP 8.5 scenario [139]. RCP 8.5 is the high emission case scenario for long-term change [140]. The substantial regional variations highlighted in [139] emphasize the relevance of geographically focused assessments with higher resolution models to understand the impacts fully.

Climate change can also be beneficial for wind energy development. The analysis of wind potential from CORDEX data in Europe indicates that climate change can lead to profitable prospects for wind energy production in the Baltic Sea as projections show increasing annual wind energy output combined with lower intra-annual variability [141]. This study also projects raising challenges in western Europe in countries like France, some parts of Germany and Iberia due to higher intra-annual fluctuations indicating larger spatiotemporal variations.

CMIP6 are used to investigate climate change impacts on wind resources in other parts of the world. Martinez shows that on-shore wind energy densities in the US and Canada will decline. He also finds robust increases for the long-term future in some focal regions including Central America with up to 30% increase for example in southern and northern Mexico [60]. Furthermore, the release of CMIP6 models enables the revise the findings extracted from CMIP5 models. The analysis of the results have to be interpreted with care because CMIP5 and CMIP6 are not formulated on the basis of the same scenarios; CMIP5 scenarios are formulated on the basis of RCP 2.6, 4.5 and 8.5 which are now replaced with the Shared Socioeconomic Pathways (SSP) scenarios for land-use and greenhouse gases emissions SSP2-4.5 and SSP5-8.5 (intensive GHG

emissions) [142]. Therefore the change in the formulation of the scenarios does not enable to directly compare the results. Carvalho et. al provide with projections of future wind energy resources using climate models from CMIP5 data with the purpose of evaluating the prospects of wind in coastal environments in the Black Sea and review the changes with CMIP6 [143], [144]. The comparison of the two models highlights diverging results in Europe about the future of wind energy resources; the increase in wind found in some regions from CMIP5 models is contradicted by an opposite trend with CMIP6 models. CMIP6 results indicate a strong decline in most of the continent by the end of the century whereas the results from CMIP5 indicate an increase [144]. This difference in the results can be explained by stronger radiative forcing in CMIP6 scenarios as opposed to their predecessors [144].

Assessment studies of past and future wind speed trends rely on various data, including climate models, measurements, and reanalysis. Climate projections provide valuable data to evaluate the future of wind resource availability in wind farms, and hind-cast simulations inform on their past operations as few have operated consistently over the time scales associated with climate change. Reanalysis products and climate models are particularly important because they enable us to overcome the lack of available and regular measurements in some regions. Only a limited number of studies including K. Kim et al. and Solaun et al. look at climate change impact on future wind resources using climate projections embedded with real wind farm operation data [145], [146].

The climate in India is characterized by its complex nature with monsoon and topography variations across its domain. High-resolution regional climate models (RCMs) are required for reproducing the climatic features and simulating future projections are essential for climate change studies in such regions. CORDEX is an international initiative launched by the World Climate Research Program (WCRP) to produce world-wide high-resolution regional climate change projections. The results of CORDEX feed climate change impact and adaptation studies, using forcing scenarios to produce projection experiments with boundary conditions provided by different GCMs. Prior to the CORDEX-COmmon Regional Experiment (CORE) RCMs (CORDEX core;[147]), the Indian Institute of Tropical Meteorology (IITM) and the Swedish Meteorological and Hydrological Institute (SMHI) collaborated to produce CORDEX WAS-44 models for the South Asian domain at $0.44°$ horizontal resolution (or 50 km). There are notable enhancements in the performance of CORDEX WAS-44 models in reproducing monsoon precipitation in India with respect to seasonal and annual cycle modeling as well as the mean monsoon rainfall simulations [130]. Such improvements increase the confidence in the results of the studies relying on those models. The analysis of CORDEX WAS-44 performance in simulating offshore wind potential highlighted that there were remaining challenges for CORDEX WAS-44 in precipitation simulations over the homogeneous monsoon zones [148].

Giorgi et al provides with a comprehensive review of the progress done in RCMs in terms of computing abilities and atmospheric processes representation [149]. Such progress was motivated by their growing importance in the impact assessment community. The release of the latest generation of CORDEX-core models marks the transition to convection-permitting RCMs. This

was made possible by increasing available computing power and improvements in physical parameterizations. The new generation of models with higher resolution is expected to provide updated information on the impact of climate change on local winds and supplement previous work of Kulkarni et al. in India [148], [150].

CORDEX core RCMs allow assessing the coherence of climate change signals and differences in comparison with lower horizontal resolution versions. The increase of model spatial resolutions is expected to enable a better understanding of regional climate change signals. However, this result is nuanced by some exceptions and shall be verified; the study of Y. Shi et al on the role of resolution in regional climate change projections in China concludes that downscaling to finer resolutions does not necessarily imply greater confidence in the models [151]. Thus, it is important to investigate this result.

The availability of wind farm data would enable their comparison with climate data. To the best of our knowledge, CORDEX-core models outputs for surface wind speed for South Asia (noted CORDEX WAS-22 or WAS-22 hereafter) have not been evaluated before and nor compared with their lower resolution predecessor CORDEX WAS-44 models (noted WAS-44 hereafter). This study complements others by using common climate models to study climate change impacts on future wind speed trends and proposes a new method to investigate their consistency both in space and time.

Acknowledging the significant uncertainties associated with future climate and repercussions on wind energy development, the aim of this study is: first, to evaluate the reliability of monthly surface wind speeds from WAS-22 RCMs and examine their performance at existing wind farms locations and other local stations in India; second, to analyze future wind speed trends from projections in the Indian sub-continent; and lastly, to suggest a decision-making tool that enables to measure the spatio-temporal consistency of these trends using a method inspired from the variogram formulation. The study is structured as the following: Section 1.2 outlines the general approach, details the data used and introduces the methods, Section 1.3 outlines the results; Section 1.4 summarizes the findings and their limits and finally Section 1.5 ends the manuscript with a short conclusion.

1.2 Materials and methods

1.2.1 General approach

The general approach adopted in this study is to analyze long-term wind speed annual and seasonal trends using CORDEX monthly simulations over the Indian sub-continent. The comparison to validate climate models in existing wind sites with local data relies also on measurements from the integrated surface database (ISD [152]) measurements and two reanalysis datasets to verify if CORDEX data reproduce local wind patterns in locations for which the wind farm operations' data were available. Therefore, prior to this step, we compare the two reanalysis

datasets considered with ISD measurements at various location in India and use the one with the closest characteristics to local wind speeds as a reference. Furthermore, we compare WAS-22 monthly outputs with their predecessor WAS-44 produced at a lower spatial resolution, and investigate the consistency of the trends from these models. We use the open source statistical software R [153] to conduct the analysis.

1.2.2   Study area and wind farms location

In this research, we focus on the Indian sub-continent and define the study area as the domain limited by latitudes from 6.7°N to 35.6°N and longitudes from 68.1°E to 97.5°E. The wind farms were chosen from the wind portfolio of CLP Group in India for their technical features and data availability. The wind farm measurements are available for the periods described in Table 1.1 (additional wind farms characteristics summarized in this table are referenced from the wind power database. Tejuva is located in the state of Rajashtan and has the longest data history with seven years of wind speed measurements. Jath is located in Maharashtra and has two years of data available. Theni is located in Tamil Nadu, and three years of data are available for this wind farm.

Table 1.1: Summary of the wind farm characteristics used in the analysis.

Wind farm	Latitude	Longitude	hub height in meters (m)	Data availability
Tejuva (Rajasthan)	27.02°N	74.23°E	90 m	2015-2017
Jath (Maharashtra)	19.75°N	75.71°E	90 m	2016-2018
Theni (Tamil Nadu)	11.13°N	78.66°E	78 m	2011-2018

1.2.3   Data used

CORDEX RCMs

CORDEX climate data are typically available from 1970 to 2100. The period extending from 1970 to 2005 is the so-called historical period, and climate projections period runs from 2006 to the end of the century. We construct the surface wind speed (10 m) using the module of the meridional and zonal components at the surface (noted u_{as} and v_{as} in [m/s] respectively). WAS-22 high-resolution models include two RCMs, the Abdus Salam International Centre for Theoretical Physics (ICTP) Regional Climatic model V4 (RegCM4-7; http://gforge.ictp.it/gf/project/regcm), and the CLMcom-ETH-COSMO-crCLIM-v1.1 model prepared by ETH Zurich in collaboration with the Climate Limited-area Modelling Community (COSMO-crCLIM-v1-1; http://cordex.clm-community.eu/). These two RCMs are used to downscale three CMIP5 GCMs: MPI-M-MPI-ESM-MR, MIROC-MIROC5 and NCC-NorESM1-M for RCP 2.6 and RCP 8.5 scenarios; the fourth, GCM ICHEC-EC-EARTH, is downscaled for RCP 8.5 only. The list of the WAS-22 scenario runs considered in this study with their RCM name, driving GCM model, and RCP scenarios is given in Table 1.2. We convert COSMO models from polar rotated to regular longitude-latitude coordinates to conform with the format of RegCM4-7 models.

Table 1.2: WAS-22 models used in this study, with their RCM name, driving GCM, model acronym, and IPCC scenarios.

RCM name	Driving GCM	Acronym	IPCC scenarios
RegCM4-7	MPI-M-MPI-ESM-MR	RegCM4-MPI	RCP 2.6 & 8.5
	NCC-NorESM1-M	RegCM4-NCC	RCP 2.6 & 8.5
	MIROC-MIROC5	RegCM4-MIROC	RCP 2.6 & 8.5
COSMO-crCLIM-v1-1	MPI-M-MPI-ESM-LR	COSMO-MPI	RCP 2.6 & 8.5
	NCC-NorESM1-M	COSMO-NCC	RCP 2.6 & 8.5
	ICHEC-EC-EARTH	COSMO-ICHEC	RCP 8.5

The same approach is repeated to construct monthly surface winds for the lower resolution WAS-44 models. The RCMs used in WAS-44 are two dynamically downscaled models forced by different GCMs from the Coupled Model Inter-comparison Project Phase 5 (CMIP5 [154]); the Regional Climatic Model version 4 (RegCM4-4 [155]) produced by the Indian Institute of Tropical Meteorology, and the Rossby Centre regional atmospheric model version 4 (RCA4 [156]) prepared by the Swedish Meteorological and Hydrological Institute. WAS-44 scenario runs and their details are summarized in Table 1.3.

Table 1.3: WAS-44 models used in this study, with their RCM name, driving GCM, model acronym, and IPCC scenarios.

RCM name	Driving GCM	Acronym	IPCC scenarios
IITM-RegCM4	MPI-M-MPI-ESM-MR	IITM-MPI	RCP 4.5 & 8.5
	CSIRO-QCCCE-CSIRO-Mk3-6-0	IITM-CSIRO	RCP 4.5 & 8.5
	CCCma-CanESM2	IITM-CCCma	RCP 4.5 & 8.5
	NOAA-GFDL-GFDL-ESM2M	IITM-NOAA	RCP 4.5 & 8.5
	CNRM-CERFACS-CNRM-CM5	IITM-CNRM	RCP 4.5 & 8.5
	IPSL-CM5A-LR	IITM-IPSL	RCP 4.5 & 8.5
SMHI-RCA4	NCC-NorESM1-M	SMHI-NCC	RCP 4.5 & 8.5
	MIROC-MIROC5	SMHI-MIROC	RCP 4.5 & 8.5
	MPI-M-MPI-ESM-LR	SMHI-MPI	RCP 4.5 & 8.5
	ICHEC-EC-EARTH	SMHI-ICHEC	RCP 4.5 & 8.5
	MOHC-HadGEM2-ES	SMHI-MOHC	RCP 4.5 & 8.5
	CCCma-CanESM2	SMHI-CCCma	RCP 4.5 & 8.5
	NOAA-GFDL-GFDL-ESM2M	SMHI-NOAA	RCP 4.5 & 8.5
	CNRM-CERFACS-CNRM-CM5	SMHI-CNRM	RCP 4.5 & 8.5
	IPSL-IPSL-CM5A-MR	SMHI-IPSL	RCP 4.5 & 8.5
	CSIRO-QCCCE-CSIRO-Mk3-6-0	SMHI-CSIRO	RCP 4.5 & 8.5

Reanalysis data

Reanalysis data are commonly used in wind resource assessment and provide valuable information about the local climate. In this study, we use reanalysis datasets as a reference to get around the lack of available reliable gridded historical surface wind speed data in the domain studied. In addition to the Modern Era Retrospective-Analysis for Research and Applications dataset (MERRA2 [157]), we include in the analysis the European Centre for Medium-Range Weather Forecasts (ECMWF) most recent reanalysis datasets (ERA5 [158]). MERRA2 is also a widely adopted reanalysis dataset in wind assessment. From these reanalysis datasets, we use surface wind speed data at the monthly time resolution. ERA5 data coverage extends from 1979 to present with a horizontal resolution of $0.281° \times 0.281°$. The data coverage for MERRA2 extends from 1980 to present with a horizontal resolution of $0.5° \times 0.625°$. ERA5 has the highest resolution among others reanalysis datasets. Ramon et al. recent research comparing various global reanalysis products with observations concludes that ERA5 represents the best near-surface winds and offers the closest values for the inter-annual variability [159]. This study also finds that none of the reanalysis stood out regarding the seasonal average wind speeds. Therefore, we compare ERA5 and MERRA2 with ISD data and pick the reanalysis used as a reference to assess the ability of WAS-22 and WAS-44 models in reproducing regional wind speed properties for a 30-years period extending from 1980 to 2010.

Wind farms measurements

In this study, we use hub-height wind speed measurements from Tejuva, Jath and Theni wind farms. The original 10 min average wind speed data collected by the Supervisory Control and Data Acquisition (SCADA) system of the wind turbines are aggregated to monthly resolution and then compared to WAS-22 models for the period for which they overlap.

Local wind measurements

We use wind speed measurements at 10 m from the Integrated Surface Database (ISD). The standard resolution of ISD data is from 3 hours to daily, and 534 stations are accessible across India. For each wind farm, we search for the ISD stations obtainable in its vicinity and extract the nearest one. In addition to the stations close to the three main wind farm sites for which wind farm data are at our disposal, we extend the comparison other 15 stations. We found that wind speed data are sparse and only available for short periods of time in many stations and only picked stations data available for at least three consecutive years. Table 1.4 summarizes the characteristics of the stations considered in this study.

Table 1.4: Summary of the specifications of ISD stations used as a reference for the wind farms considered, distance to the wind farm sites, and period of availability for the data.

Station name	Latitude	Longitude	Elevation	Time availability
Jaisalmer	26.90°N	70.90°E	231 m	2006-2020
Anantapur	14.58°N	77.60°E	36.4 m	2006-2020
Coimbatore	11.00°N	77.00°E	404 m	2006-2020
Belgaum	15.90°N	74.60°E	75.8 m	2006-2018
Porbandar	21.60°N	69.70°E	5 m	2016-2020
Rajkot	22.30°N	70.80°E	13.4 m	2006-2020
Chamarajnagar	11.93°N	76.90°E	76 m	2015-2020
Bangaluru	13.20°N	77.70°E	91.5 m	2008-2020
Kolhapur	16.70°N	74.30°E	60.8 m	2006-2020
Bangalore	13.00°N	77.60°E	92.1 m	2006-2020
Thanjavur	10.80°N	79.10°E	6.8 m	2015-2020
Ahmadnagar	19.10°N	74.80°E	65.7 m	2015-2020
Udhagamandalam	11.40°N	76.73°E	224.9 m	2009-2020
Madurai	9.84°N	78.10°E	13.1 m	2011-2020
Coonoor	11.30°N	76.80°E	174.7 m	2015-2020
Palakkad	10.80°N	76.70°E	9.7 m	2015-2020
Davangere	14.50°N	75.90°E	620 m	2015-2020
Dharwad	15.50°N	75.00°E	678 m	2015-2020

1.2.4 Methods

Comparison of surface wind speeds from reanalysis data and local measurements

The performance of reanalysis data when compared to local observations can be highly specific. Therefore, we compare ERA5 and MERRA2 datasets with local ISD wind speed measurements in 18 stations to identify their shortcomings and pick the reanalysis dataset used as a reference to analyze CORDEX models. The comparison is focused on the time period for which ISD data are available and based on the fraction bias (fBias), the mean absolute error (MAE), Pearson correlation coefficient (P.corr), and the coefficient of determination R^2. Furthermore, before comparing the various data sources, we re-gridded the data to a common 0.2° spatial resolution using the climate data operator (cdo) through bilinear interpolation. We perform the exercise for reanalysis and local stations data at the daily and monthly resolution. The results indicate higher correlation at the monthly timescales on Table A.1, therefore we focus on data at the monthly resolution.

Comparison of surface wind speeds from CORDEX and reanalysis data

We compare gridded data from WAS-22 and WAS-44 ensemble with the reference reanalysis dataset based on the differences in annual and seasonal wind climatology, variability, and trends for a 30 years extending from 1980 to 2010.

WAS-22 outputs comparison with local observations

We evaluate the performance of monthly WAS-22 scenarios runs in reflecting local wind attributes against four reference datasets, namely CLP wind farm measurements, reanalysis data (ERA5 and MERRA2), and ISD data for the period for which the data overlap. The period of evaluation depends on the availability of the observations. We calculate the fBias, MAE, P.corr and R^2 for WAS-22 multi-model ensembles (under each scenario) with ISD, reanalysis data, and CLP measurements at each location investigated. In the comparison of climate simulations with wind farm measurements, we project monthly simulations to hub-height using the wind profile power law [160], [161]:

$$v_H = v_h \left(\frac{H}{h}\right)^{\alpha}, \tag{1.1}$$

where v_H is the extrapolated wind speed at hub height H in meters, h is equal to $10m$, v_h is the surface wind speed at $10m$, and the exponent factor α is equal to the standard value of $1/7$ for neutral stability conditions [162]. The second step in the validation of CORDEX models with the local wind data consists of standardizing all monthly wind speeds (using the average and standard deviation) at each location and decomposing the time series into seasonality, trends, and fluctuation using the R package STL. The STL decomposition enables separating time series into seasonal, trend, and irregular (randomness) signals using Loess method [163]. In the STL framework, time series are de-trended before extracting the seasonal signal. Next, we can examine the standardized wind speeds and their seasonal signals in the wind sites to assess CORDEX models' ability to recover local monthly trends and seasonality.

Trend analysis of CORDEX projections and uncertainty

We compute the annual and seasonal trends from WAS-22 projections (period extending from 2006 until the end of the century) and investigate if changing patterns could be detected and how these trends could be related to yearly or seasonal climate patterns. We use the non-parametric procedure developed by Sen [164] to calculate the magnitude of the trends. Non-parametric methods are considered more robust than parametric methods against the outliers in a time series and are more applicable for variables like wind speeds that do not fulfill the normality requirement [165]. We consider a trend significant if the Mann-Kendall test yields a p-value of less than 0.05 for the null hypothesis of no trend (i.e, 95% confidence level). We express the inter-model uncertainty of the trend using the relative standard deviation (RSD) which is the ratio between the standard deviation and the mean expressed in percent.

A measure of wind trends spatio-temporal consistency

The analysis of WAS-44 models shows that significant spatial and temporal disparities characterize wind speed trend projections. We find it difficult to make conclusions on the future trends. We

define a tailored metric to measure the spatio-temporal consistency of the trends from climate model projections. The method is in the form of a structure-function. Our main contribution in this work is to use the annual wind speed trends at each cell of our domain as an input to understand their variability in space and time. The spatio-temporal consistency $C(\Delta x, \Delta t)$ is a function of separation between the locations and times, and for all the cells in the study area, its general equation is:

$$
\begin{aligned}
C(\Delta x, \Delta t) = &\frac{1}{N(\Delta x)} \sum_{(i,j) \in N(\Delta x)_{i=j}} [\tau(x_i, T) - \tau(x_j, T)]^2 \\
&\frac{1}{N} \sum_{i=1}^{N} \sum_{k=1}^{K} \frac{1}{N(\Delta t)} [\tau(x_i, T) - \tau(x_i, T_k)]^2,
\end{aligned}
\tag{1.2}
$$

where x_i and x_j are cells separated by distance Δx, Δt is the sub-period considered, $\tau(x_i, T)$ is the value of the trend at cell x_i estimated for the full length T of climate models projections (i.e from 2006 to 2100); $N(\Delta x)$ is the number of pairs of cells in the domain located at a distance Δx from each other, N is the total number of cells in the domain analyzed, and $N(\Delta t)$ is the number of sub-periods of length $T_k = \frac{T}{k}$ where $k \in 1, 2, 3, ..., K$, where K is such as each sub-period contains at least 10 years, and $\tau(x_i, T_k)$ is the trend estimated for the kth sub-period of length k. The shape of the 2D surface resulting from equation (1.2) characterizes the spatio-temporal consistency of the wind speed trends data from these models, and more precisely how the trends in two locations vary as a function of the distance between them while also accounting for the temporal dimension. Therefore, when applied to a specific region, the measure suggested enables to estimate the distance from a wind farm at which the trends remain unchanged, and help make decisions on the installation of wind farms.

1.3 Results

1.3.1 Comparison of reanalysis datasets with local data

We present the results of the comparison of reanalysis datasets with local data in Table 1.5.

Table 1.5: Comparison of the statistical metrics of MERRA2 and ERA5 with ISD stations.

	RMSE		MAE%		fBias		P.corr		R^2	
Stations	MERRA2	ERA5	MERRA2	ERA5	MERRA2	ERA5	MERRA2	ERA5	MERRA2	ERA5
Jaisalmer	2.79	0.87	1.44	0.34	2.44	1.00	0.89	0.90	0.79	0.81
Anantapur	4.21	1.00	2.61	0.53	3.61	1.37	0.89	0.84	0.80	0.70
Coimbatore	2.33	1.06	0.84	0.33	1.84	0.69	0.86	0.87	0.74	0.76
Belgaum	5.95	2.59	26.3	8.57	27.30	9.55	0.84	0.88	0.71	0.77
Porbandar	3.19	0.84	1.01	0.20	2.01	1.09	0.83	0.77	0.69	0.59
Rajkot	2.88	1.02	0.98	0.28	1.98	0.78	0.82	0.84	0.67	0.71
Charmarajnagar	3.60	0.98	3.53	0.78	4.53	1.61	0.77	0.72	0.59	0.52
Bangaluru	2.72	1.47	0.86	0.30	1.85	0.77	0.69	0.64	0.48	0.41
Kolhapur	4.13	1.22	1.81	0.48	2.81	0.97	0.66	0.54	0.43	0.29
Bangalore	4.40	1.46	3.07	0.80	4.07	1.69	0.55	0.55	0.30	0.31
Thanjavur	4.79	1.53	5.24	1.50	6.24	2.46	0.53	0.47	0.28	0.22
Ahmadnagar	5.33	2.07	40.6	11.8	41.6	12.8	0.45	0.41	0.20	0.17
Udhagamandalam	3.37	1.51	6.85	1.92	6.85	1.92	0.39	0.41	0.15	0.17
Madurai	4.35	1.17	6.48	1.58	7.48	2.50	0.20	0.06	0.04	0.00
Coonoor	4.00	0.89	5.11	0.92	6.11	1.77	0.21	0.20	0.04	0.04
Palakkad	3.66	1.33	3.69	1.27	4.69	1.90	-0.21	-0.08	0.04	0.01
Davangere	5.77	2.62	10.9	4.15	11.90	5.13	0.03	0.06	0.00	0.00
Dharwad	5.39	2.63	10.2	4.26	11.20	5.23	-0.03	-0.10	0.00	0.01

The RMSE values obtained with MERRA2 at the 18 ISD stations examined are higher than those found for ERA5. This indicates that MERRA2 consistently overestimates local wind speeds. For ERA5, RMSE values are close to or equal to 1 at five sites; Jaisalmer, Rajkot, Anantapur, Coimbatore, and Chamarajnagar. The results of the fBias also demonstrate the better estimation of wind speeds for ERA5 with values close to or equal to one at three sites; Jaisalmer, Kolhapur, and Porbandar. The fbias for MERRA2 reaches values as high as 41.60 at Ahmadnagar. The coarsest spatial resolution may be a reason for the poor performance of MERRA2 in reproducing local winds. Correlation values (between 0.69 and 0.90) for ERA5 and MERRA2 are found in 8 out of the 18 sites, namely Jaisalmer, Anantapur, Coimbatore, Belgaum, Porbandar, Rajkot, Chamarajnagar and Bengaluru. All these sites are located in the northwest or southwest, with elevations ranging between 76m and 404m. At Kolhapur, Bangalore, Thanjavur, and Ahmadnagar, the values of the Pearson coefficients are lower and range between 0.41 and 0.66. At Udhagamandalam, a station located at a high elevation, we find moderated correlation values of about 0.40 for both reanalysis datasets. Low correlation values of about 0.20 are found at the stations located in the mountainous region (Madurai and Coonoor) and elevations of 620 m above ground (Davanger and Dharwad). These poor correlation values indicate that the replica of local wind at high elevations remains a challenge for reanalysis datasets. This is probably because most assimilated stations are at low elevations. Taszarek et al. discuss this challenge when comparing ERA5 and MERRA2 over Europe and North America and infer on reanalysis

limits in coastal zones and mountains [166]. A closer look at the surroundings of some stations indicates that unsatisfactory results can be explained by the existence of trees obstructing their surroundings.

We conclude that ERA5 is an improvement over MERRA2 with smaller biases in surface wind speeds (e.g., average RMSE of 1.31 for ERA5 and 3.87 for MERRA2, an MAE of 2.02 for ERA5 and 7.12 for MERRA2, and a fBias of 2.73 for ERA5 and 8.05 for MERRA2). This result is confirmed by the study of Hofer et al., suggesting that recent reanalysis with higher spatial resolutions and observation processing show notably better skill than previous reanalyses [167]. Other recent assessments infer the higher reliability of ERA5 for renewable energy analysis and its outperformance in reproducing climate variables, including surface wind speeds, due to its improved resolution [168]–[171]. Furthermore, the analysis of the statistical metrics values from data at the daily and monthly resolution in the appendices (on Table A.1) demonstrates higher correlation coefficients higher at the monthly than daily timescales (correlation coefficients of 0.62 for monthly ERA5 and 0.50 for daily ERA5). ERA5 dataset is used as a reference in Section 1.3.2 in the comparison of CORDEX WAS-22 and WAS-44 models.

1.3.2 Comparison of CORDEX WAS-22 and WAS-44 with reanalysis data

In this section, we analyze WAS-22 and WAS-44 multi-model ensembles and evaluate their ability in reproducing surface wind speeds from ERA5. This ability is determined by examining annual and seasonal surface wind characteristics in terms of the bias in annual and seasonal climatology, variability and trends in the domain studied for the period extending from 1980 to 2010. We acknowledge that the analysis of the ensemble masks some substantial differences among the individual model and therefore investigate individual models' annual wind speed trends consistency in Section 1.3.3. We compare the annual climatology of ERA5 with the ensemble mean for WAS-22 and WAS-44 in Figure 1.1.a.
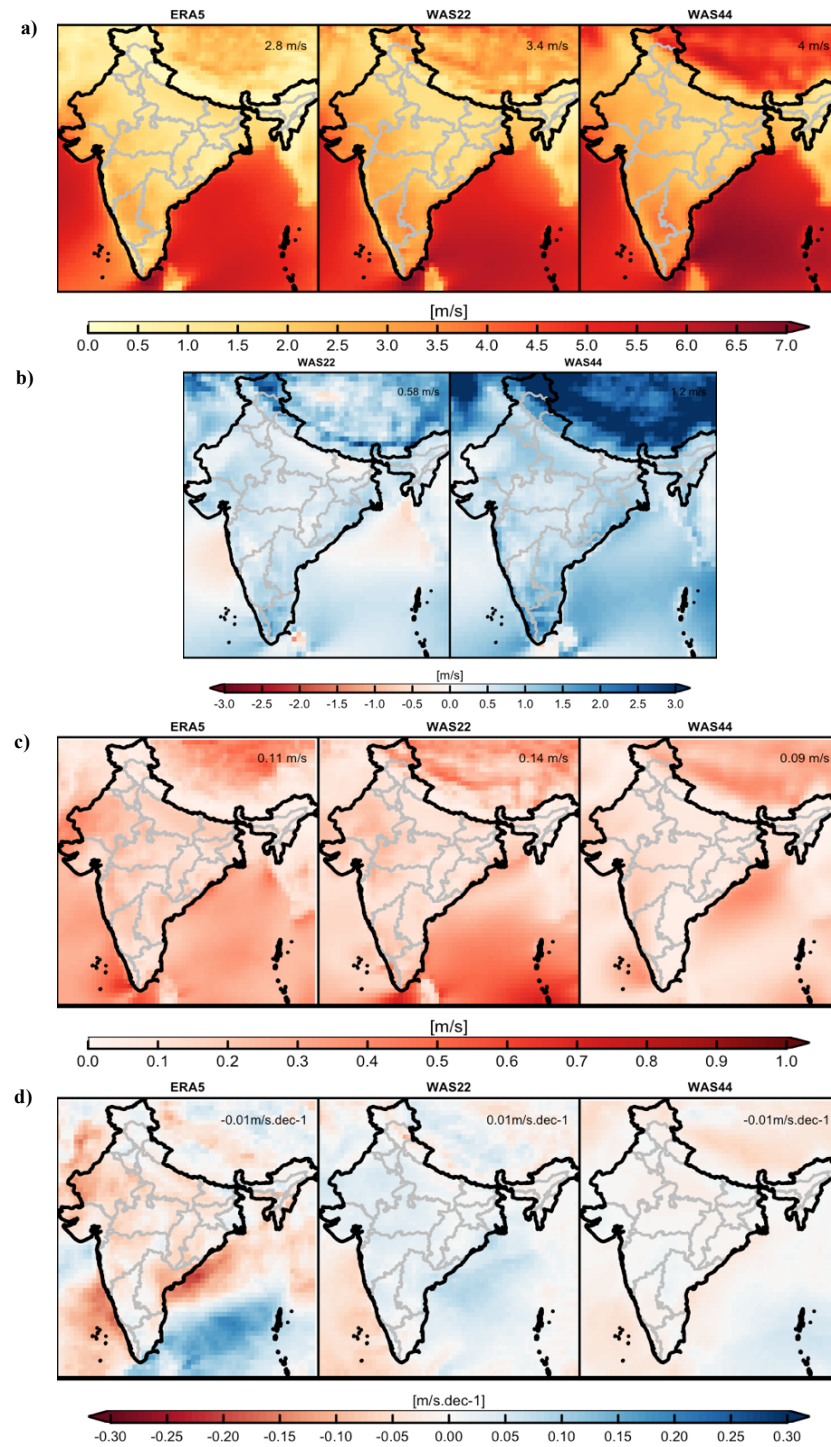
Figure 1.1: Geographical distribution of annual wind speed climatology **(a)**, annual climatology bias **(b)**, annual variability **(c)**, and annual trends **(d)** for ERA5, WAS-22 and WAS-44 multi-model mean ensembles (1980-2010).

Chapter 1. Future trends in wind resources and their consistency

ERA5 annual wind climatology range from 0.2 to 6.8 m/s, WAS-22 from 0.5 m/s to 6.9 m/s, and WAS-44 from 0.8 m/s to 7.8 m/s. The spatially averaged climatology for ERA5 equals 2.8 m/s. The bias in annual climatology (Figure 1.1.b) for WAS-22 with ERA5 is 0.58 m/s and 1.2 m/s for WAS-44, which is more than twice as large. The analysis of the annual variability for the 30 years analyzed in Figure 1.1.c shows that the spatial average of the annual variability for ERA5 is equal to 0.11 m/s. The values of the annual variability for WAS-22 are higher than the ones reported by WAS-44 (0.14 m/s for WAS-22 and 0.09 m/s for WAS-44). The spatial variability in WAS44 is smaller than in WAS22, which could be explained by the low spatial resolution that does not enable resolving the local topographical complexity. The value of the spatially averaged bias in the annual variability is -0.01 m/s for WAS-22 and -0.08 m/s for WAS-44. The spatial pattern of the variability exhibits more regions where the bias with ERA5 is higher for WAS-44 than WAS-22.

We compare annual trends for ERA5, WAS-22, and WAS-44 in Figure 1.1.d. The spatial average of the annual trends found for ERA5 (-0.01 m/s dec^{-1}) during the 1980 to 2010 period supports the stilling effect or decrease in land surface winds described in the literature (e.g.[172], [173]). The trends obtained for WAS-22 and WAS-44 do not reflect the stilling effect described by reanalysis datasets and in the literature. The spatial pattern of the trends from climate models' ensembles fail at reproducing the spatial pattern of the trends by ERA5. Therefore, we investigate the spatial pattern of the annual trends for ERA5 and MERRA2 with the ensemble mean and individual models of WAS-22 and WAS-44 models (Figure 1.2 and Figure 1.3).

The comparison of ERA5 with the RegCM4 WAS-22 model (Figure 1.2) shows a high similarity in the geographical distribution of the annual wind speed trend and magnitude. The results for COSMO-ICHEC and COSMO-NCC suggest a similar geographical distribution of the pattern in the western and southern parts of the country while differences emerge in the east. The geographical distribution of the annual trends for ERA5, MERRA2 and WAS-44 individual models from 1980 to 2010 is presented in Figure 1.3. The visual inspection of SMHI models from the WAS-44 experiment in Figure 1.3 displays a larger differences in the pattern of the annual trend among the models and also greater bias with ERA5.

The results of the seasonal wind characteristics for ERA5, WAS-22 and WAS-44 are presented in Figure 1.4. The analysis of the geographical distribution of the seasonal winds in Figure 1.4.a indicates that the highest wind values stretch along the northwestern coast. The comparison of the seasonal climatology bias in Figure 1.4.b demonstrates that the bias in WAS-22 ensemble seasonal climatology is lower than for the WAS-44 ensemble, WAS-22 experiment has a higher ability in producing results more aligned with ERA5 in regions where the elevation is high and topography is complex. Therefore, the reduction in bias found for the estimation of the annual climatology from WAS-22 compared to WAS-44 is also valid for the seasonal climatology. The seasonal bias values of WAS-44 and WAS-22 with ERA5 are about 3 and 3.6 times higher during pre-monsoon and monsoon seasons. The bias of WAS-22 with ERA5 in the pre-monsoon is -0.38 m/s for WAS-22 and -1.2 m/s for WAS44. The bias in the monsoon is -0.25 m/s for WAS-22 and -0.9 m/s for WAS-44. The bias during the post-monsoon season is 1.75 times
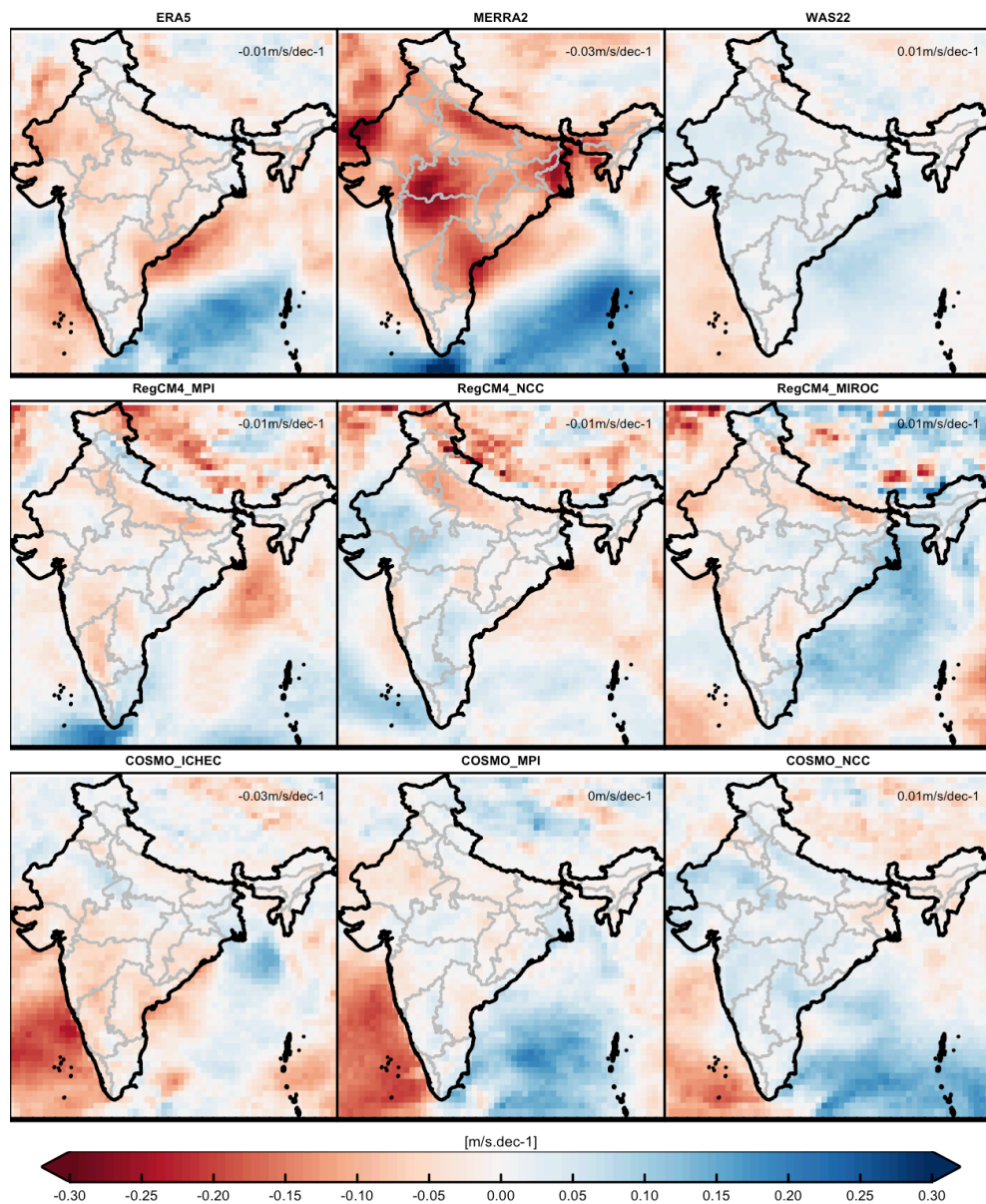
Figure 1.2: Geographical distribution of annual wind speed trends for ERA5, MERRA2, WAS-22 multi-model mean ensemble and individual models (1980-2010).

higher for WAS-44 than WAS-22 (-0.86 m/s for WAS-22 and -1.5 m/s for WAS-44), 1.6 higher during the winter season (-0.96 m/s for WAS-22 and -1.6 m/s for WAS-44). The bias in the seasonal climatology indicates that WAS-22 results are closer to ERA5. The seasonal trends found for ERA5 on (Figure 1.4.c) are underestimated by WAS-22 (Figure 1.4.d) and WAS-44 (Figure 1.4.e). We note that the magnitude of the trends during the 1980-2010 period is higher than the future trends discussed later in this chapter. The seasonal trends bias of ERA5 with
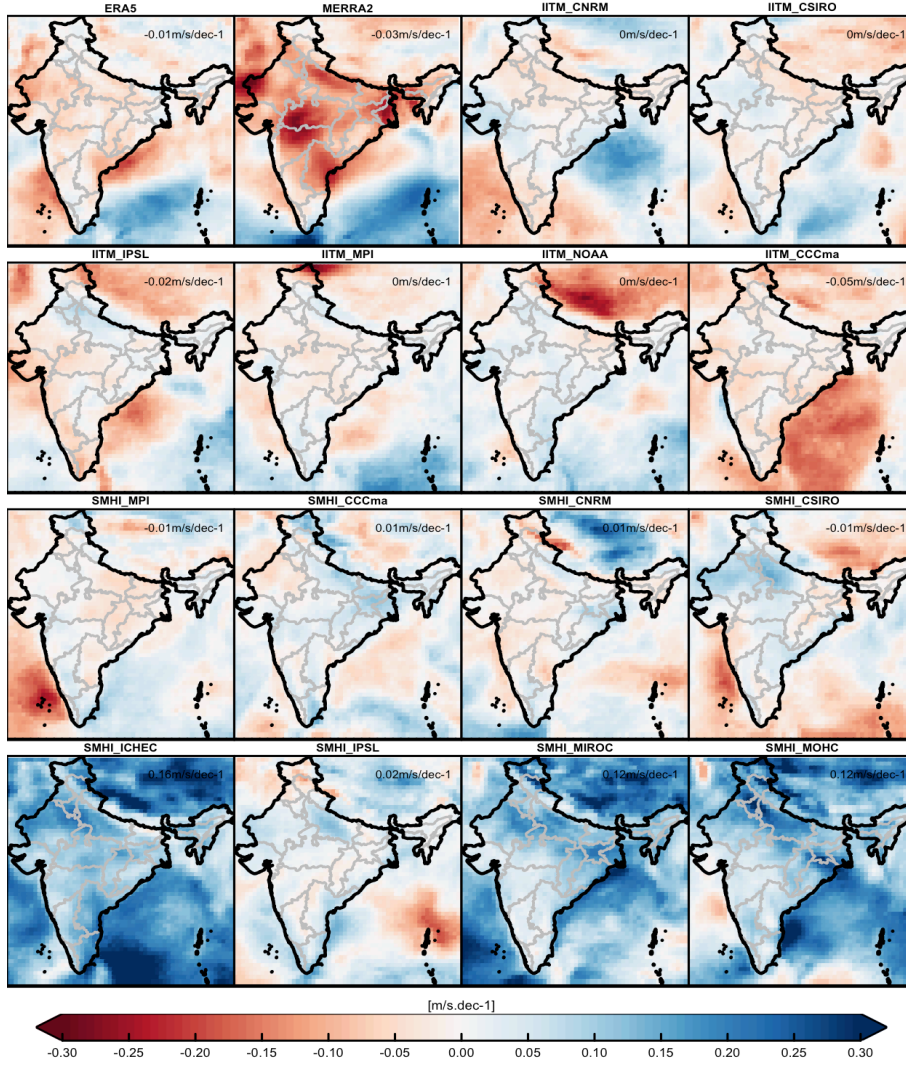
Figure 1.3: Geographical distribution of the annual wind speed trends for ERA5, MERRA2, WAS-44 multi-model mean ensemble and individual models (1980-2010).

WAS-22 is -0.18 m/s dec^{-1} for the pre-monsoon (MAM), -0.29 m/s dec^{-1} the monsoon (JJAS), -0.34 m/s dec^{-1} for the post-monsoon (ON), and -0.09 m/s dec^{-1} for the winter season (DJF). The bias in seasonal trends found for WAS-44 are the following -0.22 m/s dec^{-1} for MAM, 0 m/s dec^{-1} for JJAS, -0.51 m/s dec^{-1} for ON, and 0.07 m/s dec^{-1} for DJF. Therefore, WAS-22 outlines more differences with the trends reproduced by ERA5 than WAS-44 as illustrated by the spatially averaged seasonal trends values. The analysis of the spatial pattern of the seasonal trends shows WAS-22 improvements in simulating the seasonal pattern in the west coast during the pre-monsoon season. WAS-44 ensemble estimates the changes occurring during the monsoon season better than WAS-22 and displays a greater similarity with the trends found for ERA5 during the winter season compared to WAS-22.
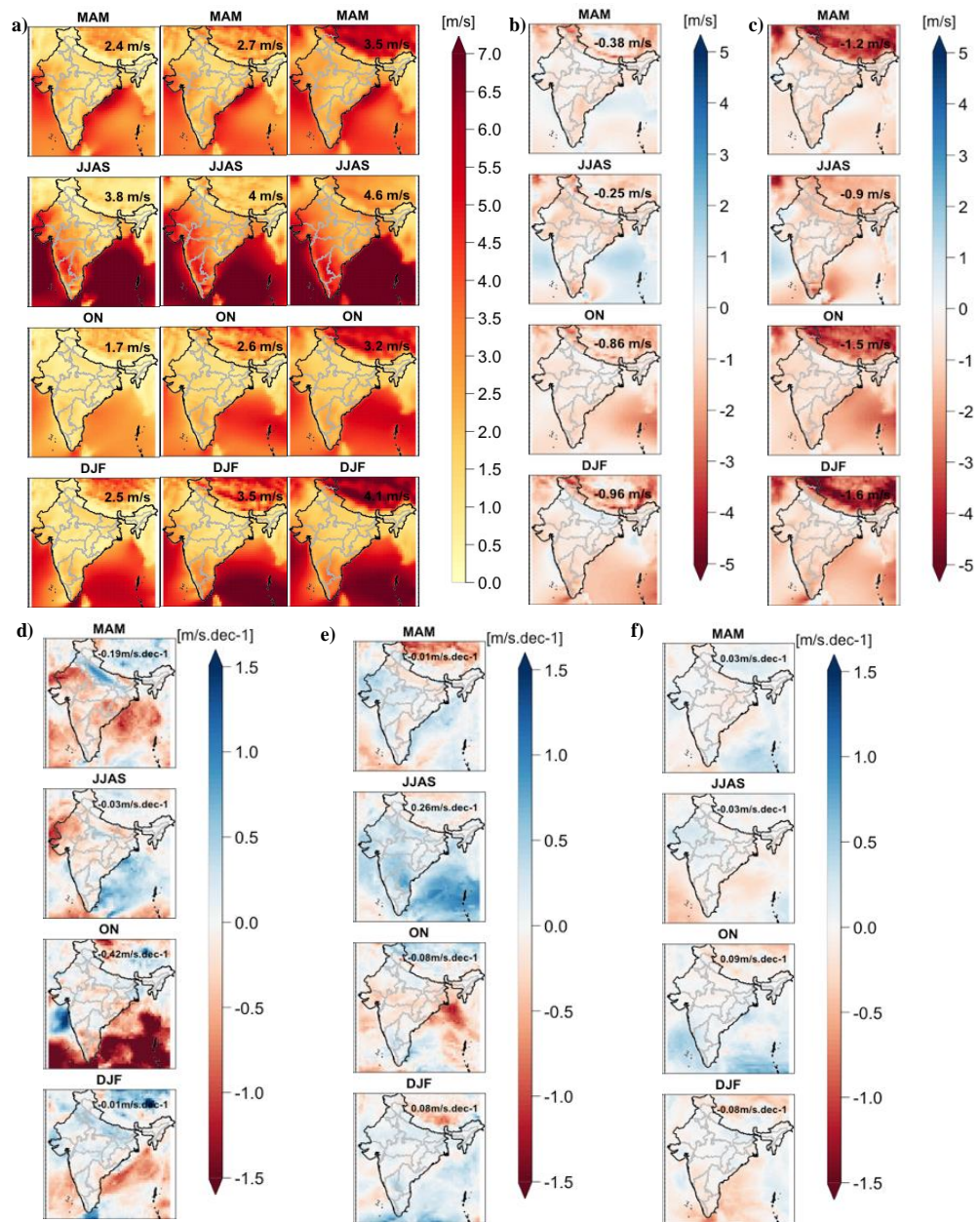
Figure 1.4: Geographical distribution of **(a)** seasonal wind speed for ERA5 (column 1), WAS-22 (column 2) and WAS-44 (column 3), seasonal climatology bias of WAS-22 with ERA5 **(b)**, seasonal climatology bias of WAS-44 with ERA5 **(c)**, seasonal wind speed trends for ERA5 **(d)**, WAS-22 **(e)** and WAS-44 **(f)** (1980-2010).

Chapter 1. Future trends in wind resources and their consistency

Despite having a larger trend bias, WAS-22 simulations add value to the representation of wind speeds from 1980 to 2010 compared to their WAS-44 counterparts in the Indian sub-continent by:

1. Improving the estimation of the annual climatology (difference in long-term annual wind with ERA5 equal to 0.71 m/s for WAS-22 as opposed to 1.40 m/s for WAS-44).

2. Outlining a spatial variability pattern closer to the reference dataset with a similar spatial average.

3. Improving the seasonal mean spatial patterns of wind speeds in regions with complex topography.

4. Simulating more realistically the geographical distribution of the annual wind speed trend and magnitude.

1.3.3 Evaluation of the consistency in the trends

The geographical distribution of wind speed trends from climate projections for RCP 8.5 scenario from 2006 to 2100 is presented in Figure 1.5.
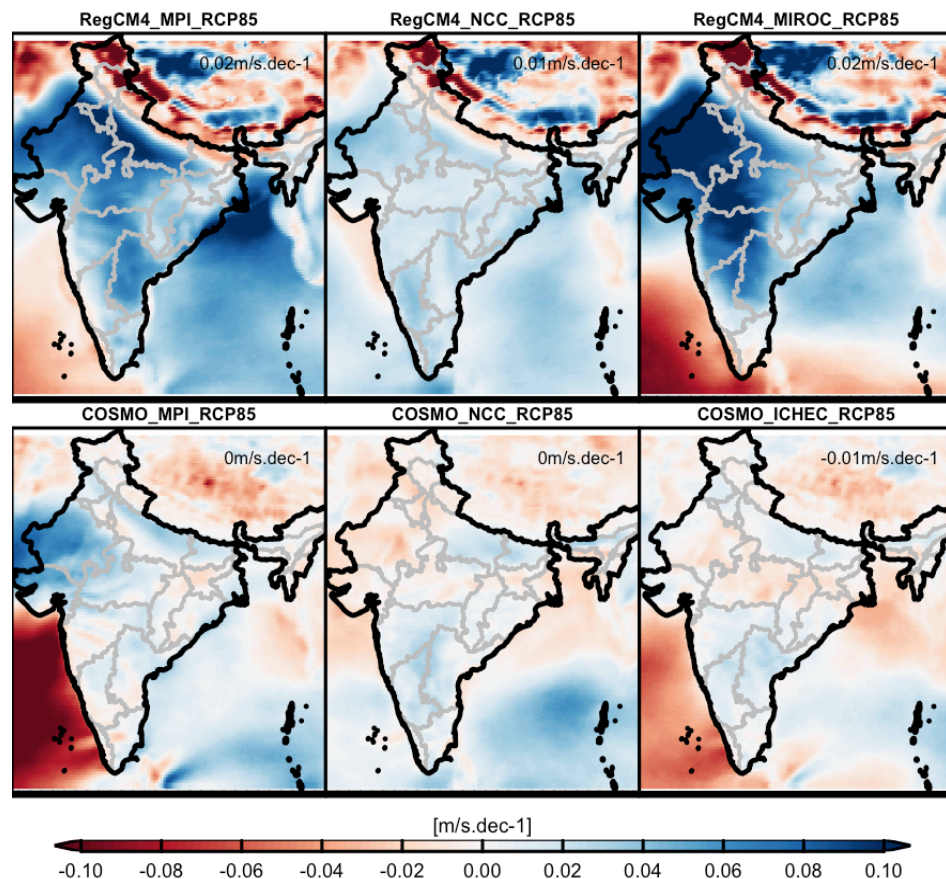
Figure 1.5: Geographical distribution of WAS-22 wind speed trends for climate scenario RCP 8.5 for the period extending (1980-2010).

WAS-22 models shown in Figure 1.5 exhibit a higher agreement among individual models in the projections of future wind speed trends compared to WAS-44 models for the same scenario (RCP 8.5) shown in Figure 1.6.

In what follows, we concentrate on WAS-44 individual models that use a common driving model with WAS-22 experiment and RCP 8.5 scenario to enable a proper comparison. We analyze the consistency of the trends in two selected regions of the domain for the two versions of CORDEX; one sub-domain in the northeastern part of India and another one in central India where we apply the consistency measure discussed in the methods selection to demonstrate its application.

The Northeastern region is characterized by a complex orography and a higher variability compared to other regions in the study area. The central region is selected as another focus region
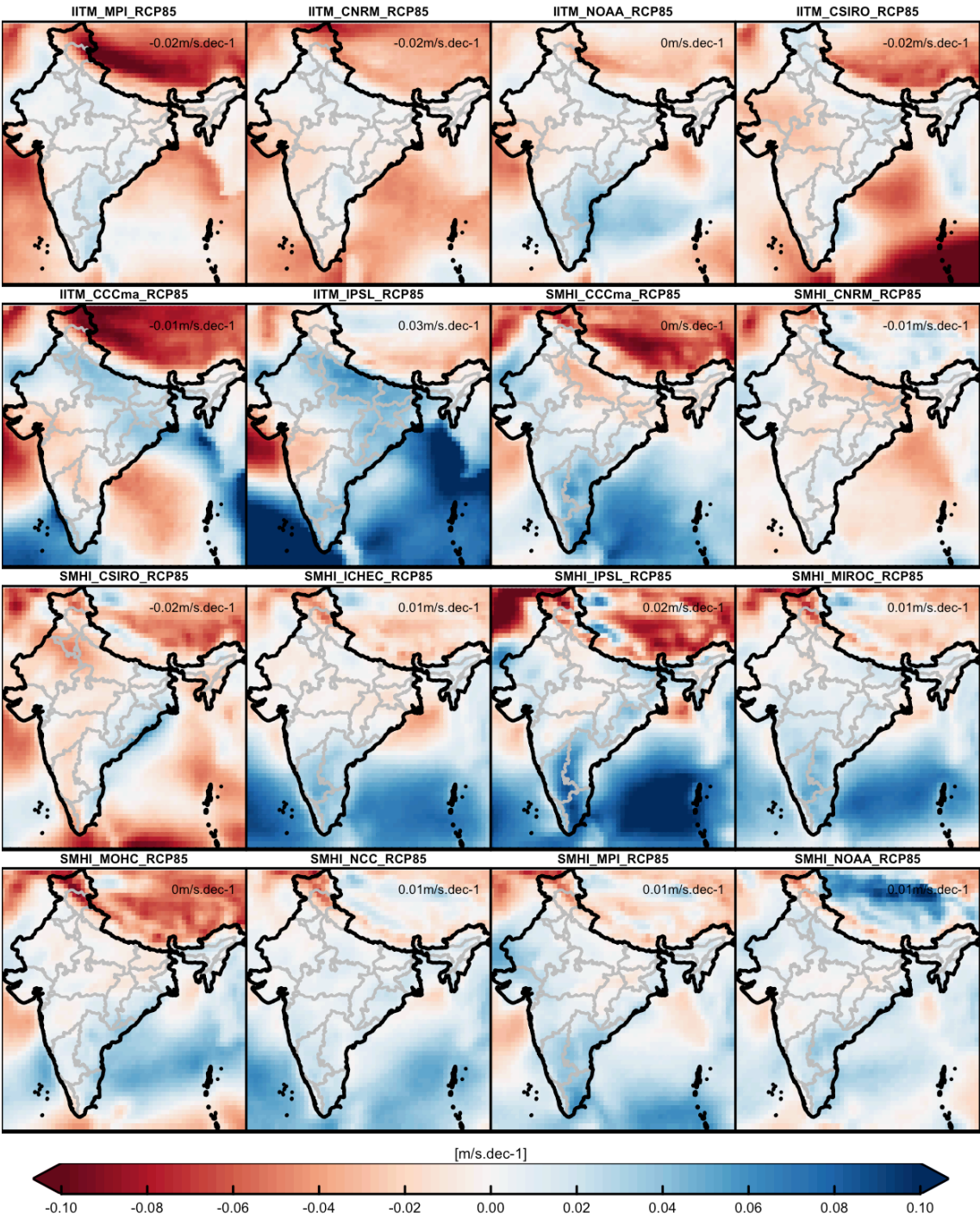
Figure 1.6: Geographical distribution of WAS-44 wind speed trends from climate projections for RCP 8.5 scenario (2006-2100).

and is characterized by a topography that is less complex and where the variability is moderate. Similarly to the previous section, WAS-22 models are down-sampled and interpolated to the same grid spacing of CORDEX WAS-44.

The results of the temporal part of Eq (1.2) for the two regions and the two families of models show a similar parabolic shape of the curve, indicating that the shorter the time slices get, the more considerable variability we find, and the analysis is inconclusive at this point because we are unable to detect any distinctive pattern.

The visualization of the combination of results for both the temporal and spatial terms of Eq (1.2) on a 3D plot is unsatisfactory because the temporal part dominates over the spatial dimension.

We proceed to a separate analysis of the spatial term of Eq. (1.2) and it leads to the unveiling of spatial consistency characteristics as illustrated by the results in Figure 1.7. The spatial consistency range defined in the methods is higher for WAS-22 than WAS-44 in the two regions. COSMO-ICHEC displays the lowest values of $C(\delta x, \delta t = 0)$ among WAS-22 in the two regions, while RegCM4-MPI has the highest values in the northeast and the center and is followed by COSMO-MPI (with a common driving model) in the northeast and RegCM4-MIROC in the other region.

The consistency is interpreted not as a quality check for the models but as a way to measure how trends change as the distance from a specific wind farm changes based on the spatial consistency plot in a specific region.
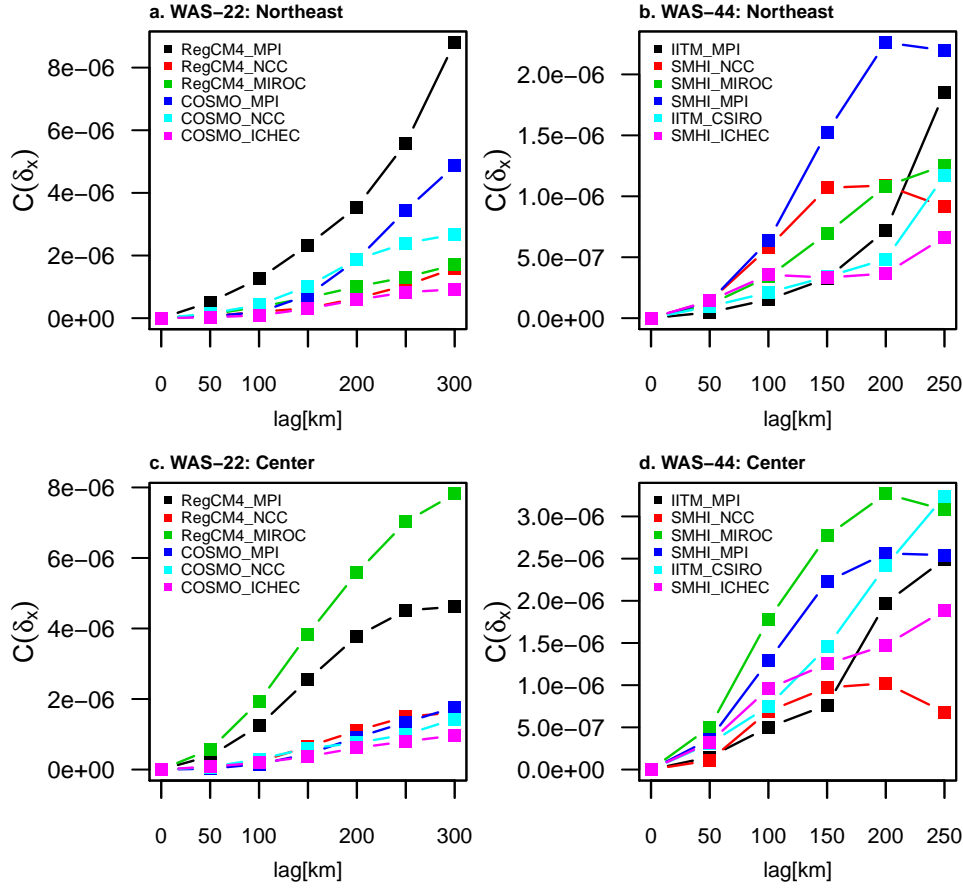
Figure 1.7: Spatial consistency of WAS-22 and WAS-44 individual models in the northeast (a and b) and in the center (c and d).

1.3.4 WAS-22 models comparison with local measurements

Table 1.6 summarizes the results of the correlation and bias analysis for WAS-22 multi-model ensemble mean under RCP 2.6 and RCP 8.5 scenarios in Tejuva, Theni, and Jath with ISD, ERA5 and CLP data.

Table 1.6: Summary of the fraction bias (fBias) and Pearson correlation (P.corr) values of WAS-22 with ISD, ERA5 and CLP data in Tejuva, Theni and Jath.

|	Reference datasets	ISD		ERA5		CLP	
Metrics	**Sites**	**RCP 2.6**	**RCP 8.5**	**RCP 2.6**	**RCP 8.5**	**RCP 2.6**	**RCP 8.5**
	Tejuva	1.25	1.37	1.93	2.05	0.70	0.74
fBias	Theni	3.83	4.96	2.94	3.68	0.71	0.91
	Jath	1.28	1.36	1.80	2.00	0.73	0.75
	Tejuva	0.63	0.65	0.64	0.66	0.53	0.60
P.Corr	Theni	0.22	0.23	0.58	0.60	0.55	0.53
	Jath	0.34	0.42	0.68	0.68	0.59	0.63

The values obtained for RCP 2.6 and RCP 8.5 are close at the three wind farm sites. In Tejuva, the values of the fraction bias of WAS22 models and ISD data are over 1 (1.25 for RCP 2.6 and 1.37 for RCP 8.5) and indicate that WAS-22 models tend to overestimate ISD data. The fraction bias values found in comparing WAS-22 models in Tejuva with ERA5 highlight even higher values (1.93 under RCP 2.6 and 2.05 under RCP 8.5). However, the fBias values obtained in comparing WAS-22 values with CLP farm data show lower values (0.70 for RCP 2.6 and 0.74 for RCP 8.5) and indicate an underestimation. The underestimation is challenging to explain but could be due to the simple projection used to estimate wind speed at hub height. The Pearson correlation coefficient of WAS-22 ensemble mean for RCP 2.6 and RCP 8.6 in Tejuva indicates values from 0.60 to 0.66 in comparing the ISD, ERA5, and CLP data. Therefore, WAS-22 data can acceptably reproduce local wind characteristics in Tejuva (fraction bias not indicating significant differences and good correlation coefficient with the other datasets).

The fraction bias values obtained for WAS-22 in Theni indicate poor scores with values nearly equal to 4 when ISD data are taken as a reference, and one possible explanation for that is the distance between the site and the station leading to significant differences in the wind values. The fraction bias in Theni was obtained for 3.93 when ERA5 is taken as a reference. A bias score lower than one is also found on this site compared to wind farm data. The inability to reproduce local climate indicated by the high overestimation of the wind speeds shown by the results in Theni for the fraction bias comes in line with the poor correlation coefficients found for ISD. The correlation coefficients found for WAS-22 with ERA5 are moderate, with values between 0.59 and 0.60 and slightly lower for CLP data (0.53 and 0.55). The bias results found In Jath show similar trends as Tejuva, with values between 1.28 (for RCP 2.6) and 1.36 (for RCP 8.5) when ISD is taken as a reference, nearly equal to 2 when ERA5 is the reference, and between 0.73 and 0.75 when CLP data are the reference. Regarding the correlation coefficients, low values are found when ISD is the reference (0.34 for RCP 2.6 and 0.42 for RCP 8.5). In Jath, we find stronger values when ERA5 is the reference (0.68) and between 0.59 and 0.63 when CLP data is

the reference. The quality of ISD data varies depending on the location, and further efforts are needed to enhance it. At the three wind farm sites, WAS-22 models have an average correlation of 0.64 with ERA5 and 0.57 with wind farm measurements. ISD measurements and WAS-22 ensemble in Theni and Jath have the lowest correlation. The low correlation coefficients with ISD measurements obtained in Theni (0.22) and Jath (0.38) are attributed to the difference in the local climate because of the considerable distance between wind installation sites and ISD stations (in Table 1.4 the distance is 71 km for Theni and 36 km in Jath in contrast with Tejuva, where the distance between the two is about 1.3 km). This observation emphasizes the limitations faced in validating climate projections linked to the lack of reliable reference data in some locations to evaluate the models. Furthermore, we extend the comparison to the other ISD sites in Table A.2 that shows a similar pattern with correlations averaging 0.36 with ISD measurements and 0.60 with ERA5. For the bias, when ISD data are compared to WAS-22, we found 8 sites where the values do not exceed two and range between 1.08 in Bangaluru and 1.91 in Anantapur.

Figure 1.8 and Figure 1.9 represent standardized monthly wind speeds and the seasonality components obtained with the STL method of WAS-22 (RCP 2.6 and RCP 8.5).

Figure 1.8: Comparison of standardised monthly wind speeds for ISD (dashed black line), ERA5 (brown line) and WAS-22 (green line for the RCP 2.6 ensemble and red line for the RCP 8.5 ensemble) with CLP measurements (dashed green) in Tejuva (top), Jath (middle), and Theni (bottom).

Figure 1.8 shows that the WAS-22 RCMs are not able to match exactly the measurements at the three locations. The plots indicate that the RCMs follow closely ERA5 data. In Tejuva, the pattern of ISD and CLP measurements overlaps with the two reanalysis datasets and WAS-22

models. On the other hand, the overestimation of ISD and ERA5 by climate models indicated by the fBias values is corroborated by the normalized wind speeds comparison in Theni and Jath (Figure 1.8).

The seasonal cycle analysis demonstrates the WAS-22 performance in reproducing the seasonal patterns at the three sites 1.9. Hence, the strong correlation values discussed earlier are attributed to the seasonality. A close look at the results indicates a mismatch in the short and medium-term time evolution of wind speeds reported by the local measurements and the simulations. This discrepancy between observations and model projections is explained by low-frequency climate modes playing a large role in the observations and not being well reflected in the climate models [174]. In conclusion, WAS-22 models cannot exactly reproduce local observations and cannot accurately predict the real climate variability for the period analyzed (the short-span of the comparison period with the observations is one explanation of that). However, WAS-22 models can be trusted with respect to their mean trend prediction, which will be looked at in the following subsection.
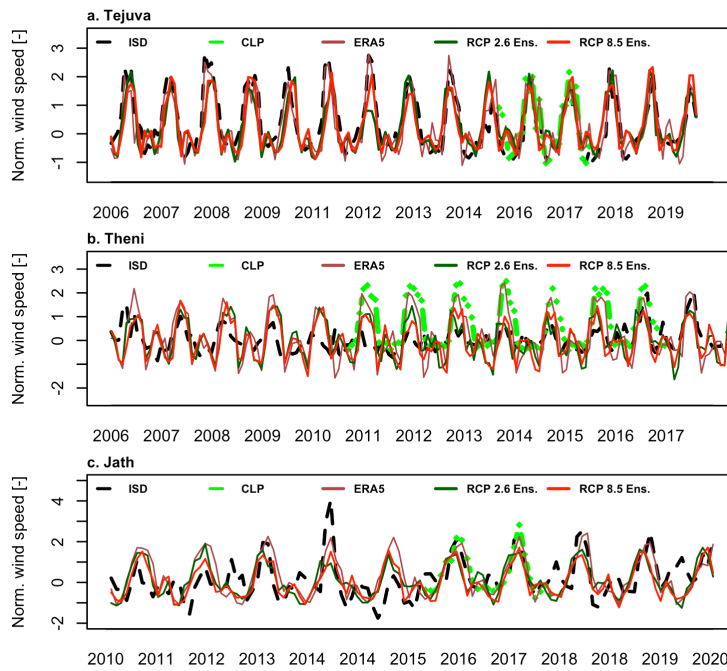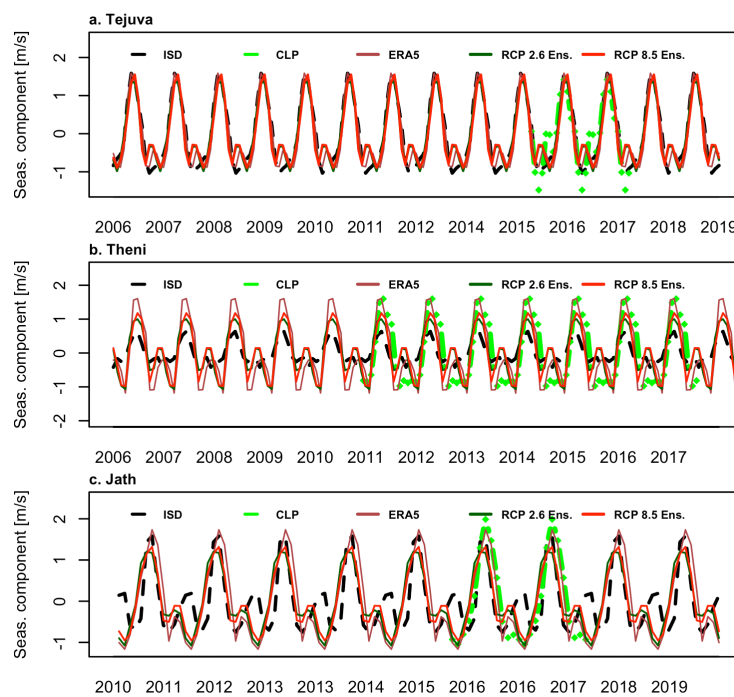

Figure 1.9: Comparison of the seasonality signal of monthly winds for ISD (dashed black line), ERA5 (brown line) and WAS-22 (green line for the RCP 2.6 ensemble and red line for the RCP 8.5 ensemble) with CLP measurements (dashed green) in Tejuva (top), Jath (middle), and Theni (bottom).

1.3.5 WAS-22 projections annual trends in the Indian sub-continent

We divide the study area into five sub-domains and analyze the annual trends in each one of them for the full length of the climate projections (2006-2100) for the two ensembles of RCP scenarios. The latitude and longitude ranges of the five sub-domains are summarized in Table 1.7.

Table 1.7: Sub-domains definition.

Sub-domains	Latitude range	Longitude range
North-west (N-W)	23°N to 30°N	68°E to 80°E
Top-north (T-N)	30°N to 36°N	74°E to 80°E
Center	18°N to 23°N	73°E 80°E
East	18°N to 26°N	80°E to 88°E
South	8°N to 18°N	74°E to 80°E

From 2006 to 2100, we detect almost no change in annual trends in the five study regions for the low-end scenario (see Table 1.8). For the other scenario, we find 0.04 m/s per decade ($\pm 8\%$) in the north-west, 0.03 m/s per decade ($\pm 11\%$) in the center, 0.02 m/s per decade ($\pm 19\%$) in the east, and the standard deviation is higher than the mean in the top-north which indicates that it is not significant. The results remain valid by recalculating the trends in these three sub-domains for two times periods; the period starting five years after 2006 and extending to 2100, and the period starting in 2006 and ending five years before 2095 [175]. While the magnitude of the changes seems low, it can have an impact on wind energy generation because of the cubic relationship between wind speed and power production. The trends found in the top-north and south reflect a high uncertainty $\pm 44\%$ in top-north and $\pm 64\%$ in the south due to the complexity of the climate in those regions.

Table 1.8: WAS-22: Area-averaged mean annual trends and standard deviation (SD) for the period 2006-2100 (*indicates trends with a RSD value higher than 1).

Scenarios	RCP 2.6		RCP 8.5	
Regions	Mean	SD	Mean	SD
N-W	*0.00**	0.00	0.04	0.00
T-N	*-0.01**	0.01	-0.02	0.01
Center	*0.00**	3.10×10^{-3}	0.03	3.10×10^{-3}
East	*0.00**	3.10×10^{-3}	0.02	3.10×10^{-3}
South	*0.00**	5.30×10^{-3}	0.01	5.30×10^{-3}

The individual trends results for each model output (Table A.3 and Table A.4) show that the uncertainty for RegCM4 models family under RCP 8.5 scenario is always smaller than for COSMO ones.

Consistently with the analysis of the spatial average per region, the visual inspection of the geographical distribution of the annual trends of RCP 2.6 scenario results as shown in Figure 1.10 shows almost no significant change. The results for RCP 8.5 scenario in Figure 1.10 indicate

an increase in the western part of India, including some parts of the north. This result remains valid after filtering out wind speeds lower than 2 m/s to verify that the areas of positive trends are reflecting regions with exploitable wind resources.
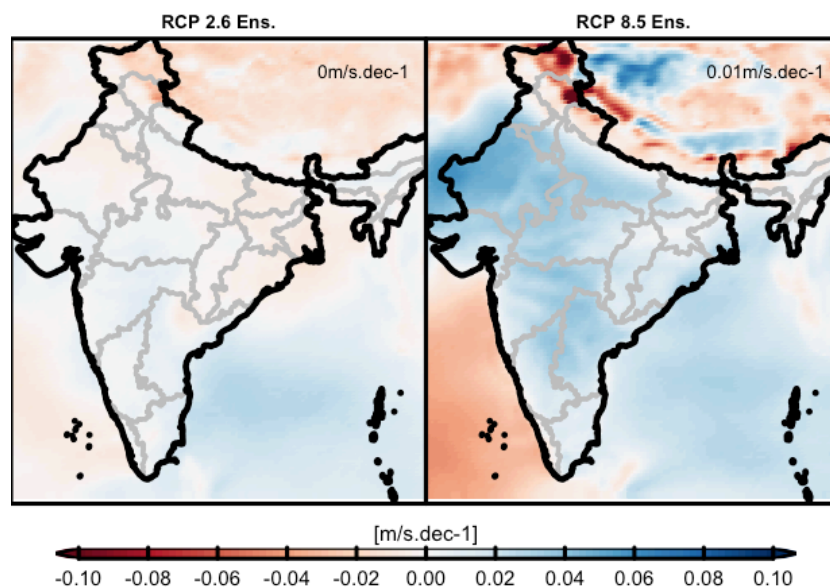
Figure 1.10: Geographical distribution of WAS-22 ensemble annual trends for climate change scenario RCP 2.6 (left) and RCP 8.5 (right) (in m/s per dec.) from 2006 to 2100.

Within each RCM family, RegCM4, on the one hand, and COSMO, on the other hand, we notice that the magnitude of wind speeds reproduced by the models is proportional to parent GCMs temperature sensitivity. In fact, the highest trends magnitude are found for the models with parent GCMs with the highest temperature sensitivity (MIROC-MIROC 5 high sensitivity, followed by MPI-ESM-MR and ICHEC-EC-Earth, medium sensitivity model, and finally, Nor-ESM-NCC with the lowest sensitivity; https://cordex.org/experiment-guidelines/cordex-core/cordex-core-simulation-framework/). The temperature sensitivity of the parent GCM impact on the magnitude of wind speed trends was also discussed by [176]. In what follows, we assess the evolution of the annual trends during two periods of 30 years between 2025 to 2055 and 2065 to 2095.

The results of the spatial average for the five sub-domains defined earlier are presented in Table 1.9. No trends are distinguished during the first period, and uncertainty values found exceed the value of the mean for the two RCP scenarios. From 2065 to 2095 under RCP 8.5 scenario, we find an increase of 0.05 m/s per decade ($\pm$48%) in the north-west, and 0.04 m/s per decade ($\pm$48%) in the east. Uncertainty values found elsewhere exceed $\pm$80% and are not discussed.

Table 1.9: WAS-22 ensemble: Area-averaged mean annual trends and standard deviation (SD) periods 2025-2055 and 2065-2095 (*indicates trends with a RSD value higher than 1*).

Periods	2025-2055				2065-2095			
Scenario	RCP 2.6		RCP 8.5		RCP 2.6		RCP 8.5	
Regions	Mean	SD	Mean	SD	Mean	SD	Mean	SD
N-W	*-0.01**	0.02	*-0.01**	0.02	-0.03	0.022	0.05	0.02
T-N	*-0.01**	0.04	*-0.02**	0.037	*0.00**	0.021	*0.00**	0.021
Center	*-0.01**	0.01	*0.00**	0.01	-0.02	0.01	*0.00**	0.01
East	*-0.01**	0.03	*-0.01**	0.03	*-0.02**	0.02	0.04	0.02
South	*-0.01**	0.03	*0.00**	0.03	*-0.01**	0.02	-0.03	0.02

The visual inspection of the spatial distribution of the annual trends for the RCP 8.5 ensemble during the first period displays increasing trends in the Andhra Pradesh, and Tamil Nadu states close to Theni and almost no change in trends throughout the rest of the Indian territory. For the long-term future, the same analysis reveals negative trends in some parts of Tamil Nadu in the south, mild positive trends in the northeast (south of Odisha), and high positive trends in the north toward the south of Nepal along a region extending from the south of Bihar, across Uttar Pradesh reaching the south of Punjab.

1.3.6 Seasonal trends

Wind speed seasonality affect wind energy planning because of its impact on wind operations; wind turbines schedule optimizes harvesting energy when winds are high and shutting them down when they are not.

Well aware of the diversity of the impacts and their dependence on the local geographical specificities, we discuss hereafter in more detail the geographical distribution of the seasonal wind speed trends in the Indian subcontinent for the climate projections with a focus on the RCP 8.5 scenario. To extract information useful for wind energy development, we look at the significant seasonal trends for the full length of climate projections and focus on wind speeds higher than 2 m/s. In Figure 1.11, we can see that significant positive trends of up to 0.15 m/s per decade are expected throughout all parts of the Indian lands during the pre-monsoon season. The monsoon winds are projected to increase in India's Northwestern parts and the parts of the east distant from the coast with a magnitude ranging from 0.025 to 0.075 m/s per decade. No significant change in trends is found for the winter season. In a similar fashion to the future annual trends, we analyze the spatial average of the seasonal trends for the full length of WAS-22 projections in five regions of the Indian sub-continent under both RCP scenarios in Table 1.10. The results for RCP 2.6 scenario indicate no significant change in trends, except in the center,
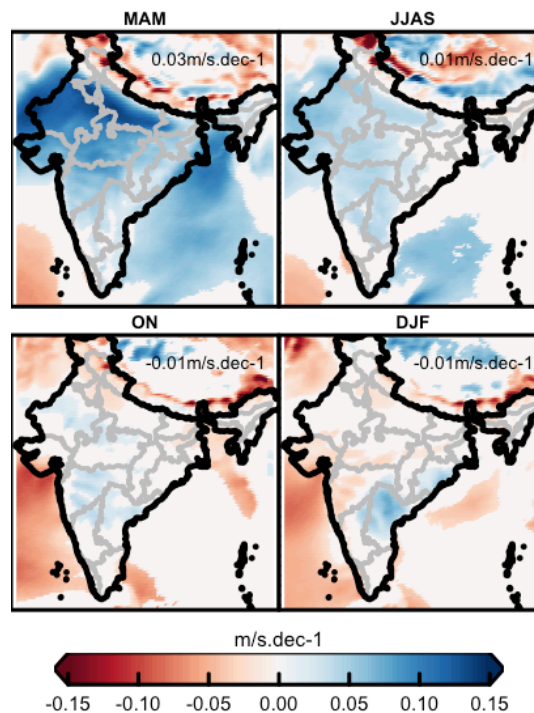
Figure 1.11: Geographical distribution of WAS-22 ensemble seasonal trends for climate change scenario RCP 8.5 (2006-2100).

where there is a increase of 0.1 m/s yet the uncertainty is large ($\pm62\%$). In the five sub-domains, we find an increase in trends of 0.1 m/s per decade $\pm7\%$ during the pre-monsoon season under RCP 8.5 scenario. In the north-west, we find an increase in monsoon winds of 0.01 m/s per decade ($\pm23\%$). In the center, results indicate an increase equal to 0.04 m/s per decade $\pm20\%$ during the monsoon and the post-monsoon, and a decrease of -0.01 m/s per decade during the winter season, but the uncertainty is large ($\pm51\%$). In the east, the main change in trends occurs during the monsoon season with a magnitude of 0.02 m/s per decade ($\pm53\%$). The results also indicate a decrease in monsoon wind in the top-north (-0.04 m/s), and similarly to the annual trends, the uncertainty in this particular region is large ($\pm48\%$). The trends discussed are robust to the sensitivity analysis conducted by calculating the trends during the two periods (2011-2100) and (2006-2095). Looking at the seasonal trends results of WAS-22 projections under RCP 8.5 scenario, we find that change in wind speeds occur mainly during the pre-monsoon, and the highest trends occur during the monsoon period. Similarly to other regions in South Asia, India, the monsoon season carries massive winds to the Indian subcontinent, and is intensely sensitive to climate change [177].

Table 1.10: Area-averaged mean seasonal trends [m/s per decade] and standard deviation (SD) of 2006-2100. MAM: months from March to May (pre-monsoon), JJAS: months from June to September (monsoon), ON: months of October and November, DJF: months from December to February (winter) (*indicates trends with a RSD value lower than 1).

Seasons	MAM				JJAS				ON				DJF			
Scenarios	RCP 2.6		RCP 8.5		RCP 2.6		RCP 8.5		RCP 2.6		RCP 8.5		RCP 2.6		RCP 8.5	
Regions	Mean	SD	Mean	SD	Mean	SD	Mean	SD	Mean	SD	Mean	SD	Mean	SD	Mean	SD
N-W	0.01*	0.01	0.10	0.01	-0.01*	0.10	0.01	0.10	0.01*	0.01	0.00*	0.01	0.00*	0.01	-0.01*	0.01
T-N	0.01*	0.01	0.10	0.02	-0.02*	0.02	-0.04	0.02	-0.01*	0.01	-0.02*	0.01	-0.01*	0.01	0.01*	0.01
Center	0.01*	0.01	0.10	0.01	0.01	0.01	0.04	0.01	0.01*	0.01	0.04	0.01	0.00*	0.00	-0.01*	0.00
East	0.01*	0.01	0.10	0.01	-0.01*	0.01	0.02	0.01	0.00*	0.01	0.00*	0.01	0.00*	0.00	0.00*	0.00
South	0.01*	0.01	0.10	0.01	0.02*	0.02	0.01*	0.02	0.01*	0.01	0.00*	0.01	0.00*	0.01	0.00*	0.01

We analyse the projections of the seasonal trends during the near-term future (2025-2055) (Table 1.11) and the long-term future (2065-2055) (Table 1.12) to understand the evolution of the seasonality throughout the century. Analogously to the results found for the full length of climate models projections, wind speeds increase in all five sub-domains with a magnitude of 0.01 m/s per decade ±7% under RCP 8.5 scenario in the near and long-term future. In the near future, we detect a decrease in monsoon winds in the north-west with a magnitude of nearly −0.3 m/s per decade under both RCP scenarios, and in the center by the same magnitude under RCP 8.5, although the standard deviation value is nearly 63% of the trend found. The results for the 30 years between 2065 to 2095 indicate an increase during the pre-monsoon in all the regions. Monsoon winds increase by 0.01 m/s per decade (30%) in the north-west and 0.2 m/s per decade (±49%) in the center and by 0.5 m/s per decade (±31%) in the east. Although the understanding of the interplay between climate change and monsoon patterns has not yet been fully addressed ([178], [177]), analysis of future precipitation from CORDEX models indicated that an intensification of the Indian Ocean Dipole in the future would enhance the monsoon throughout India and the increase in wind speed as reflected by our results. [179] found that RegCM4, even at a lower resolution in CORDEX WAS-44 at 50 km, was able to reproduce the seasonal circulation pattern over South Asia, including the evolution of monsoonal pattern, which increases confidence in WAS-22 models with their higher spatial resolution.

Table 1.11: Area-averaged mean seasonal trends [m/s per decade] and standard deviation (SD) of 2025-2055 (*indicates trends with a RSD value higher than 1).

Seasons	MAM				JJAS				ON				DJF			
Scenarios	RCP 2.6		RCP 8.5		RCP 2.6		RCP 8.5		RCP 2.6		RCP 8.5		RCP 2.6		RCP 8.5	
Regions	Mean	SD	Mean	SD	Mean	SD	Mean	SD	Mean	SD	Mean	SD	Mean	SD	Mean	SD
N-W	0.01*	0.01	0.10	0.01	-0.30	0.10	-0.26	0.10	0.01*	0.12	0.09*	0.12	0.09*	0.15	0.06*	0.15
T-N	0.01*	0.01	0.10	0.15	-0.14*	0.15	-0.07*	0.15	0.09*	0.28*	0.05	0.28*	-0.06	0.17*	-0.11*	0.17
Center	0.01*	0.01	0.10	0.01	-0.08*	0.17	-0.27	0.17	-0.07*	0.16	-0.12*	0.16	-0.13*	0.15	0.10*	0.15
East	0.01*	0.01	0.10	0.01	-0.29*	0.31	-0.13*	0.31	0.00*	0.14	-0.09*	0.14	-0.08*	0.09	0.12*	0.09
South	0.01*	0.01	0.10	0.01	0.31*	0.25	0.12*	0.25	-0.30*	0.23	-0.50	0.23	-0.10*	0.15	0.24*	0.15

Table 1.12: Are-averaged mean seasonal trends [m/s per decade] and standard deviation (SD) of 2065-2095 (*indicates trends with a RSD value higher than 1*).

Seasons	MAM				JJAS				ON				DJF			
Scenarios	RCP 2.6		RCP 8.5		RCP 2.6		RCP 8.5		RCP 2.6		RCP 8.5		RCP 2.6		RCP 8.5	
Regions	Mean	SD	Mean	SD	Mean	SD	Mean	SD	Mean	SD	Mean	SD	Mean	SD	Mean	SD
N-W	*0.01**	0.01	0.10	0.01	*-0.01**	0.10	0.01	0.10	*0.01**	0.13	*0.17**	0.13	*0.15**	0.14	*0.01**	0.14
T-N	*0.01**	0.01	0.10	0.21	*0.06**	0.21	*0.13**	0.21	*0.15**	0.17	*0.02**	0.17	*-0.30**	0.39	*-0.08**	0.39
Center	*0.01**	0.01	0.10	0.01	*-0.14**	0.12	0.24	0.12	*-0.11**	0.11	*0.15**	0.11	*0.12**	0.10	*0.06**	0.10
East	*0.01**	0.01	0.10	0.01	*-0.01**	0.14	0.46	0.14	*-0.27**	0.28	*0.23**	0.28	*0.15**	0.21	*-0.02**	0.21
South	*0.01**	0.01	0.10	0.01	*0.06**	0.17	*-0.14**	0.17	*-0.23**	0.27	*0.00**	0.27	*0.21**	0.24	*0.17**	0.24

1.4 Discussion

The release of the latest version of the CORDEX experiment for South-Asia, WAS-22, provides a valuable opportunity to investigate the future of wind speeds in the Indian subcontinent with high-resolution RCM projections. While CORDEX WAS-22 high resolution shall represent better the local physics and the spatial variability, various studies indicated that the ability to downscale to higher resolution does not necessarily imply increased model accuracy or reduced model bias 884073:20334651. Hence, we verify the improved performance of WAS-22 against the previous WAS-44 version at a lower resolution and compare its consistency in two regions with different spatial characteristics. We find that WAS-22 outperforms WAS-44 models by reducing the bias in annual and seasonal climatology and simulating the seasonal pattern extracted from reanalysis datasets for a reference period extending from 1980 to 2010. WAS-22 ensembles are also characterized by a higher agreement in the projections among the individual RCMs compared to WAS-44 projections. The use of a spatio-temporal consistency measure helped compare WAS-22 and WAS-44 differences quantitatively. The analysis of the temporal part of the equation was, in this case, inconclusive. Comparing the $C(\Delta x, \Delta t = 0)$ values of the two experiments in the two regions by quantifying the average range distance at which 50% of the maximum value is reached indicates a higher value for WAS-22 models and a higher consistency across models. The application of this metric is preliminary in this study; we suggest exploring it further in future work; the shape of the curve of $C(\Delta x, \Delta t)$ in a particular region could serve for wind planners addressing decision-making purposes to investigate how trends values change as a function of the distance from the wind sites.

We find a strong correlation between WAS-22 outputs, reanalysis datasets, and local measurements, which is primarily credited to their performance in reproducing the seasonal cycle. The long distance between the reference sites and ISD stations explains the low correlation between WAS-22 models and ISD measurements in Theni and Jath, where they are far from each other. ISD measurements highlighted quality limitations, as illustrated by their discrepancies with other reference datasets in some of the sites analyzed and the short-span of the data available. Therefore, model evaluation challenges remain, and further efforts are needed to improve access to readily accessible local wind measurements. Nevertheless, the comparison with local wind data confirms the good performance of WAS-22 in reproducing the local variability and the seasonal wind cycle, making them a valuable source of information to understand future wind patterns. We obtained estimates of wind speed trends under future climate change scenarios and analyzed their spatial

distribution in the Indian-subcontinent. The analysis of the full length of WAS-22 projections reveals that nearly no significant annual trends are detected in the Indian sub-continent under the low emission scenario RCP 2.6. The results of the same analysis under RCP 8.5 scenario indicates positive trends in the north-west (0.04 m/s per decade ($\pm 8\%$)), the center (0.03 m/s per decade ($\pm 11\%$)) and the east (0.02 m/s per decade ($\pm 19\%$)). In some regions, the complex topography impacts the trends calculated, as shown by the large uncertainty values obtained in these regions (top-north close the Himalayas and the south). We verify that the increase in annual wind speed concerns winds higher than 2 m/s and is more pronounced towards the long-term future as revealed by the results of the annual trends between 2065 and 2095, especially in the north-west (0.05 m/s per decade ($\pm 48\%$)) and the east (0.04 m/s per decade ($\pm 48\%$)). Our results align with other climate studies highlighting differences among warming scenarios being more pronounced towards the end of the century than at mid-century [180].

The analysis of seasonal trends under the RCP 2.6 scenario indicates nearly no significant change (except an increase in the center during the monsoon). For RCP 8.5, seasonal changes are detected throughout the domain studied and are often occurring during the pre-monsoon (an increase of 0.1 m/s per decade ($\pm 7\%$) throughout the five sub-regions) and monsoon seasons. Seasonal variations impact electricity production and their prediction is essential for the future of wind energy. Monsoon changes could have various socio-economic impacts, particularly in the southern and western parts of the Indian sub-continent, where most wind farms are currently deployed [181]. The seasonality analysis of the full length of WAS-22 projections predicts monsoon winds increase in the north-west (0.01m/s per decade ($\pm 23\%$), the center (0.04 m/s per decade $\pm 20\%$), and the east (0.02 m/s per decade ($\pm 53\%$)). The trend of the monsoon winds in the top-north reveals the opposite direction of the change with a -0.04 m/s per decade. Thus, while significant perturbations often occur during the pre-monsoon, the highest ones happen during the monsoon season, emphasizing monsoon sensitivity to climate change. Between 2025 and 2055, under RCP 8.5, we detect a decrease in monsoon winds with a magnitude of nearly -0.3 m/s per decade in the north-west (under both RCP scenarios) and the center. Between 2065 and 2095, we find an increase during the pre-monsoon in all five regions, and during the monsoon in the north-west (0.01 m/s per decade ($\pm 30\%$)), the center (0.2 m/s per decade ($\pm 49\%$)) and even most notably in the east (0.5 m/s per decade ($\pm 31\%$)).

Previous studies in India enhance confidence regarding north-west trends found. For example [148], using lower resolution RCMs, found that wind speeds along the northwestern coastline had high accuracy. No significant changes are found for the winds during the winter season. The results for the south need further investigation, and [148] concluded that most RCMs fail to simulate the wind along the southwestern coastline because of the very high variability caused by the southwest monsoon. Despite model improvement and the ability to represent more processes in greater detail with higher resolution, the regional models used in CORDEX have only the land surface component. The atmosphere-ocean coupling is still missing, which is probably one factor that hinders more accurate simulations, particularly close to the coast.

Our work drives more collaboration between the climate research community and the wind industry and intends to push forward the practical use of climate models in investment and planning decisions and support wind energy stakeholders in anticipating wind speed changes.

1.5   Conclusion

This work assesses WAS-22 models and their predecessors, WAS-44, comparing them with local measurements and reanalysis datasets, ERA5 and MERRA2. The comparative results indicate the improved performance of WAS-22. Furthermore, a method to quantify wind speed trends consistency is developed and applied to WAS-22 and WAS-44 models. We also examine the differences in normalized winds and seasonal trends of WAS-22 monthly outputs with ERA5 and wind farm measurements at existing wind energy sites. Ultimately we analyze long-term wind speed annual and seasonal trends using WAS-22 monthly projections over the Indian sub-continent. From the analysis, it is clear that under climate change scenario RCP 8.5, future changes indicate increasing patterns in some locations. Promoting climate models into decision-making tools may be beneficial both from an energy policy point of view since an exacerbation of climate change impacts in the Indian sub-continent is expected. In future work, the availability of downscaled CMIP6 models would enable us to revise our conclusions.

2 Assessment of climate change and climate-resilient wind and solar assets

Background This chapter is adapted from a published manuscript. The information included in the supplementary material is not presented and can be accessed in the published version.

Manuscript information

Title: Climate Change Impact Assessment for Future Wind and Solar Energy Installations in India.

Authors: Zakari Yasmine, Vuille François and Lehning Michael.

Journal: Frontiers in Energy Research.

Status: Published in 2022.

Contributions: Conceptualization, data collection and analysis, visualization, manuscript writing (original draft, review and editing).

DOI: 10.3389/fenrg.2022.859321

2.1   Introduction

India is favored with an abundance of wind and sunlight availability across most of its geography with wind-rich regions in the south and west [182], and promising locations for solar energy in the south [183] but even more so - largely untapped - in the mountains [184]. Wind and solar energy offer benefits in mitigating greenhouse gas emissions and increasing energy security. Frequent and severe heatwaves, heavy rainfall events, and rising sea levels are among the foreseeable natural disasters mainly due to climate that India is already witnessing today [185]. Global climate models (GCMs) within the Coupled Model Inter-comparison Project Phase 5 (CMIP5) and CMIP6 (latest simulations) predict an increase in monsoon precipitation and variability in the future with climate change [47], [49]. In order to avoid these dramatic consequences predicted by climate models, the government of India has publicized striving plans for renewable energy deployment to decarbonize its energy production [86]–[90], [186]. The aggressive renewable energy policies of India combined with its huge renewable resource potential favor a fast growth in wind and solar power generation throughout the country. India aims at reaching a target of 450 Gigawatts of renewable capacity by 2030 [31], which represents many opportunities for investors, as wind and solar are excepted to cover a substantial portion of India's future demand for electricity [97]. The decarbonization of the power sector in India faces numerous risks adding to the complexity of facing the threat of climate change. [187] assessment of recent wind policy development in India highlights that the slowing growth in wind energy development observed since the beginning of the global pandemic can hinder its renewable energy ambitions.

Besides their intrinsic variability and seasonal disparity, wind and solar energy are also sensitive to climate. The variability of the monsoon under future climate conditions is a crucial factor likely to impact wind energy production [182], [188]. [189] and [190] provide an exhaustive overview of climate change impacts on wind energy production. [25] identify a decrease in wind energy at the global scale under the influence of future global warming. These studies conclude that climate change affects wind production via changes in daily and seasonal distribution of wind speed and temperature. These changes may be caused by large-scale circulation and seasonal patterns such as El Nino Southern Oscillation or local land-use changes including urbanization and deforestation [191]. India has experienced a depression in monsoon circulation, and a delay in monsoon onset because of the Indian Ocean warming as a result of increased greenhouse gases and changes to the regional aerosol emissions [192], [193]. During the last decades of the twentieth century, wind resources in India were affected by the stilling effect, a decrease in wind speeds, also reported at the global level [194]. This stilling, or reduction in wind power potential, is attributed to an increase in temperatures in the Indian Ocean [195]. [196] warn about the possibility of a shortening of the monsoon season in the future. This shortening could hinder wind energy production in the regions where most of the production relies on monsoonal winds. Hence, it is beneficial to examine the effects of changing climatic conditions on current and future wind sites.

Climate change impacts the quantity of solar radiation reaching the surface of the planet driven by the change of radiation as a result of changes in the snow cover and cloudiness [197]. The

factors that impact solar Photo-Voltaic (PV) production and can be aggravated by climate change are surface temperatures, solar irradiation, wind speed, and changing concentrations of dirt, dust, snow, and atmospheric particles [79], [198]. Monsoon anomalies can provoke extreme weather events [199], also likely to impact PV power output [64]. Solar radiation has not remained constant over the past decades in India [200]. [201] describe the occurrence of the solar dimming phenomenon which is the systematic reduction of solar radiation reaching the ground in the cities of Jodhpur, New Delhi, Nagpur, and Kolkata up to 2003, while solar brightening (increase of solar radiation reaching the ground) was observed in some other regions since 1990 driven by the efforts to reduce pollution. Project developers need to be wary of such phenomena even though reductions in the amount of solar radiation received do not necessarily imply decreases in solar energy production because the later depends mostly on changing temperatures [202].

The scientific community quantifies climate change impacts on wind and solar power generation in various regions. [190] reviews most relevant studies that present quantitative results. As an example, regional assessments in Asia indicate that wind energy density throughout the twenty-first century is projected to decline in Taiwan, and slight wind variations are expected in China [95]. [182] use East Asia CORDEX simulations to study changes in wind resources availability in India and China to assess projected changes under climate change scenarios and find an overall decline of two percent in the annual generation potential of India up to the year 2060. [182] do not include the projections for solar potential which is another renewable energy source subject to regional climate changes and key to a successful energy transition. We demonstrate that wind projections from climate models indicate an increase in some parts of India, triggering more enthusiasm for wind development in the northwest of the country [129]. Solar PV output is estimated to decrease in large parts of the world due to global warming and decreasing all-sky radiation over the coming decades. Positive trends in solar PV are expected in regions where the cloud cover decreases substantially, or clear-sky radiation increases [203].

RCMs are the most modern tool for projecting climate conditions in specific areas [204]. Estimates of future changes in climate are expressed in terms of mean changes [205], or predictions of future trends in wind speeds, temperature and radiation. These estimates can also be converted to impacts such as changes in energy production. Despite the engagement of the climate modeling community for RCMs improvements [66], the uncertainty of the trends predicted by climate models can be high. In Chapter 1, we studied trends in wind alone for CORDEX WAS-22 projections in India under climate change scenarios and found that some of the trends were highly uncertain. The availability of a large number of climate projections enables to produce multi-model ensembles (MME) that can be exploited to assess mean changes in climate over different time periods and related uncertainties. [206] indicates that projections are considered to be robust when the magnitude of change is smaller than the associated uncertainty. Uncertainty assessments in regional climate projections range from methods based on simple agreement heuristics to characterize positive or negative trends in a climate variable from different RCMs, quantitative uncertainty estimates based on the median and inter-model range of a variable across a series of model projections, to attaching probabilities to a group of scenarios on a regional scale [207].

The sources of uncertainty in climate projections are scenario uncertainty, model diversity and inherent natural variability. Their quantification in ensembles of climate projections supports the understanding of where targeting efforts to reduce them [208]. The methods to characterize the different sources of uncertainty associated with the projections of climate variables include advanced Bayesian analysis of variance (ANOVA) [209], and QUALYPSO [205] which is another statistical approach to calculate the total uncertainty of projections. These methods are computationally expensive and time-consuming procedures. Therefore, although the partitioning of uncertainty sources increases understanding of the future role of climate change in India, its study is beyond the scope of this article and will be in the focus of our future research.

The perceived inaccuracy of climate models has so far limited their consideration in strategic planning. That being said, it suggests that to encourage their adoption, risk-averse decision-makers could benefit from planning tools that reduce uncertainty [101]. Portfolio theory is one these tools and diversifies investments between multiple assets (things in which one could invest) to reduce uncertainty in total future returns with minimized loss in the expected value of returns [210]. [102] use mean-variance analysis in Italy to show the benefits of spatial diversification. The spatial diversification means that the variability may be partly mitigated by aggregating the production from different sources and sites at different places. [103] used the same framework to optimize the geographical location of wind and solar portfolios in China and reduce the variability which limits the use of storage in the system. In this study, we suggest the adaptation of portfolio theory to use it as a tool to reducing the uncertainty of climate predictions when the impacts are converted to energy estimates.

Solar and wind resources are often negatively correlated in space and time [102], [103]. Combining the energy production from wind and solar sources reduces the variability in the power supply thanks to the balancing between meteorological variables. [184] demonstrate that skillfully complementing and coordinating renewable energies over large regions in Switzerland can smoothen intermittencies by reducing correlations among generators and consumers. It shows that optimizing the spatio-temporal variability of wind, solar, and hydropower reduces storage needs and fits the local demand. The southwestern monsoon and the annual solar cycle drive the variability in wind and solar energy in India. Peak wind resources occur during the monsoon season, precisely when the cloud cover affects solar PV production. Solar energy, on the other hand, peaks during the summer precisely when wind energy is at its lowest [211]. Hence, India can be a hub of green energy supply if it exploits geographical advantages in energy supply sources [212]. Climate change makes the Indian monsoon season more chaotic and impacts its predictability, which could be dramatic for resource planning and energy production scheduling [193], [213]. Yet, should the monsoon become stronger or weaker in the future and should its patterns shift, exploiting the correlation between wind and solar could serve to reduce the uncertainty on their respective future trends, given that the combined perspective has a lower error that the individual ones. Can we use the anti-correlation of solar and wind resources to reduce uncertainty in the estimation of future yield if the combined generation of solar and wind power is considered?

In order to answer this research question, we divide the analysis into two parts. In the first part, we analyze CORDEX simulations to understand future trends of the climate variables influencing solar and wind production under climate change scenario RCP 8.5. Then we select regions where future wind and solar farms could be installed and use portfolio methods to exploit the negative correlation between wind and solar and assess its impact reducing the uncertainty climate simulations trends.

2.2 Material and methods

2.2.1 Data used

In this manuscript, we use CORDEX WAS-22 regional downscaled experiments for all Coupled Model Inter-comparison Panel 5 (CMIP5) models available on the Earth System Grid Federation (ESGF). We focus on three climate variables from CORDEX, namely near-surface wind speeds (sfcWind) at 10 m height, surface temperature (tas) and downward surface radiation (rsds) at the monthly resolution and 0.22° (about 22 km) horizontal spacing. We define the study area in India as $6.70°N$ to $35.5°N$, and $68.1°W$ to $97.3°W$. CORDEX simulations are available for a historical period (1979–2005) and future projections starting from 2006 to the end of the century with Representative Concentration Pathways (RCPs) scenarios RCP 2.6, the lower emission scenario for CMIP5, and RCP 8.5, the scenario assuming a continued increase in greenhouse gases throughout the end of the century [214]. Three RCM families are available for CORDEX WAS-22; 1) the Abdus Salam International Center for Theoretical Physics (ICTP) RegCM system (ICTP-RegCM4-7 [215], noted RegCM4 hereafter), 2) COSMO-crCLIM-v1-1.v1 (COSMO [216]), and 3) REMO2015.v1 (REMO [217]). Table 2.1 summarizes RCM names, with their driving GCM parent, scenarios available and acronym of CORDEX simulations.

Table 2.1: Summary of the models used in this study

Regional climate model	Driving model	Scenarios	Model's acronym
ICTP-RegCM4-7	NCC-NorESM1-M	hist, RCP 2.6, RCP 8.5	RegCM4-NCC
	MPI-M-MPI-ESM-MR	hist, RCP 2.6, RCP 8.5	RegCM4-MPI
	MIROC-MIROC5	hist, RCP 2.6, RCP 8.5	RegCM4-MIROC
COSMO-crCLIM-v1-1.v1	NCC-NorESM1-M	hist, RCP 2.6, RCP 8.5	COSMO-NCC
	MPI-M-MPI-ESM-L	hist, RCP 2.6, RCP 8.5	COSMO-MPI
	ICHEC-EC-EARTH	hist, RCP 8.5	COSMO-ICHEC
REMO2015.v1	NCC-NorESM1-M	hist, RCP 2.6, RCP 8.5	REMO-NCC
	MPI-M-MPI-ESM-LR	hist, RCP 2.6, RCP 8.5	REMO-MPI
	MOHC-HadGEM2-ES	hist, RCP 2.6, RCP 8.5	REMO-MOHC

As a necessary prerequisite for this work, we evaluate monthly CORDEX WAS-22 simulations for the three climate variables over the period 1981–2005, by comparison to ERA5 reanalysis dataset [218]. We examine how well they reproduce the spatial distribution of annual and seasonal means during specified time periods (denoted climatology) and trends at each grid point, and the spatial averages.

2.2.2 Variability at local wind and solar sites

We analyze the temporal patterns of wind speed at three existing wind sites and radiation and temperature at four solar sites for ERA5 and the individual CORDEX WAS-22 models. Table 2.2 outlines the name, location and total capacity in Mega-Watt (MW) of the sites considered in this study. They are selected because they all belong to CLP Group and are used as a benchmark of a real-life portfolio whose structure will be the model of the portfolios simulated later on in India. On the selected sites, we evaluate the standardized monthly anomalies derived during a 25 years period extending from 1981 to the end of 2005 to examine the seasonal variations.

Table 2.2: Summary of the characteristics for the CLP sites used in this study

Asset type	Site name	Location (state)	Gross capacity in MW
Wind	Tejuva	Rajasthan	100.8
	Jath	Maharashtra	60
	Theni	Tamil Nadu	99
Solar	Veltoor	Telangana	100
	Gale	Maharashtra	50
	Clean Solar PVT LTD	Telangana	30
	DSPL	Telangana	50

2.2.3 Evaluation of future changes

One way to use RCM projections is to assess the magnitude and degree of consistency in the simulations in terms of changes in i) climate variables or ii) impacts when the wind speed or solar radiation and temperature are converted to energy estimates [207]. These changes can be expressed in linear trends of annual, seasonal or monthly mean quantities between certain time periods. For the evaluation of future changes, we analyze annual and seasonal climatology and trends in surface wind speeds, temperature and radiation from CORDEX WAS-22 models in the Indian sub-continent for RCP 2.6 and RCP 8.5 scenarios during two sub-periods; from 2025 to 2055, and from 2065 to 2095. We focus the discussion in the main text on simulations with RCP 8.5 to identify the largest bounds of changes in wind, radiation and temperatures in the models. The length of the two sub-periods simulates the economic lifetime of wind and solar assets. When the seasonality is considered, we refer to winter as the months from December to February, pre-monsoon the months from March to May, monsoon as the months from June to September (noted JJAS), and the post-monsoon (months of October and November) seasons. We use linear regression and Theil-Sen [219], [220] non-parametric method to analyze trend magnitudes, which are tested for statistical significance using the Mann-Kendall test [221], [222]. To illustrate the spread of model projections, we take the most extreme as well as the median trend values of all considered models at every grid point. Thus, we evaluate the smallest trends; strongest negative or smallest positive trends, the largest trends; strongest positive or smallest negative trends, and the median trends. After analyzing the whole study domain, we divide it into five sub-regions described in Figure 2.1 to summarize the regional trends. This step is motivated by the need to identify regions where wind and solar monsoon trends are anti-correlated as this is

a binding condition in our work. Once these regions are identified, we focus on two out of them for this analysis. In each region, we select three locations for wind assets and four others for solar assets. For the application of portfolio methods, we produce energy time-series for wind and solar PV at selected locations according to the method discussed in Section 2.2.4.
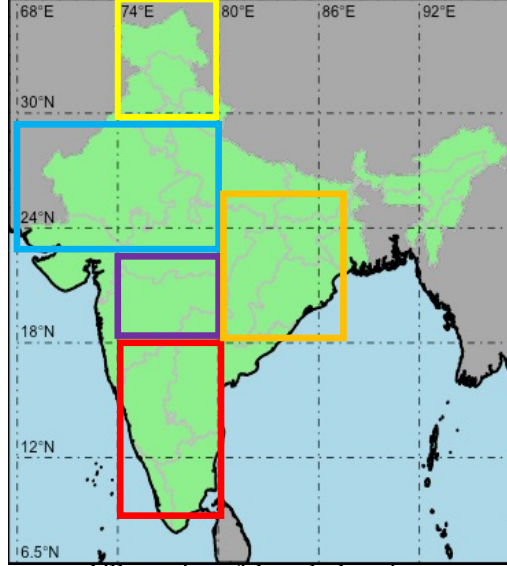
Figure 2.1: Map of the study area and illustration of the sub-domains represented by boxes: North (yellow), Northwest (blue), central West (purple), East (orange) and South (orange) that are utilized for analysis

2.2.4 Energy production estimates

After identifying the regions where wind and solar are anti-correlated during the monsoon season, we pick the locations for wind and solar sites. Hereafter, we lay out the method used to estimate the returns of the wind and solar PV assets which then serve as an input in the portfolio analysis explained in Section 2.2.5. We determine the energy production for each wind and solar asset using CORDEX data and express this return in the form of capacity factors and PV potential as actual production estimates depend on local weather and installations. For wind assets, the capacity factor CF_{wind} is defined as the fraction of the potential production of wind power at the wind site and the maximum possible energy (P rated, times the amount of time energy was produced, t):

$$CF_{wind} = \frac{E_{produced}}{P_{rated} * t} \tag{2.1}$$

At the three wind farm locations considered, we assume 30 Suzlon 111 wind turbines installed at a hub height of 90 m with a turbine diameter equal to 111.9 m and a rated power of 2.1 MW. To project surface wind speed to hub height, we extrapolate wind speed data v_1 at 10 m height to the 90 m hub height using the power law [223] to obtain v_2:

$$v_2 = v_1 \left(\frac{z_2}{z_1}\right)^{\alpha} \tag{2.2}$$

Where the friction coefficient α is equal to $\frac{1}{7}$. The total energy production of each wind farm is estimated by summing the production (resp. nameplate capacity) of each wind turbine over the life of the asset. We assimilate the life of the turbines to 25 years to align with time periods selected to evaluate the impact of climate change. Our analysis is independent of a specific investment life-cycle. Therefore, we do not assume that all turbines need to be installed at a certain point in time and the conclusions do not depend on the 25-year assumption.

For solar sites, in order to make a first order estimate and translate solar radiation and temperature into potential changes in PV generation, we use the methods presented in [224] and [81] to calculate PV_{pot}, which is defined as the fraction of the power output under standard conditions that a PV module may have according to Eq. (2.3):

$$PV_{pot} = P_R \frac{rsds}{rsds_{STC}} \qquad (2.3)$$

PV_{pot} is unit-less, $rsds$ is the surface downward radiation at each time from ERA5, $rsds_{STC}$ is radiation under standard conditions which is equal to $1000 Wm^{-2}$ and P_R is the performance ratio calculated from Eq. (2.4):

$$P_R = 1 - \gamma(T_{cell} - T_{STC}) \qquad (2.4)$$

Where T_{STC} is equal to 25°C, $\gamma = 0.005°C^{-1}$ assuming the behavior of mono-crystalline silicon solar panels, and T_{cell} is the temperature of the PV cell calculated with Eq. (2.5):

$$T_{cell} = c_1\ c_2 T\ c_3 rsds - c_4 sfcWind \qquad (2.5)$$

$sfcWind$ is surface wind speed, c_1, c_2, c_3 and c_4 values are listed in Table 2.3 along with the other variables and constants and their units.

Table 2.3: Definition of the values for the parameters in Eqs. (2.3), (2.4) and (2.5)

Variable name	Value	Units
$rsds_{STC}$	1000	Wm^{-2}
γ	0.005	$°C^{-1}$
T_{STC}	25	$°C$
c_1	4.3	$°C$
c_2	0.943	-
c_3	0.028	$°C\ W^{-1}m^2$
c_4	1.528	$°C\ m^{-1}s$

In Section 2.2.5, we show how CF_{wind} and PV_{pot} estimated from CORDEX data, are used in the portfolio analysis framework to investigate the impact of combining wind and solar assets on the uncertainty of portfolio returns.

2.2.5 Portfolio analysis

Portfolio analysis supports decision-making subject to the trade-off between the expected return and the volatility of this return. The framework enables the assignment of weights to assets included in a portfolio such that the total return is maximized and the volatility of this return is minimized. Decision-makers can evaluate the performance of each optimal portfolio formed by a combination of assets. The optimal solutions of the trade-off in the portfolio analysis are graphically represented on an efficient frontier which is a plot of optimal returns and their volatility. In the following, we explain how it is adapted to calculate the uncertainty on returns calculated from climate models. First of all, we use as an input to the bi-objective function a set of wind and solar sites. We consider that these candidates are part of a portfolio whose structure mimics the existing portfolio discussed earlier, with three wind farms and four solar PV assets. The sites selected sit on locations where wind and radiation trends are anti-correlated during the monsoon season. We solve the bi-optimization problem three times for each set of locations in a way that we have as an input, 1) only wind sites, 2) only solar sites, and 3) wind and solar sites combined. By doing so, we can compare the efficient frontiers obtained from the standalone perspective with wind only or solar only portfolios, and the mixed portfolios. The examination of the three efficient frontiers obtained enables us to highlight the effects of the combination of wind and solar in the portfolio and its impact on the volatility of the return, as opposed to the non-mixed portfolios. The analysis is repeated for each individual RCM model for a certain RCP scenario. Finally, by doing so we can measure the spread between the curves of the efficient frontiers for each one of the portfolio types and examine how the combination of asset types affects this spread.

Formally, the mean-variance analysis consists of a bi-optimization problem Eqs. (2.6) and (2.7), where μ_k is the average production of wind or solar power in each location k, the mean portfolio return μ_p (approximated by its total capacity factor) is maximized while its variance σ_p^2 is minimized, subject to the constraints that the sum of the weights w_k is equal to one, and that all capacity factors are positive.

$$\begin{aligned} \max \quad & \mu_p = \sum_k w_k \mu_k \\ \text{s.t.} \quad & \sum_k w_k \leq 1 \end{aligned} \tag{2.6}$$

$$\begin{aligned} \min \quad & \sigma_p^2 = \sum_k \sum_m w_k w_m \text{cov}_{(k,m)} \\ \text{s.t.} \quad & \sum_k w_k \leq 1 \end{aligned} \tag{2.7}$$

Hence, we calculate the average production at each location k, namely the mean μ_{wind} that is approximated by CF_{wind} in the case of wind sites and by PV_{pot} in the case of solar sites. In Eqs. (2.6) and (2.7), w_k are the weights of each asset in the portfolio. For the minimization of the portfolio variance σ_p^2 in Eq. (2.7), we calculate the covariance matrix $cov_{(k,m)}$ between the different assets k and m based on their geographical distribution using the time-series.

Furthermore, we limit the weight for each asset in the optimal portfolio cannot be larger than 50%. After solving the bi-objective function presented earlier, we obtain the efficient frontiers or the set of optimal portfolios; each point on the frontier is a combination of assets according to certain weights to form a portfolio with a certain return and its corresponding volatility value). The algorithm defines the assets considered in the portfolio.

We simulate returns for five assets to illustrate the concept of the efficient frontier in Figure 2.2. The five points represent the mean return and standard deviation for each one of the five individual assets. The resolution of the bi-optimization problem described in Eqs. (2.6) and (2.7) enables to find the combination of assets where returns are maximized for a given level of volatility, or minimized volatility for a given level of return. The set of these optimal solutions constitutes the efficient frontier. On this graph, the higher a point is to the left, the better is an asset because the expected return is higher and the related volatility is lower.
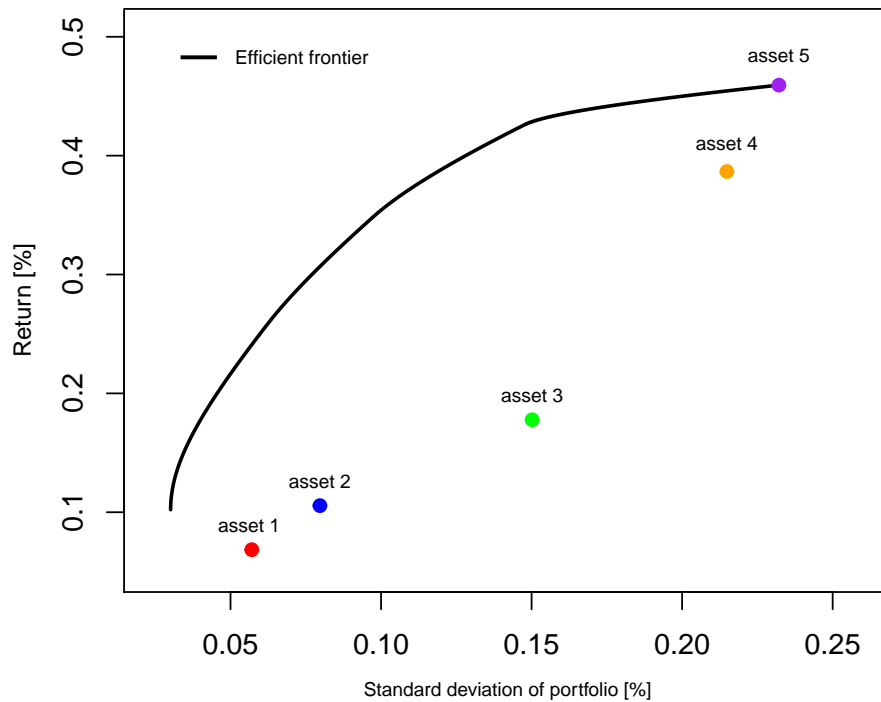
Figure 2.2: Illustration of the efficient frontier for five assets

2.3   Results and discussion

2.3.1   Evaluation of the performance of CORDEX WAS-22 against ERA5

The results of the comparison between CORDEX WAS-22 models and ERA5 are presented in
Figure 2.3 for sfcWind, Figure 2.4 for tas, and Figure 2.5 for rsds.
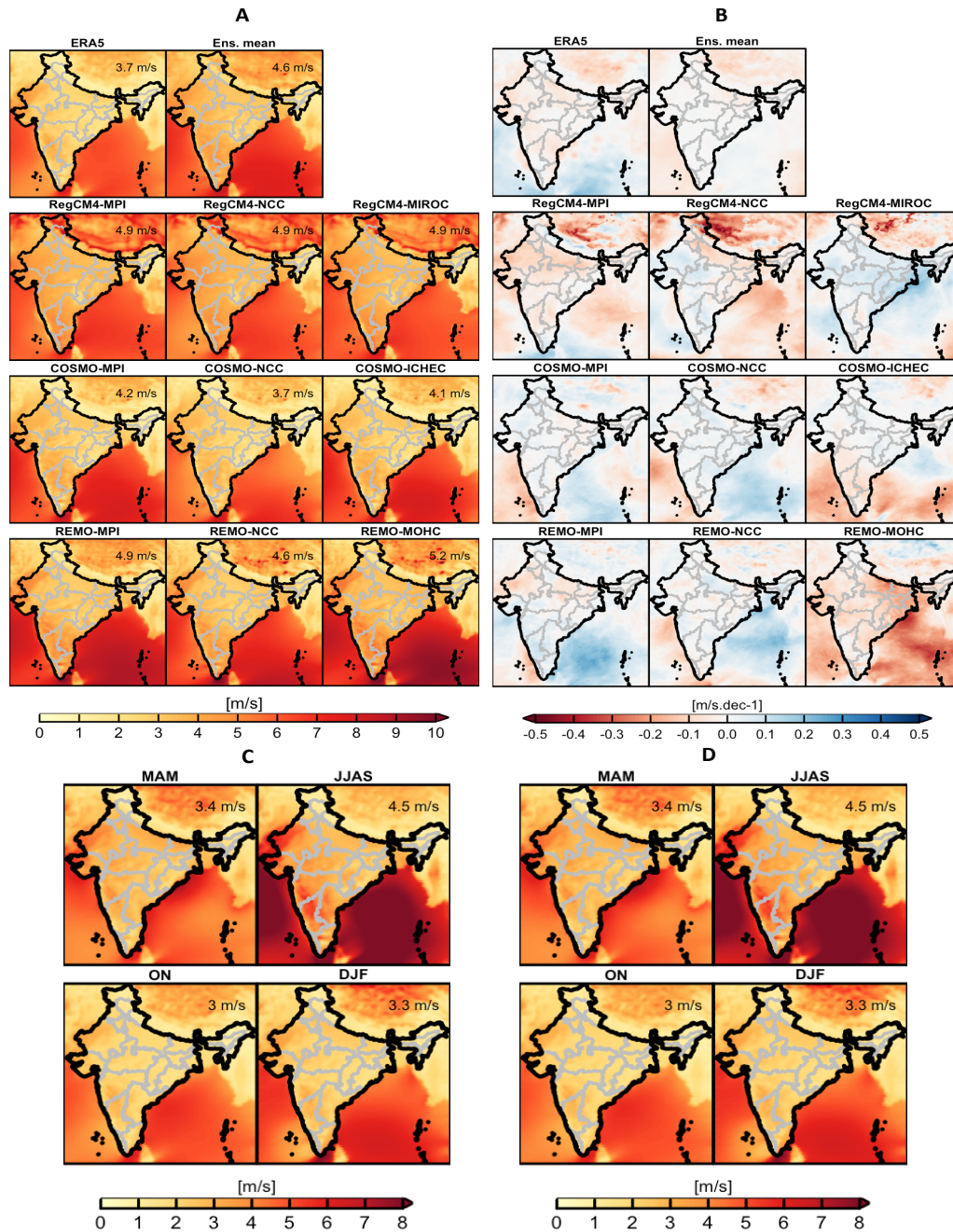
Figure 2.3: Surface wind speeds: comparison of the annual climatology **(A)** and trends **(B)** of ERA5 and
WAS-22 (first row), and seasonal climatology **(C)** and **(D)** (second row).

Regarding the annual climatology of wind speeds, the results in Figure 2.3**A** demonstrate that the geographical pattern of CORDEX WAS-22 models resembles the one found for ERA5 although differences exist in the south of Tibet. For the annual trends of surface winds, the comparison in Figure 2.3**B** shows that not all individual climate models reproduce the pattern of ERA5. In general, we find that ensemble mean for wind speed, noted sfcWind$_{hist}$ (first row and second column in Figure 2.3**C** satisfactorily captures wind speed annual trends, and shows similarities in the pattern of the monsoonal trend (Figure 2.3**D**). This result is in general a key finding because it increases confidence in the ability of CORDEX models in reproducing the monsoon pattern which is a majorly impacting climatological feature on wind energy in India.

We include a similar assessment for temperature and solar radiation as they are used to estimate solar energy time series. We find a strong resemblance in the spatial pattern of annual temperature climatology between ERA5 and CORDEX WAS-22 individual models displayed in Figure 2.4**A**. Discrepancies in the annual climatology for temperature are found in mountainous areas towards the Himalayas in northern India because the resolution of climate models cannot capture the complexity of local spatial variability. There is also a good agreement in the annual temperature trends (Figure 2.4**B**) and all datasets exhibit trends with a positive slope. Accordingly to the results for wind speeds, we find large similarities in the seasonal temperature climatology between ERA5 (Figure 2.4**C**) and the historical ensemble (Figure 2.4**D**).

Figure 2.4: Surface temperature: comparison of the annual climatology **(A)** and trends **(B)** of ERA5 and CORDEX WAS-22 (first row), and seasonal climatology **(C)** and **(D)** (second row).

We see in Figure 2.5**A** that differences exist in the spatial pattern of the annual climatology for radiation while ERA5 data and the ensemble mean outline a good agreement with only a slight difference in the spatial average (230 Wm^{-2} for ERA5 and 220 Wm^{-2} for the ensemble mean). We notice a high variability between ERA5 and the individual models for the annual radiation

trends in Figure 2.5**B**. Similarly to the annual pattern, we find a significant similarity in the seasonal climatology for radiation between ERA5 (Figure 2.5**C**) and the historical ensemble (Figure 2.5**D**).
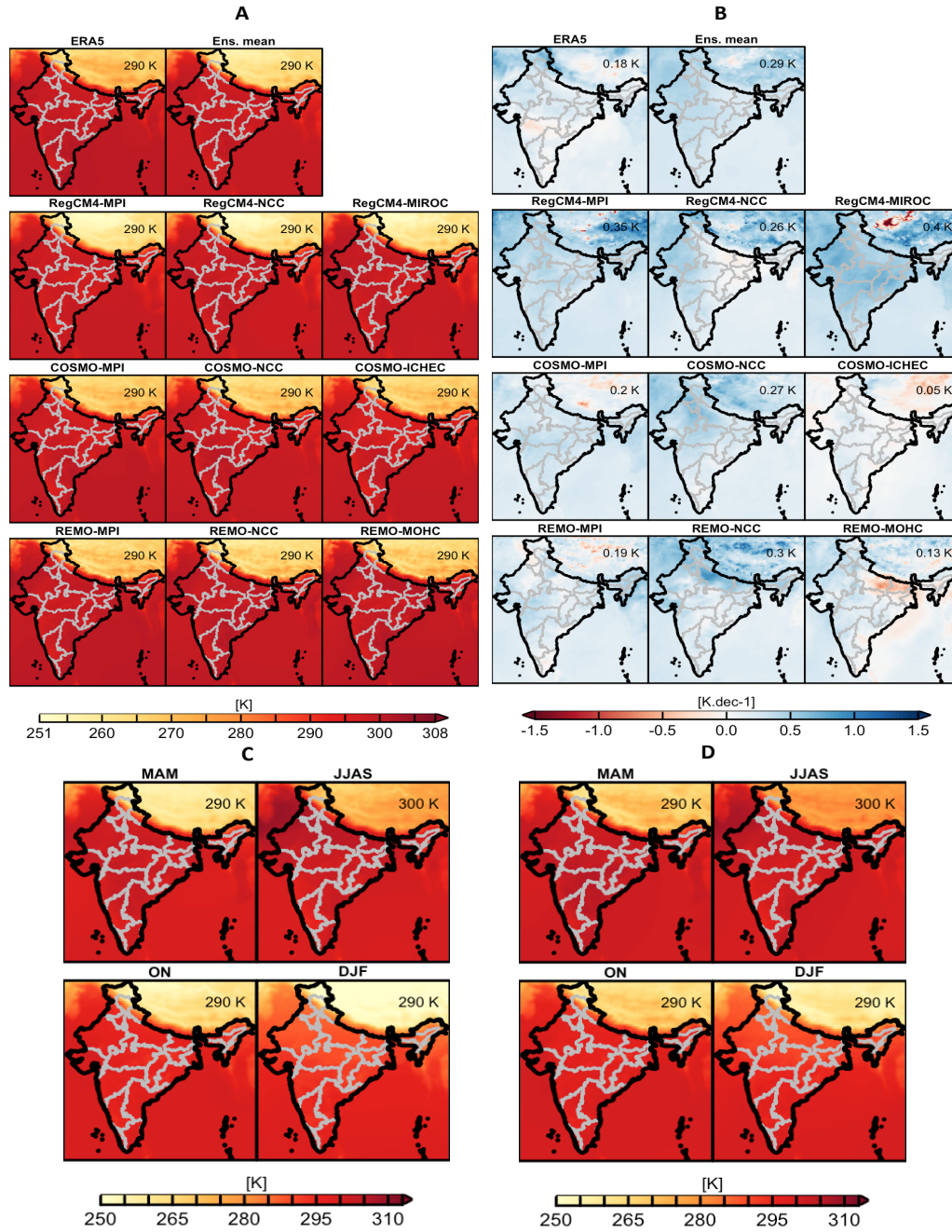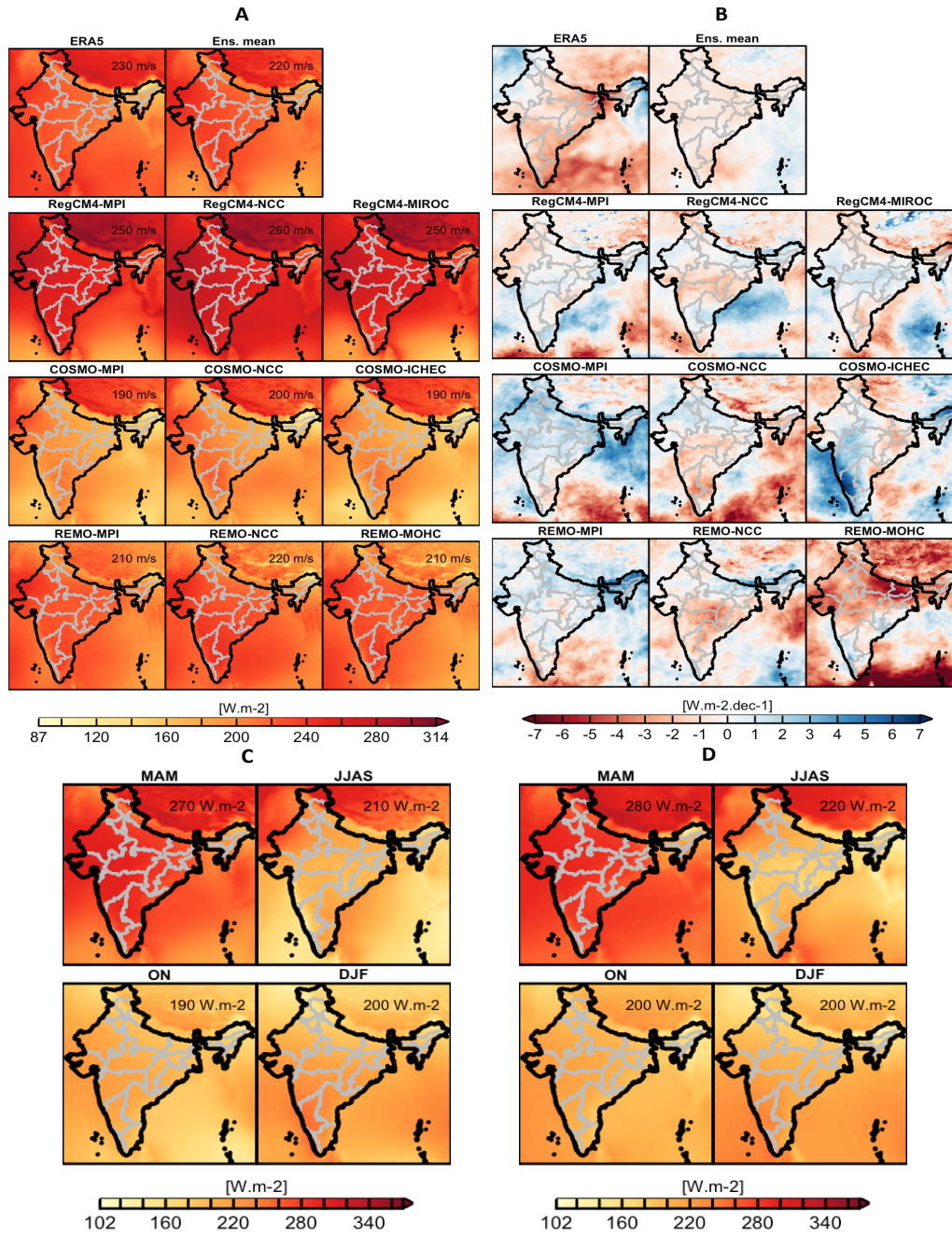

Figure 2.5: Surface shortwave downward radiation: comparison of the annual climatology **(A)** and trends **(B)** of ERA5 and CORDEX WAS-22 (first row), and seasonal climatology **(C)** and **(D)** (2nd. row).

In summary, we conclude that CORDEX WAS-22 models for the three climate variables reproduce ERA5 data with a reasonable degree of fidelity, and the resemblance in the spatial distribution is stronger at the annual than seasonal level. Section 2.3.3 includes an evaluation of the temporal variability at existing wind and solar sites.

2.3.2   Analysis of the variability of CORDEX WAS-22 models at local sites

Figure 2.6**A** outlines the temporal variability of standardized wind speed at three existing wind-farm sites, and compares CORDEX models with ERA5 (black line). In the three sites, the peak in wind speeds reflected by ERA5 coincides with the monsoon season. However, REMO models represented in purple shades outline a peak delayed and occurring later during the year. The delay in the monsoon peak for wind speeds from REMO models is apparent when looking at the plots of the seasonality component. COSMO and RegCM4 models show a good correspondence in the seasonal component of the individual models with ERA5. We see that there are differences in the individual models and that in some instances, the individual models are not able to reproduce the peak in wind speed during the monsoon.

At the four solar sites, we observe that the peak in radiation (Figure 2.6**B**) reported by ERA5 (black line) occurs between March and May. The time of occurrence of the peak for RegCM4 and COSMO models coincides well with that of ERA5. REMO models (lines in the purple shade) fail to reproduce that as the peak of these purple lines occurs later around the monsoon season. This delay in peak radiation for REMO models also appears when we analyze the seasonality component for radiation. In Veltoor, the correspondence in the trends between ERA5 and RegCM4 models is the highest which could indicate that not all available models are equally suitable for a particular location. The differences between the RCMs can be partially explained by the fact that COSMO for example has difficulties over domains with a climate substantially different from that of Europe where it has been developed [225]. On the other hand, IITM-RegCM4 over South Asia was developed at an Indian institute.

For temperature (Figure 2.6**C**), the peak that happens in June or July according to ERA5 data is accurately reported by RegCM4 models (green) and COSMO ones, while REMO models persistently show a delay with a peak occurring only after the monsoon season and towards the end of the year.

The evaluation of the temporal variability between the individual models in wind and solar locations highlights one of the problems when evaluating climate change; these differences between the ERA5 data and CORDEX models can be attributed to differences in the parametrization of the models and shows that uncertainty of climate predictions may still be large. Now that we highlighted some differences in the models, we study the trends for future projections before testing how the combination of wind and solar can reduce the variability in the trends.
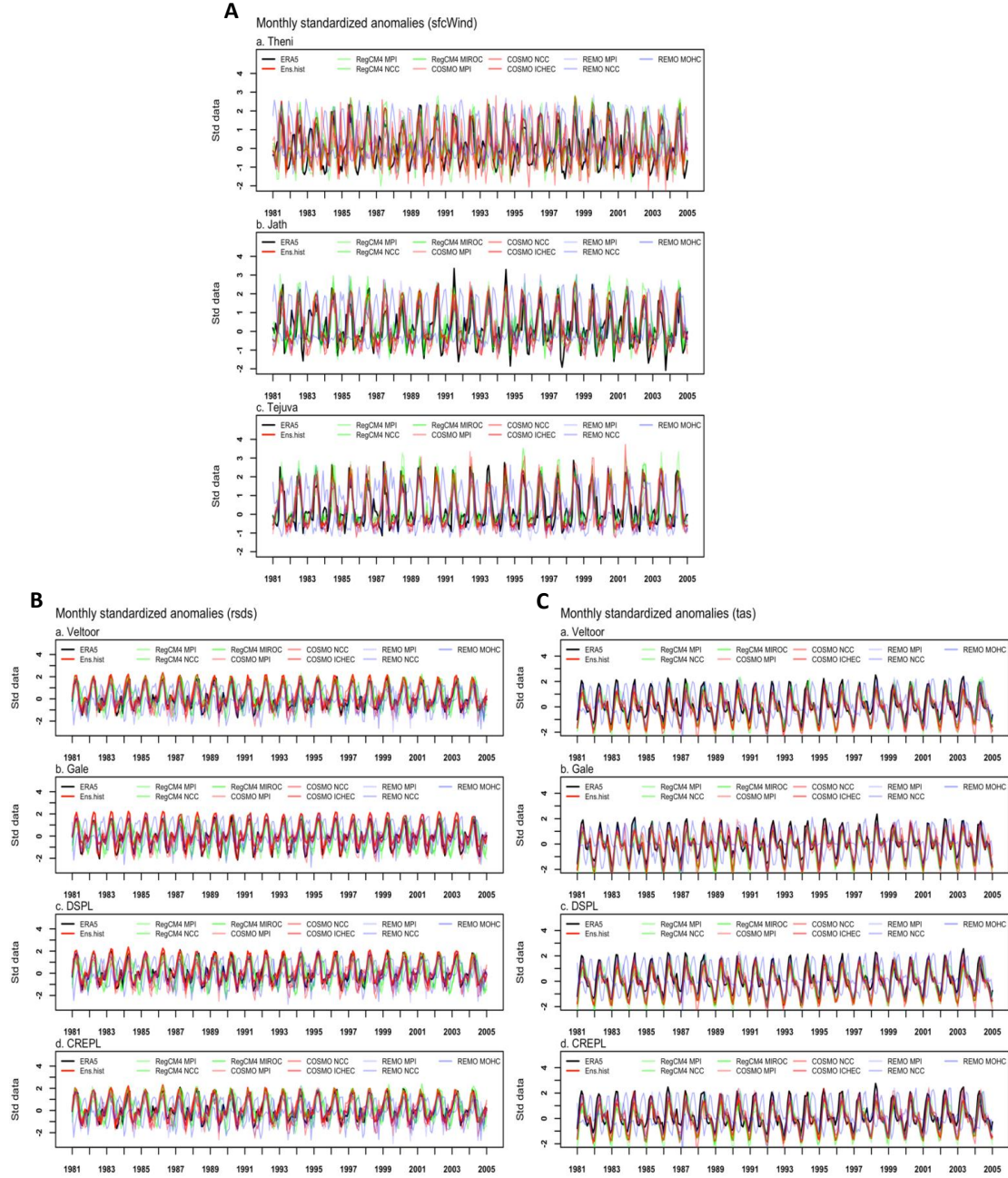
Figure 2.6: Monthly standardized anomalies for wind speeds **(A)**, surface downward radiation **(B)**, and temperature **(C)** extracted from ERA5 and CORDEX WAS-22 (1981-2005).

2.3.3 Trends in CORDEX WAS-22 predictions and seasonal variation of both wind and radiation trends

In this section, we describe the geographical distribution of long-term annual and seasonal climatology and trends for surface wind speed, temperature and radiation in India under the RCP 8.5 scenario. The results for the annual climatology for the three climate variables are presented in Figure 2.7.
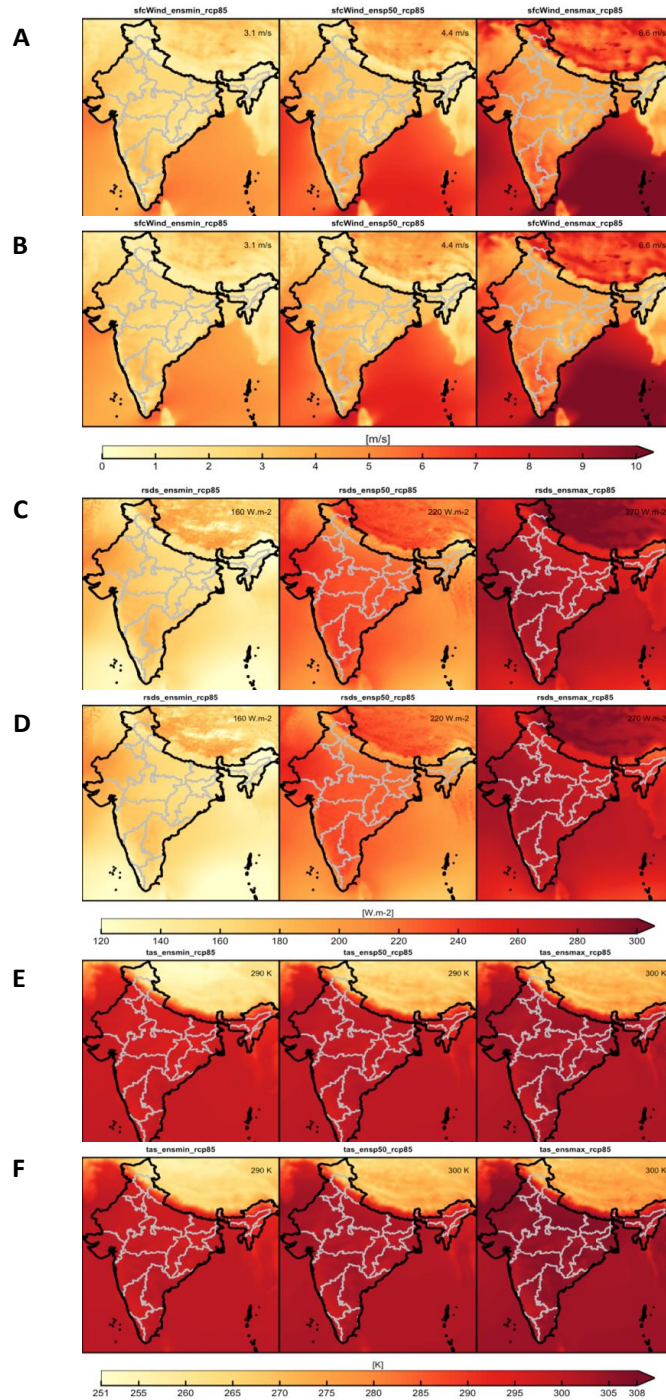
Figure 2.7: Distribution of the annual climatology (RCP 8.5): annual wind (2025-2055) **(A)** and (2065-2095) **(B)**, radiation (2025-2055) **(C)** and (2065-2095) **(D)**, and temperature (2025-2055) **(E)** and (2065-2095) **(F)**.

The evaluation of the climatology between the two periods (2025 to 2055), and (2065 to 2095) in Figure 2.7**A** and **B** shows that the median value of the annual wind speed increases by 2.6%. Looking at the seasonal climatology for surface wind in Figure 2.8, we see that the minimum seasonal values showed in Figure 2.8**A** increase for monsoon and winter winds during the first time period, while pre-monsoon and maximum monsoon wind speeds increase in the latest part of the century in Figure 2.8**F**. Regarding the seasonal trends during the first period (Figure 2.8**G**, **H** and **I**), we find a positive wind speed trend during the pre-monsoon in the northwest, and some southern areas during the monsoon and winter seasons. We also find some increase in the northeast for winter wind speeds from the maximum ensemble. During the second period extending from 2065 to 2095 (Figure 2.8**J**, **K** and **L**), we find a positive trend in the northwest and southeastern coast for pre-monsoon wind speeds. We can also report on some positive trends for monsoon wind speeds in areas located in the northwest and northeast. Looking at the maximum ensemble, we find a positive trend in the north and northeast, indicating an increase in extreme wind speeds.
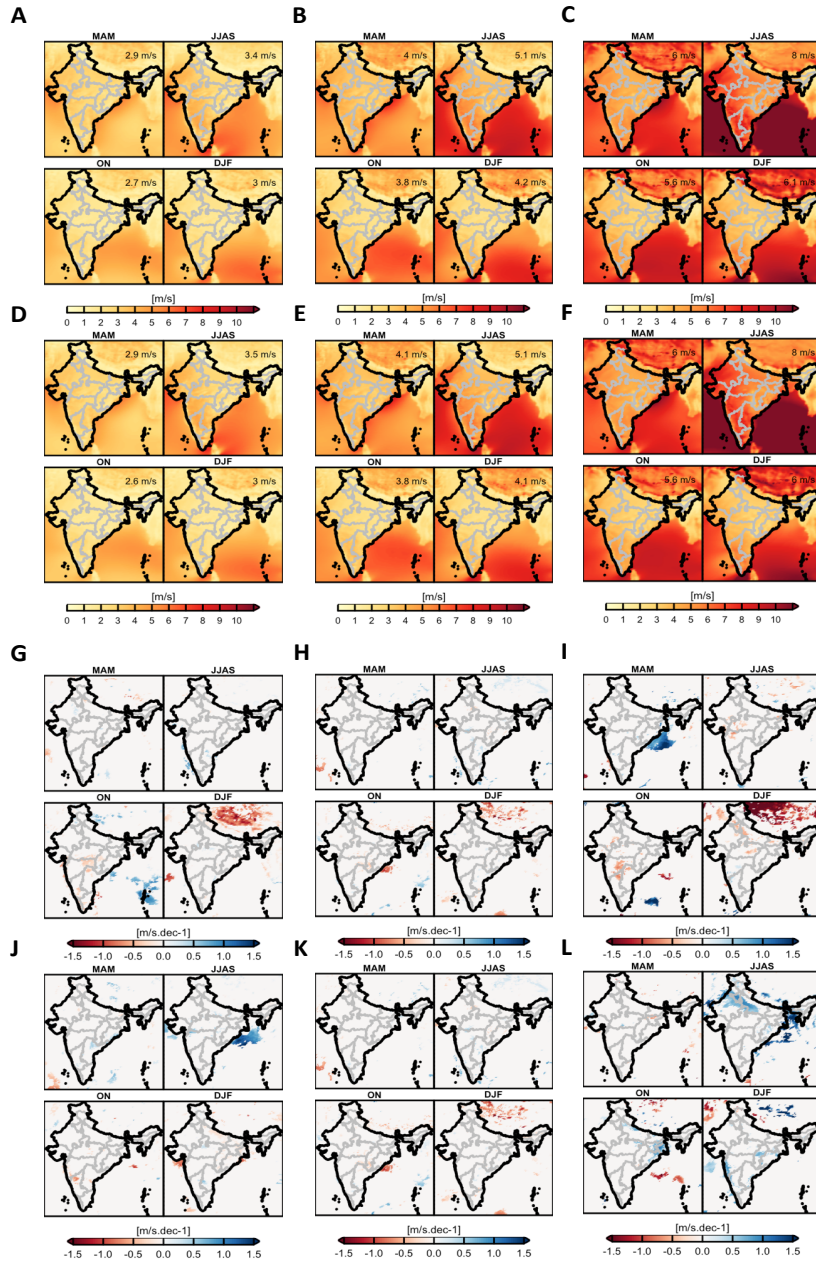
Figure 2.8: Surface winds (RCP 8.5): Seasonal climatology for the smallest **(A)**, median **(B)**, and largest **(C)** ensembles (2025-2055), and analogously **(D)**, **(E)** and **(F)** for (2065-2095). **(G)**, **(H)** and **(I)** are respectively the seasonal trends for the smallest, median and largest ensembles (2025-2055), and **(J)**, **(K)** and **(L)** are respectively the smallest, median and largest ensembles (2065-2095). White areas indicate grid points where trends are not statistically significant (p>0.05).

The spatial distribution of the annual climatology for the downward surface radiation is presented in Figure 2.9. The highest values are found in the North of India towards the Himalayas, as well as in the northwestern and southwestern parts of India. The annual and seasonal mean climatology remain the same between the first and second periods. Looking at the median ensemble for the first period (Figure 2.9**A**, **B** and **C**), we see no significant change in the pre/post-monsoon climatology. During the monsoon season (Figure 2.9**G**, **H** and **I**), the northwest and northeast near the coast have significant negative trends. During the second period, results show a positive trend in the north of India during the monsoon that would involve an increase in PV output in the region (Figure 2.9**J**, **K** and **L**).
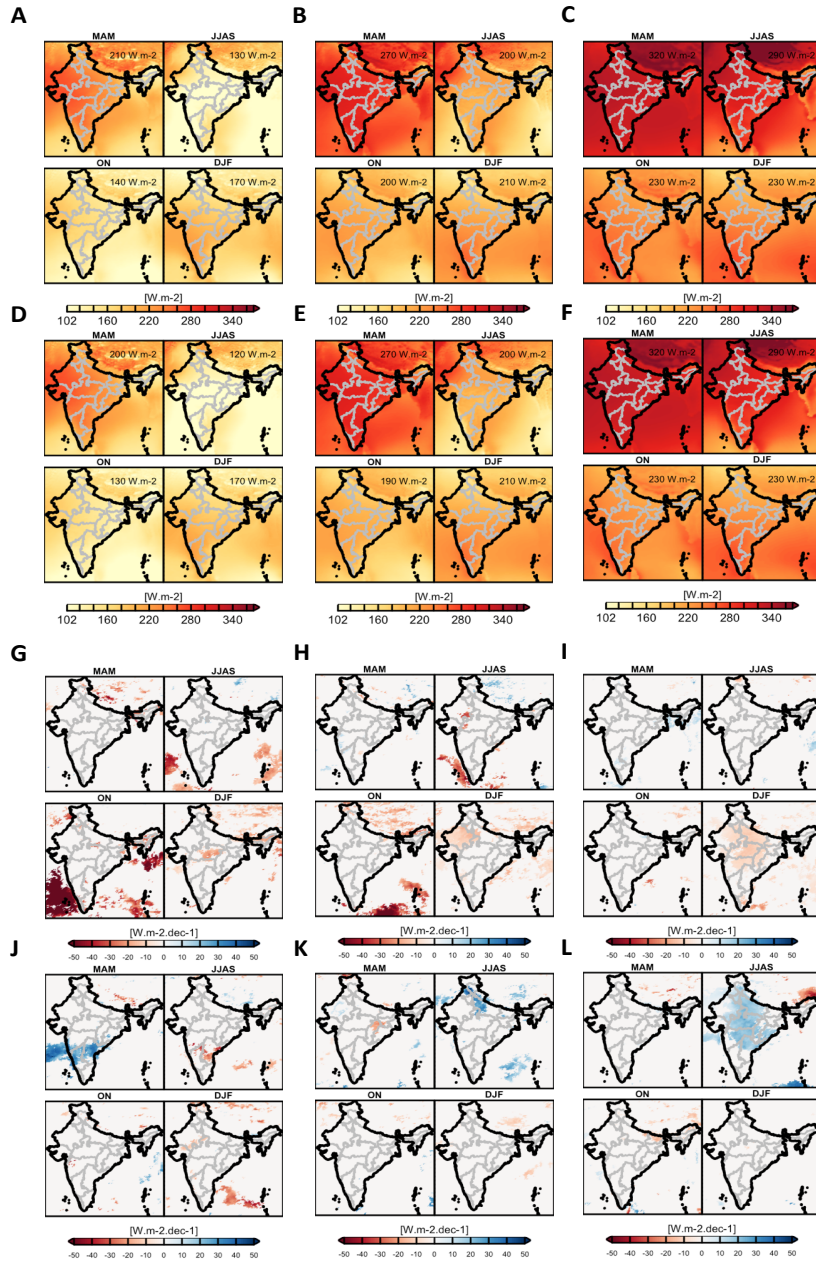
Figure 2.9: Surface downward shortwave radiation(RCP 8.5): smallest **(A)**, median **(B)**, and largest **(C)** ensemble seasonal climatology for the period between 2025 and 2055, and analogously **(D)**, **(E)** and **(F)** for the period between 2065 and 2095. **(G)**, **(H)** and **(I)** are respectively the smallest, median and largest ensembles during the 2025-2055 period, and **(J)**, **(K)** and **(L)** are respectively the smallest, median and largest ensembles from 2065 to 2095. White areas indicate that at these grid points, trends are statistically non-significant at the level 0.05.

For temperature, we find a higher climatology and positive trends towards the end of the century, and extreme temperatures increasing during the monsoon in the whole of India except the South. Assuming that there will be no changes in future solar radiation, these trends would imply decreasing power output for solar PV as solar panel decrease in efficiency with increasing temperatures [226].

Prior to the portfolio analysis, we investigate the seasonal correlation between surface downward radiation and wind speed in the sub-regions defined earlier in Table 2.4. This table shows that the two regions where the anti-correlation in wind and radiation is strongly distinguishable and consistent for the two RCP scenarios are the South from 2025 to 2055 and the North from 2065 to 2095. Hence, we select two sets of wind and solar assets in these two regions as candidates for the application of the portfolio analysis.

Table 2.4: Spatially averaged seasonal correlation coefficients between rsds and sfcWind for the five sub-domains analyzed for the two RCP scenarios and time periods defined in each quarter of the year (noted Qtr).

Scenario	RCP 2.6							
Periods	2025-2055				2065-2095			
Region	Qtr1	Qtr2	Qtr3	Qtr4	Qtr1	Qtr2	Qtr3	Qtr4
Top-North	0.52	0.47	0.46	0.53	-0.83	-0.76	-0.79	-0.85
Northwest	0.31	0.34	0.27	0.19	0.04	0.08	0.32	0.33
Center	0.06	0.07	-0.02	-0.10	0.27	0.36	0.59	0.59
East	0.20	0.15	0.15	0.16	0.12	0.31	0.47	0.34
South	-0.63	-0.44	-0.55	-0.70	0.80	0.83	0.91	0.90
Scenario	RCP 8.5							
Periods	2025-2055				2065-2095			
Region	Qtr1	Qtr2	Qtr3	Qtr4	Qtr1	Qtr2	Qtr3	Qtr4
Top-North	-0.30	-0.42	-0.34	-0.26	-0.19	-0.29	-0.16	-0.10
Northwest	0.93	0.94	0.67	0.67	0.90	0.90	0.64	0.65
Center	0.52	0.19	-0.23	-0.02	0.44	0.17	-0.21	-0.04
East	0.76	0.48	0.20	0.47	0.70	0.46	0.22	0.45
South	-0.32	-0.48	-0.66	-0.68	-0.27	-0.42	-0.62	-0.63

2.3.4 Portfolio analysis and its practical application to future wind and solar energy installations

We apply the portfolio framework in two sets of wind and solar assets in the South and the North where the two solar radiation and wind speed variables are anti-correlated. The characteristics of the two sets are summarized in Table 2.5. We analyze how the combination of wind and solar impacts the uncertainty of prediction on energy returns.

Table 2.5: Latitude and longitude of the assets in the South and North.

Assets	South		North	
	Latitude	Longitude	Latitude	Longitude
Wind 1	74.2	14.7	79.4	34.8
Wind 2	74.6	14.3	78.3	33.3
Wind 3	76.0	9.6	77.2	32.8
Solar 1	78.8	16.4	78.7	35.3
Solar 2	75.1	16.2	74.1	31.1
Solar 3	78.2	18.0	78.9	34.8
Solar 4	75.1	15.3	77.4	34.4

For the analysis of the results, we evaluate how the spread of the efficient frontiers associated with the mixed portfolios differs from the one found for wind and solar only portfolios. The results are presented in Figure 2.10 where the first row depicts the results for the set located in the South from 2025 to 2055, and the second row the ones for the set located in the North for the second time-period. In the southern region, under RCP 2.6 and during the first time-period, the evaluation of the efficient frontiers obtained for the set of asset in Figure 2.10**A** shows that for a return level of 0.25, the standard deviation of the portfolio for solar-only portfolios ranges between 0.035 and 0.045. The efficient frontier of wind only portfolios only has one optimal solution for the level of return and the standard deviation converges to a single value of 0.032. Different weights values of the three wind assets currently evaluated cannot improve the optimal return and thus its attached standard deviation. The standard portfolio for mixed portfolios ranges from 0.025 to 0.032. The mixed portfolio reduces the spread of the standard deviation of the portfolio for this return level by 30% compared to the solar-only type. In the same region and time period, under RCP 8.5, Figure 2.10**B** shows that for the same return level of 0.25, the reduction of the uncertainty range for the mixed portfolio compared to the solar-only type is also valid as the standard deviation of the portfolio for solar-only varies from 0.035 to 0.049 whilst it ranges between 0.025 and 0.035 for the mixed type which also corresponds to a reduction of 30%. In the North, where the seasonal anti-correlation between wind and solar radiation variables extends throughout the year under RCP 2.6 and between 2065 and 2095, Figure 2.10**C** highlights that for a return level of 0.31, the spread of the standard deviation of solar-only portfolios ranges from 0.041 and 0.48, from 0.082 and 0.085 for the wind only type, and from 0.039 and 0.041 for the mixed portfolio. Hence, the reduction obtained with the mixed portfolio reaches a level of 71.4% compared to the solar only, and 33.3% compared to the wind only type. For this same set, under RCP 8.5, we find that for a return level of 0.34 (Figure 2.10**D**), the spread of the standard deviation for solar-only portfolios ranges from 0.052 and 0.097, for wind-only portfolios is between 0.092 and 0.096,
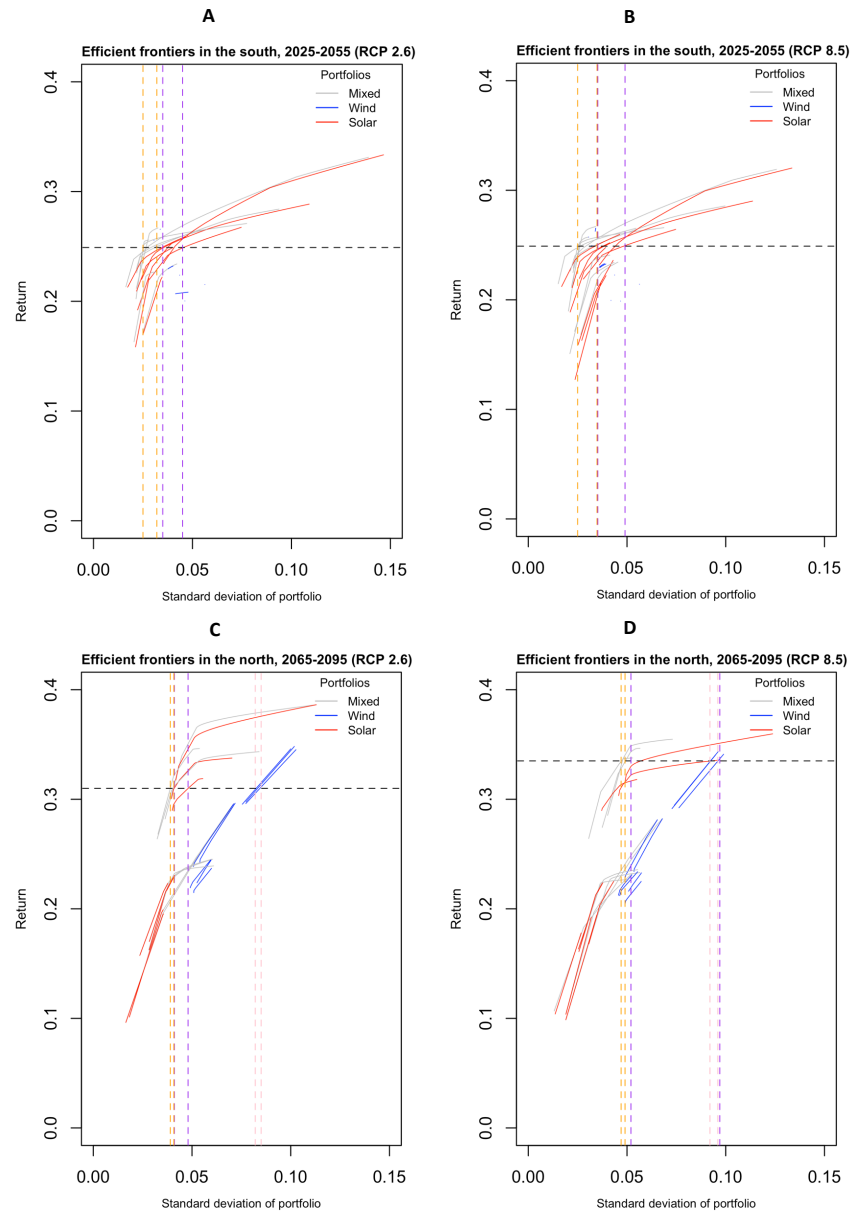
Figure 2.10: Efficient frontiers from the CORDEX WAS models in the portfolio set 1 located in the South for the period between 2025 and 2055 under RCP 2.6 scenario (**A**) and RCP 8.5 scenario (**B**). (**C**) and (**D**) are the efficient frontiers obtained for portfolio set 2 in the North for the period between 2065 to 2095 for RCP 2.6 and RCP 8.5 respectively. On each graph, the black horizontal dashed line represents the level of portfolio return examined, and vertical dashed lines represent the spread of its associated standard deviation for mixed (orange lines), wind only (pink lines), and solar only (purple lines) portfolios.

and for the mixed portfolios is between 0.047 and 0.490. This entails that the range obtained with the mixed portfolio for the return level evaluated leads to a reduction of the uncertainty on the standard deviation by 96% compared to the solar-only portfolio type and 50% compared to the wind-only one. The benefits of the portfolio method are demonstrated in the two regions

presented considering the reduction of the spread in the efficient frontiers for a certain return value when the portfolios are mixed compared to the portfolios of solar only in the first case, and both wind and solar for the second case. We highlight that we also find cases where the reduction of the spread for the mixed portfolios does not hold. Yet, we consistently find that mixed portfolios offer a great advantage in reaching higher return levels for low to medium risk portfolios (efficient frontiers on the left) and this constitutes a desired advantage for investors. The results also indicate that the reduction in the uncertainty is more substantial for the solar only portfolios compared to the wind only. The variability at the monthly time-scales is higher for wind than solar.

We investigate the impact of time resolution on the findings and re-do the analysis in the same regions with daily data for CORDEX WAS-22 data under both RCP scenarios. We evaluate the differences in the spread of the mixed portfolio compared to the single portfolio types from daily data, for the same return levels defined for monthly data. The results are included in Figure 2.11.

In the South, with daily data, the reduction in the spread of the uncertainty for the mixed portfolio compared to the solar only type is effective for return levels below 0.22. The efficient frontiers for wind portfolios from daily data have the same characteristics with a single optimal solution. In the North, with daily data, we find that mixed portfolios have a lower uncertainty spread than solar ones for high return levels (above 0.30). The conclusions found at the monthly resolution remain valid with daily data.
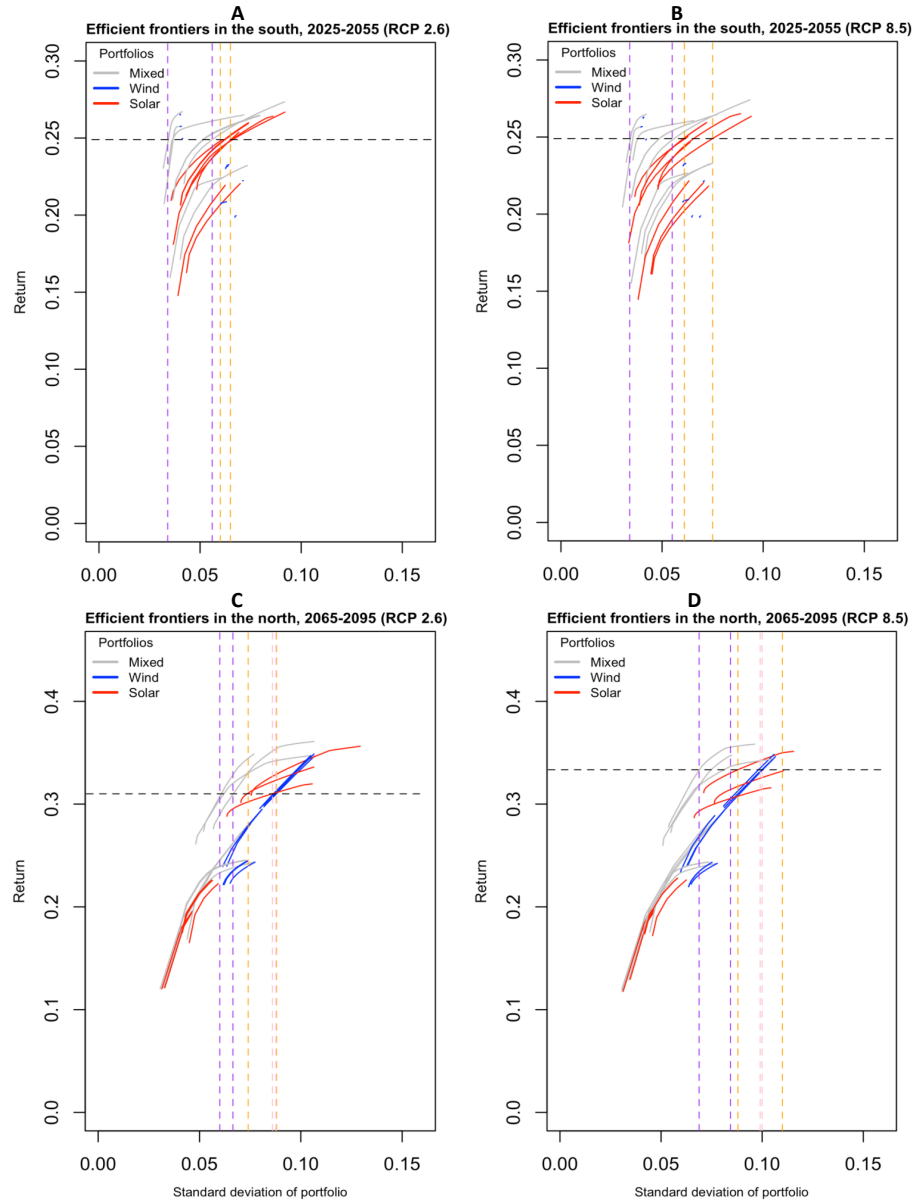
Figure 2.11: Efficient frontiers from CORDEX WAS models at the daily time resolution in the portfolio set 1 located in the South for the period between 2025 and 2055 under RCP 2.6 scenario (A) and RCP 8.5 scenario (B). (C) and (D) are the efficient frontiers obtained for portfolio set 2 in the North for the period between 2065 to 2095 for RCP 2.6 and RCP 8.5 respectively. On each graph, the black horizontal dashed line represents the level of portfolio return examined, and vertical dashed lines represent the spread of its associated standard deviation for mixed (orange lines), wind only (pink lines), and solar only (purple lines) portfolios.

2.4   Conclusion

Seasonal monsoons play a crucial role in determining the local climate in India and are also impacted by climate change. Recognizing the uncertainty in climate models, the underlying idea in this study is to highlight that if climate models wrongly predict a future modification in a weather pattern like the monsoon, then the potential loss in one parameter, for example, solar radiation, can be compensated by a potential increase in another one, wind, since these two variables are often anti-correlated. To exemplify this idea, we first compare surface wind speed, temperature, and solar radiation variables from CORDEX WAS-22 data with ERA5 to assess their performance in reproducing climatological characteristics in an historical period. The examination of the standardized anomalies for wind speed and solar radiation in different locations illustrates variability between climate models but shows in general a good performance. We then determine the annual and seasonal climatology and trends of these climate variables during two periods in the future, namely 2025 to 2055 and 2065 to 2095, and calculate the seasonal trends in five sub-regions of the Indian territory in order to identify regions where the trends between radiation and wind are anti-correlated during the monsoon. Finally, we construct two portfolios of three wind farms and four solar assets in selected locations to test if portfolio methods reduce the uncertainty of the projections. The research outcomes infer that this method does not necessarily influence the level of the total return obtained, intending the energy output expressed in terms of a capacity factor, but the uncertainty of this estimated return. Hence, we show that by accounting for the correlation between wind and solar in two different Indian regions, the application of the portfolio framework highlights not only the diversification potential, which is a known benefit, but also enables to reduce uncertainty estimates compared to a single variable, wind only, or solar only assessment. The analyses and conclusion on any upward or downward trend in wind and solar energy output are from the energy resource perspective. Whether these available resources can be fully converted into energy output would be subjected to other technical, commercial and operational factors in the life time of the asset (e.g. component or system degradation reduces the output over time).

This research is carried out in a climate change assessment perspective in an effort to push forward the inclusion of climate models in future discount cash flow models of investors that engage in the energy transition with a rapid shift to clean energy. We develop an analysis that is simple and reproducible in any other region where wind and solar trends are anti-correlated. The exercise can be carried out in existing or planned wind and solar assets without a limitation on a specific portfolio structure. Therefore, future analysis should explore other regions in South Asia heavily influenced by monsoon interactions which can be good candidates for further case studies.

We acknowledge that one major limitation of this study is the use of raw climate data to estimate portfolio returns instead of bias-corrected datasets. However, we want to point out that the portfolio method could be applied to current data from climate models as well as for current local data. The comparison between the three pairs (CORDEX, reanalysis and local data) would then allow to estimate more local effects since it is known that the climate change signal,

i.e. the difference between the current and future climate portfolio, will often be preserved during downscaling [227]. Furthermore, the use of bias correction techniques with local data would strongly be limited in our case because we do not have access to good data that we can use to compare the corrected dataset and validate the results. As an illustration, wind speed measurements in India from the Integrated Surface Database (ISD) of the National Centers for Environmental Information (NCEI) of the National Oceanic and Atmospheric Administration (NOAA) [228] present gaps, and the available stations are not necessarily close enough to the locations studied. The gap in the availability of solar data in India because of the unavailability of ground monitoring stations is discussed in the literature [183].

The first practical implication of our research for investors in India resides in the fact that there are locations where the risk is decreased when combining two asset types and other locations where the combination appears less effective. This information may be useful in picking sites for development of wind and solar renewable assets. We also see the value of our study to portfolio managers interested in investigating future investment possibilities in regions with no long-term track of wind and solar measurements. [187], [229] recommend the extension of the lifetime for existing wind farms in order to increase investment values. Therefore, further applications of portfolio methods with climate models can also tackle the threats to wind development linked to aging installations in the context of re-powering decisions to increase efficiency.

3 Generating high-resolution wind fields with a new Wind-Topo in India

Background This chapter is based on a work that is unpublished. The original Wind-Topo model was developed by Dr. Jerome Dujardin and re-adjusted for purpose of this research.

Authors: Zakari Yasmine, Dujardin Jerome and Lehning Michael.

Journal: TBD.

Status: Unpublished.

Contributions: Investigation, data collection, processing and analysis, visualization, and writing.

Data availability The data are available upon request. *DOI*: NA

3.1   Introduction

The estimation of wind flow is critical for the development of wind energy. In this context, wind speeds from reanalysis datasets are widely used in wind resource assessment. However, their spatial resolution remains unsatisfactory for unraveling local wind characteristics and extracting accurate wind information. This chapter investigates a perspective on wind predictions different from the long-term climate projections presented in chapter 1 and 2 and explores the application of machine learning methods to improve surface wind estimations. In the following, we inspect the application of a new version of Wind-Topo [115], a deep learning-based model that discovers the interactions between high-resolution topography and lower-resolution states of the atmosphere to generate near-surface wind fields and predict wind flow in two geographical locations. The original model has successfully enabled the provision of high-resolution (up to 50 meters) surface wind data in the Swiss Alps. Wind-Topo's initial conception was trained with measurements from stations in Switzerland and a numerical weather prediction model (NWP) as a predictor, the Consortium for small-scale modeling family COSMO 1 [230] at 0.01° horizontal spacing.

Given its inherent uncertainty, the prediction of wind has attracted the attention of many scholars. Current methods include physical, statistical, and machine learning techniques [231]–[233]. Since the world is moving towards green energy, conflicting land use issues emerge as sites dedicated to energy assets compete with land potentially usable for agricultural farming. The growing population and densifying agglomerations add more pressure to the competition for land use and call for exploring alternative sites. Terrains suitable for wind harvesting in mountainous regions usually consist of plains and ridges without a steep slope [234]. Kruyt et al. explore the application of COSMO 1 for wind energy predictions in complex terrains [235]. Graf et al. evaluate the ability of state-of-the-art climate models for Switzerland to represent mean winds and their seasonality in areas with a complex topography and finds that the most apparent wind speed biases are persistent over mountainous terrain [111]. With the growing interest in assessing wind energy potential in complex terrains, machine learning techniques can play a significant role in effectively providing accurate wind speed predictions [112].

Deep learning, which is a type of machine learning algorithm, imitates how humans gain specific knowledge and can redefine complex data from high-input data [236], [237]. Deep learning models dominate other sophisticated machine learning methods [238]. They have contributed to many areas like speech recognition and signal processing [239], detection of diseases like Alzheimer's [240], environmental water management including pollution prediction [241]–[243], solar photovoltaic energy generation forecast models [244], [245] and most recently wind power generation forecasting [246]. Stationarity is often a prerequisite for applying machine learning techniques [247], which may limit their application in a changing environment. However, one might assume that the relationship between the input data and the terrain is stationary, which offers the possibility of exploring deep learning applications to improve long-term wind speed prediction in regions threatened by climate change to potentially create further incentives for wind energy developers to examine the feasibility of wind sites in under-explored geographical locations.

Studies on wind energy using machine learning methods in India are still rare. A recent study suggests that machine learning methods applied in one location can be used to forecast wind speed forecasting at other points distant from the training data and at different remote areas [248]. Further research on such applications in the sub-continent can add value to researchers and wind developers because access to reliable climate measurements in India over multiple years remains challenging. Currently, the National Institute of Wind Energy (NIWE) and the Indian government operate wind monitoring stations and provide mass measurements at a cost for commercial buyers and academic institutions. Wind developers in India also invest in the collection of meteorological information, yet the data collected is limited in time and is not provided for free [249]. Neighboring countries to India, such as Nepal, where wind deployment is at an early stage, also face challenges with data access. Although initiatives for resource assessment are carried out, projects also often struggle with wind data availability [250]. Hence, there could be much value in the availability of free high-resolution data.

In this chapter, we use a new version of Wind-Topo, trained with Swiss station measurements and ERA5 data [218] instead of COSMO-1, to predict near-surface winds in India and Nepal. Our objective is to assess the model's applicability to discover the interactions between wind flows and local topography and ultimately improve the availability of wind information in the area. The rationale behind this is to leverage a model that has proved successful in providing improved wind flow estimations in the Alps, reanalysis dataset ERA5, and information from available stations in the domains analyzed to explore the possibilities and limitations of machine learning algorithms.

3.2 Approach adopted and outline

Wind-Topo is a deep learning model which has a custom architecture mostly based on Convolutional Neural Networks (CNN, [251]). Wind-Topo is a state-of-the-art 2-D to-point statistical downscaling model based on deep learning that employs kilometer-resolution numerical weather prediction model outputs and high-resolution topography to predict near-surface wind speed and direction in highly complex terrain. Details about the model can be found here [115]. Its high performance in Switzerland and flexibility motivated its application to other regions. While initially developed to provide high-resolution data in Switzerland, its performance and flexibility call for further applications. In the first steps of this analysis, we tested the original form of Wind-Topo trained with COSMO 1 to provide high-resolution data in India. COSMO 1 is not available in India. Data from ERA5 interpolated to a 1 km grid, and the same height levels as Wind-Topo are used as an alternative. The first results led to a re-adjustment of the approach. The perspective adopted consists of re-training Wind-Topo with ERA5 data in Switzerland, with 261 stations used for the calibration and 60 stations for the validation. Furthermore, ERA5 data is chosen as a substitute for COSMO 1 because of its large geographical coverage. After training the model with ERA5 interpolated to a 1 km grid spacing, Wind-Topo is applied in the state of Tamil Nadu. The results in this state proved to be limited, and a new domain was explored in the northeast overlapping with Nepal. The remainder of this chapter is structured as follows;

Section 3.3 describes the data and model, Section 3.4 presents the results, Section 3.5 discusses the limitations of the approach and the next steps envisioned for future improvements, and finally Section 3.6 presents with a conclusion to this chapter.

3.3 Data and model used

3.3.1 Domains definition and measurements

The Swiss Alps domain where the new Wind-Topo is trained and its elevation are shown in Figure 3.1 **a**. Before selecting the testing domains, we evaluated various locations in India and
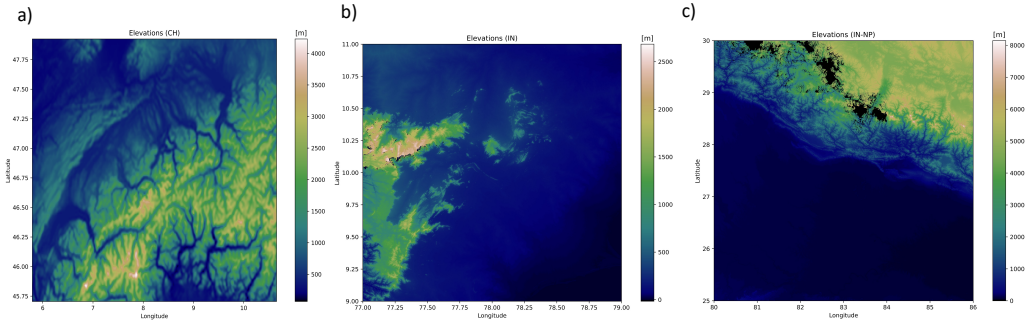
Figure 3.1: Swiss domain **(a)** and the two other candidate domains in India **(b)** and India-Nepal **(c)**.

screened ISD stations to find regions where reliable measurements were available for at least the period from 2016 to 2018. We used Google Earth to closely inspect the surrounding conditions of the ISD met station, and it revealed critical shortcomings in the data. The integrity of the measurements at multiple stations has been impacted by a surrounding environment obstructing their quality. Therefore a small number of acceptable locations were left. A practical alternative is adopted to overcome this limitation. The domain selected is constrained to the area where wind turbine data and station data are available. The domain used for the application of Wind-Topo in India is represented in Figure 3.1**b**. Measurements from the wind farm in Theni are available for thirty turbines at hub heights and ten minutes of temporal resolution. As the screening of ISD measurements uncovered an area where coherent wind speed and direction data are available in the north-east, a domain surrounding these stations is used as an input for testing the new Wind-Topo. Its elevation and limits are present in Figure 3.1**c**. We refer to this domain as IN-NP in the rest of this chapter. ISD stations considered and their characteristics are shown in Table 3.1, where the two first lines correspond to the locations in Tamil Nadu, and the last eight lines are the ones between India and Nepal. ISD measurements available at three-hourly temporal resolution are interpolated to hourly resolution.

Table 3.1: Coordinates and elevation of ISD stations used in the testing.

Name	Latitude [°N]	Longitude [°E]	Elevation [m]
Kodaikanal	28.1	81.7	2343
Valparai	28	82.5	634
Nepalgunj	28.1	81.7	165
Dang	28	82.5	634
Jumla	29.3	82.1	2300
Surkhet	28.6	81.6	720
Pokhara	28.2	84.0	827
Bhairahaw	27.5	83.4	109
Simara	27.2	85.0	137
Okhaldhunga	27.3	86.5	1720

The spatial distribution of the stations in the IN-NP domain is presented in Figure 3.2.

Figure 3.2: Illustration of ISD stations in the IN-NP domain. Each red dot represents the location of one of the eight stations considered.
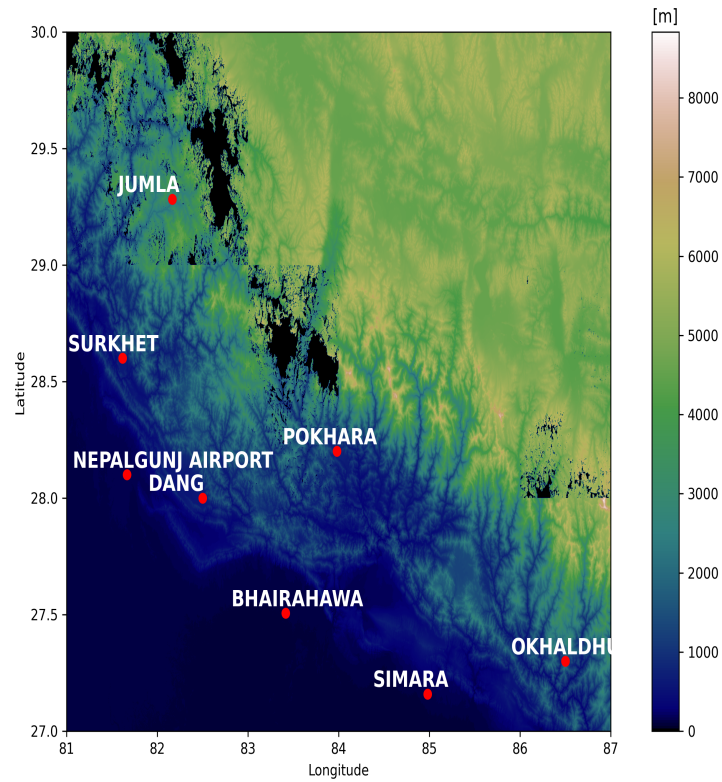
3.3.2 Construction of the predictor dataset

We use ERA5-complete at model levels[I] to construct the predictor dataset. ERA5 complete data are available at hourly time resolution and 0.25° grid spacing for 137 model levels [252]. They are obtained through the climate data store (CDS) Application Programming Interface. The variables u, v, w, and t are defined on 137 model levels. The ECMWF meteorological workstation application, Metview, is used to interpolate vertically the data from model levels to heights in meters above the ground. For u, v, and w, we use a function that interpolates a field-set on model levels onto heights in meters above ground level based on a logarithmic interpolation. The results of the vertical interpolation of the data at 10 meters above ground use ERA5 pressure data expressed as a logarithm and lead to NaN values when the values are too low. Therefore, the first height fed to Wind-Topo is readjusted to 11 meters above the ground. Once the interpolation from model levels to heights above ground is obtained, we interpolate all the variables to a 1 km horizontal resolution using the bi-cubic method. The horizontal interpolation from 0.25° grid to 1 km is performed using bi-cubic spline mapping with the Climate Data Operators (CDO) [253].

3.3.3 Analysis of ERA5 characteristics in the domains considered

As wind is influenced by local characteristics and varies in places and seasons, we evaluate annual and seasonal winds differences in the calibration domain (CH) and the testing domain (IN-NP) in Figure 3.3.

The geographical distribution of surface wind speeds in CH indicates higher wind speeds in areas where elevations are high except for the lowest level (11m). In other words, wind speed values increase with heights [235]. The examination of ERA5 wind speed in this domain indicates an inconsistency in surface wind flow pattern; winds appear to be higher in the plain than in the mountains. Wind patterns observed for levels starting from 89 or 293 m do not indicate further anomalies. Therefore, the observation of wind at the surface indicates a misrepresentation in ERA5; the sub-grid scale effect could possibly lead to an underestimation of wind at the stations located in the mountains. The 0.25° grid resolution is also most likely too large to reflect the mountain effect correctly. For stations located in the plains and sheltered areas near the ground, the flow appears to be experiencing less drag and surface wind is higher. The values in the IN-NP domain indicate that the highest wind speed values are concentrated in the northeastern regions (Figure 3.3**b**). Meanwhile, contrary to the observation in the Alps, wind speeds decrease with increasing heights in the southwest where the lowest elevations concentrate. In this case, the low-level flow appears to be blocked by the Himalayas, creating an along-barrier jet on the plains. As you move to higher altitude, the flow can progressively cross the Himalayas, creating higher winds above the mountains, and lower winds high above the plains

Figure 3.4**b** shows the seasonality of surface winds in the Swiss domain and highest wind occur during the winter season. The pattern indicates that areas where elevations are low in

---

[I]https://www.ecmwf.int/en/forecasts/documentation-and-support/137-model-levels
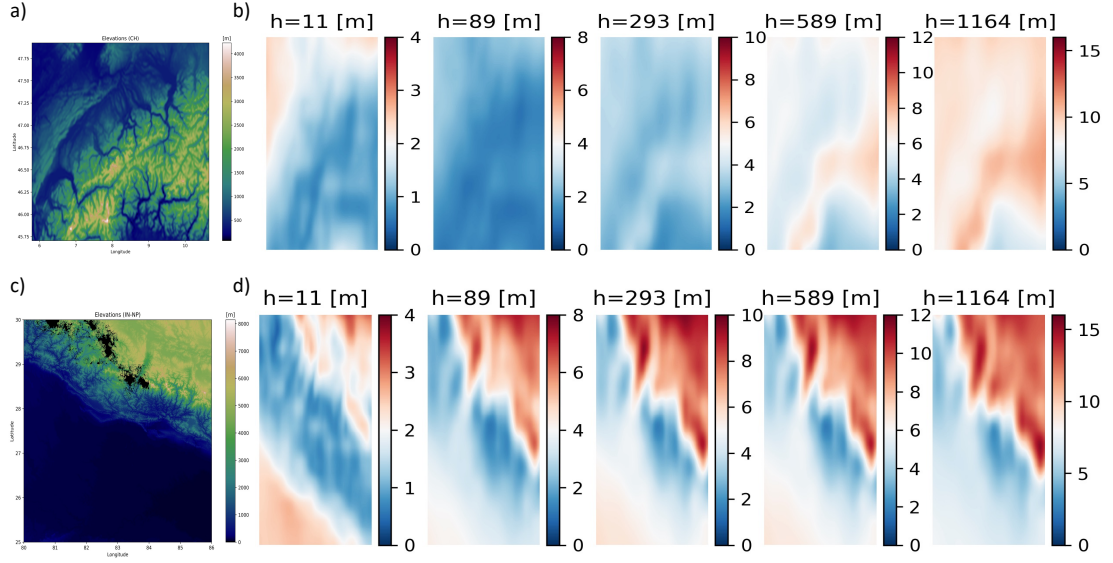
Figure 3.3: Elevation in CH **(a)** and annual wind climatology in m/s in 2017 at 5 height elevations **(b)**. Elevation in IN-NP **(c)** and annual wind climatology in m/s in 2017 at 5 height elevations **(c)**.

the northwest exhibit highest winds. The analysis of the results in the IN-NP domain (Figure 3.4**d**) show that for regions in the northeast, where elevations are the highest, wind speed has the highest magnitude in spring (MAM) and winter (DJF). For this region, low values of wind speeds occur in summer (JJA). In the south-western region, where elevations are the lowest, highest wind speeds occur in MAM and JJA. Wind speeds in India evolve from low wind speeds in January to high during monsoon months and once again decrease until November-December. The worsening in the correlation found later in some instance with Wind-Topo could be explained by the fact that the model is trained in the Alps, a geographical domain dominated by a fast-moving weather systems, while persistent patterns predominantly shape the climate in Nepal and India. In summary, except for surface wind very close to the ground, wind flows from ERA5 are higher at high altitudes in Switzerland, while they tend to be lower than expected in Nepal because of the blocking effect created by the mountainous areas; which may have to do with the way surface drag is calibrated to approximate larger scale motions and pressure distributions.

3.3.4 Wind-Topo formulation

In the original formulation of Wind-Topo, the 1.1 km resolution COSMO 1 was used as a predictor, and near-surface winds were downscaled to a 50-m resolution. In the test case, the interactions between wind and the local topography as represented by the model showed a big improvement on wind prediction. Wind-Topo requires the eastward and northward components of wind (u and v), the vertical velocity (w), temperature (t), and pressure at 10, 89, 293, 589, 1164 meters above ground. Other inputs require the ground surface sensible heat flux (sshf) and a digital elevation model (DEM) in order to predict near-surface wind flow. The Space Shuttle
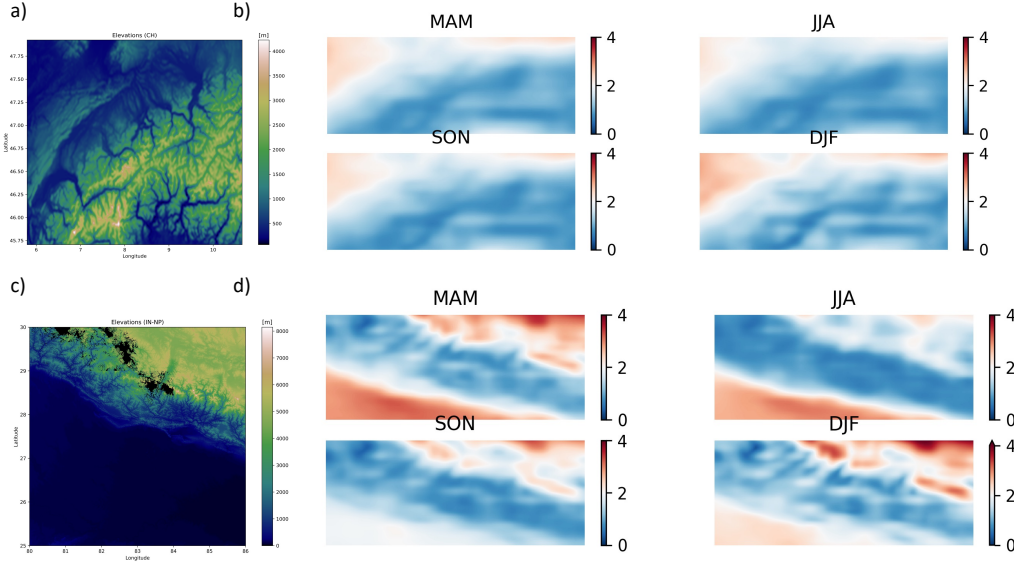
Figure 3.4: Elevation in CH**(a)** and seasonality of wind (in m/s) at the surface in 2017 for the CH domain **(b)**. Elevation in IN-NP **(c)** and seasonality of wind at the surface in 2017 (in m/s) for the IN-NP domain**(c)**.

Radar Topography Mission (SRTM) DEM available on the USGS Earth Explorer at a 30-meter resolution is used. The fact that ERA5 behaves differently in the two regions even though the difference in the altitude of the two domains is comparable, hints towards the fact that ERA5 parametrization leads to inconsistencies of the wind flow in the surface, or the resolution is too low to resolve the local effects. Furthermore, values for w (vertical wind) close to the surface appear to have problems. Therefore, the new Wind-Topo version is re-adjusted and trained without the w component of wind.

The year 2017 is used for testing in the IN-NP domain.

3.4 Results

The results of the calibration and testing are discussed in this section. The performance of the new Wind-Topo in the IN-NP domain are also presented. The performance metrics used are the mean bias error (MBE), correlation (corr), and mean absolute error (MAE) of ERA5 and Wind-Topo with the measurements.

3.4.1 Calibration and testing over the training period

The following section evaluates the results of the new Wind-Topo version at the calibration and validation stations in Switzerland. A first comparison at the wind speed values of the measurements with the values obtained from ERA5 indicates that ERA5 tends to underestimate

wind speeds in the Alps. This observation hints towards the inability of ERA5 to resolve the orographic speed-up effects at complex sites such as the Alps. Its average wind speed at the 261 stations approximates to 1.25 m/s which is not representative of the reality painted by the measurements. Wind-Topo enables to correct the underestimation bias of ERA5 and the average wind speed for the 261 stations reaches 2.6 m/s. The average correlation coefficient obtained with Wind-Topo is higher than ERA5. However, in some cases, the model has limited performance in improving the correlation with the measurements.

Table A.5 provides an overview of wind speed measurements, ERA5, and Wind-Topo and their performance for the validation stations in Switzerland. The results illustrate that at the stations where ERA5 and sizes are in the same range, Wind-Topo improves the accuracy of wind speed estimates and correlation with wind measurements. When wind speeds measured are too high, ERA5 fails dramatically at reporting the wind speed while Wind-Topo improves the estimation but the bias remains high because the values used as input are too far from reality.

To understand Wind-Topo results, Figure 3.5 displays a decomposed view for the MAE values at each Swiss station classified into three categories; exposed, sheltered, and "other".
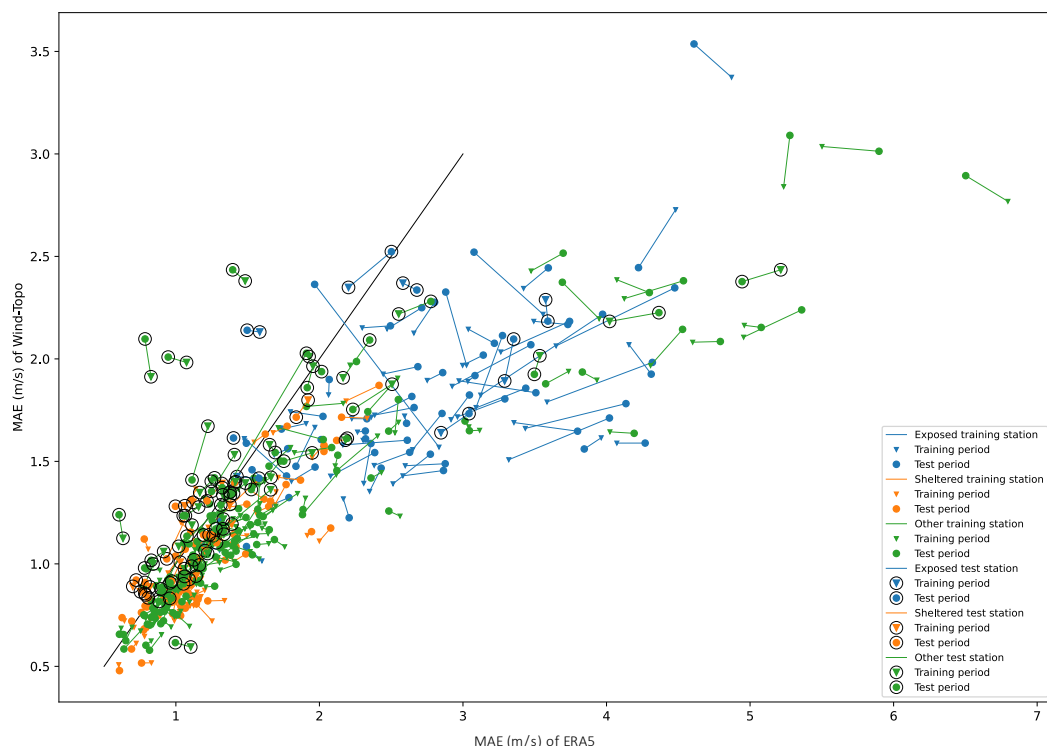
Figure 3.5: Mean absolute error of Wind-Topo at all 321 stations compared with ERA5. The segments represent the stations and colors indicate the categories. The extremities of each segment show the MAE for the training period (triangles) and the test period (circles). The stations circled in black represent the 60 test stations. Any point below the black line shows an improvement from Wind-Topo.

Each segment represents a station in Figure 3.5. The extremities of each segment are the scores

of the training and test periods. We focus on the ones circled in black to evaluate the test stations. Any point under the black curve means that Wind-Topo has a lower MAE than ERA5. The figure indicates that Wind-Topo has a lower MAE than ERA5 for the three types of stations. Wind-Topo still demonstrates some limitations at some of the "other" stations type and is significantly worse at them, where the bias is between 2 and 2.5 m/s. Wind-Topo strongly decreases the MAE at the sites with high ERA5 MAE. Furthermore, we can also examine how the MAE in ERA5 changes from one period to another and how Wind-Topo responds to it by looking at the orientation of the segments. A parallel segment orientation reflects that Wind-Topo follows the variation of score in ERA5. An upward deviation from this orientation (triangle to circle) shows that Wind-Topo has lower performance for the test period.

The clustering of exposed and sheltered sites is more pronounced where looking at the MAE results for wind directions on Figure 3.6. In this case, we observe Wind-Topo significantly improves wind direction estimation for these two site types. The MAE of wind direction obtained with Wind-Topo at sheltered sites is worse at only three stations.
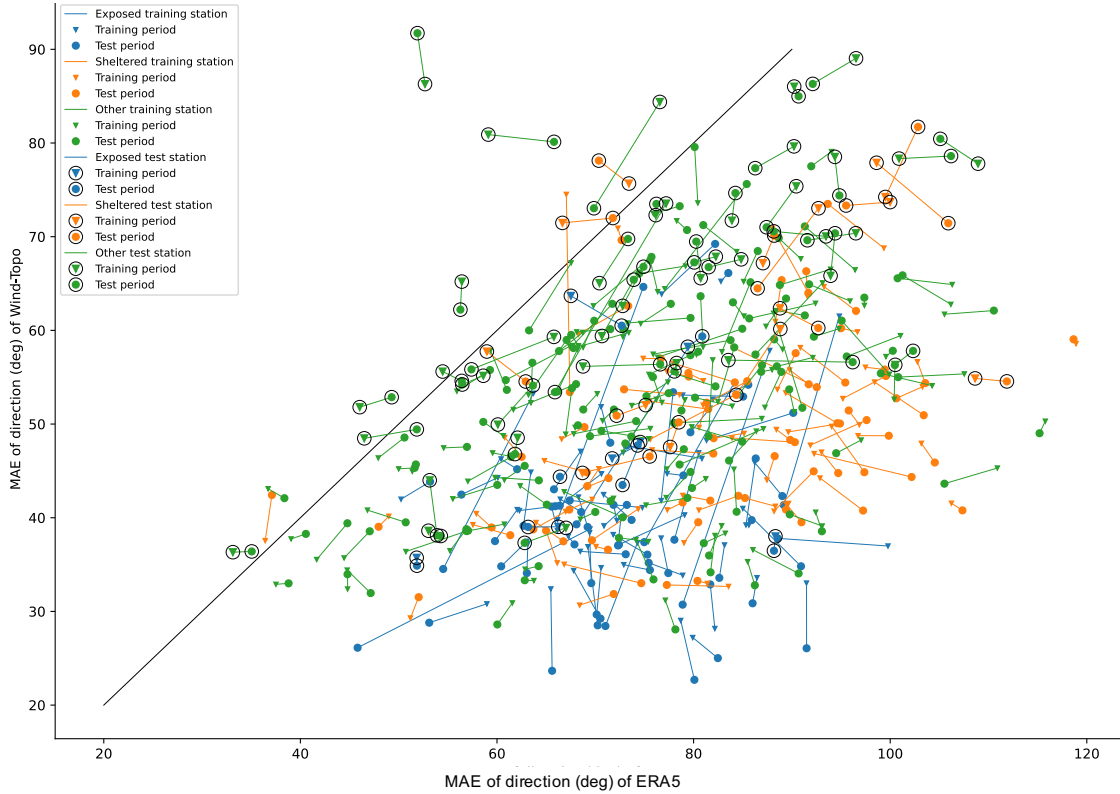
Figure 3.6: Mean absolute error of the direction for Wind-Topo at all 321 stations compared with ERA5. Similarly to the figure above, the stations circled in black represent the 60 test stations. Any point below the black line shows an improvement from Wind-Topo. The segments represent the stations and colors indicate the categories. The extremities of each segment show the MAE for the training period (triangles) and the test period (circles).

Similarly, Figure 3.7 illustrates the results of the correlation at the individual stations. The

clustering of the segments above the black line demonstrates that Wind-Topo shows improved performance at most sites. Wind-Topo is clearly better than ERA5 at all exposed stations. It is also the case for most sheltered ones.
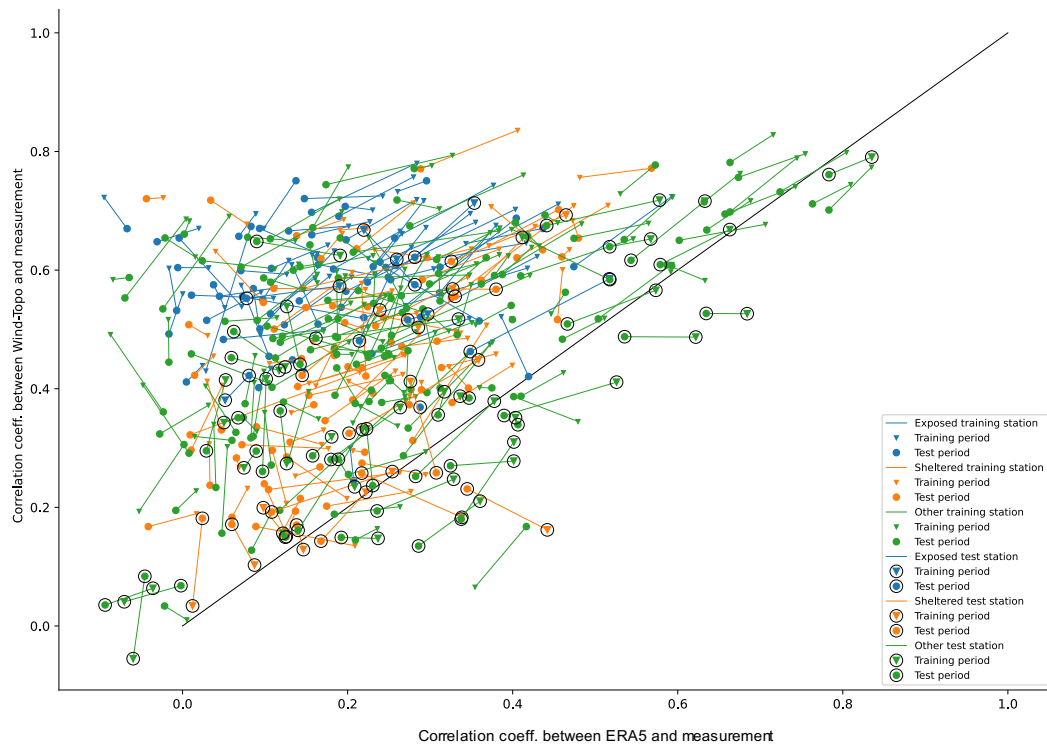
Figure 3.7: Correlation coefficient (coeff.) for Wind-Topo at all 321 stations compared with ERA5. Similarly to the figure above, the stations circled in black represent the 60 test stations. Any point above the black line shows an improvement from Wind-Topo. The segments represent the stations and colors indicate the categories. The extremities of each segment show the correlation coeff. for the training period (triangles) and the test period (circles).

Results of the temporal dimension of Wind-Topo can be evaluated in Figure 3.8. This figure includes the inter-quartile and median values obtained at the test stations in bold colors for Wind-Topo and more transparent ones for ERA5. The results on the plot at the top indicate that for ERA5, we see similar wind magnitudes at sheltered and exposed sites. This suggests that the resolution of ERA5 is not high enough to distinguish between the two. The second plot illustrates that Wind-Topo always corrects this bias. The third plot, showing the correlation, demonstrates improved Wind-Topo performance at exposed sites in winter and summer. The correlation for Wind-Topo is also better than ERA5 at the sheltered and "other" stations. Finally, wind speed and direction MAE are always lower with Wind-Topo. Hence, we can conclude that Wind-Topo performs better at almost all stations and during all seasons.
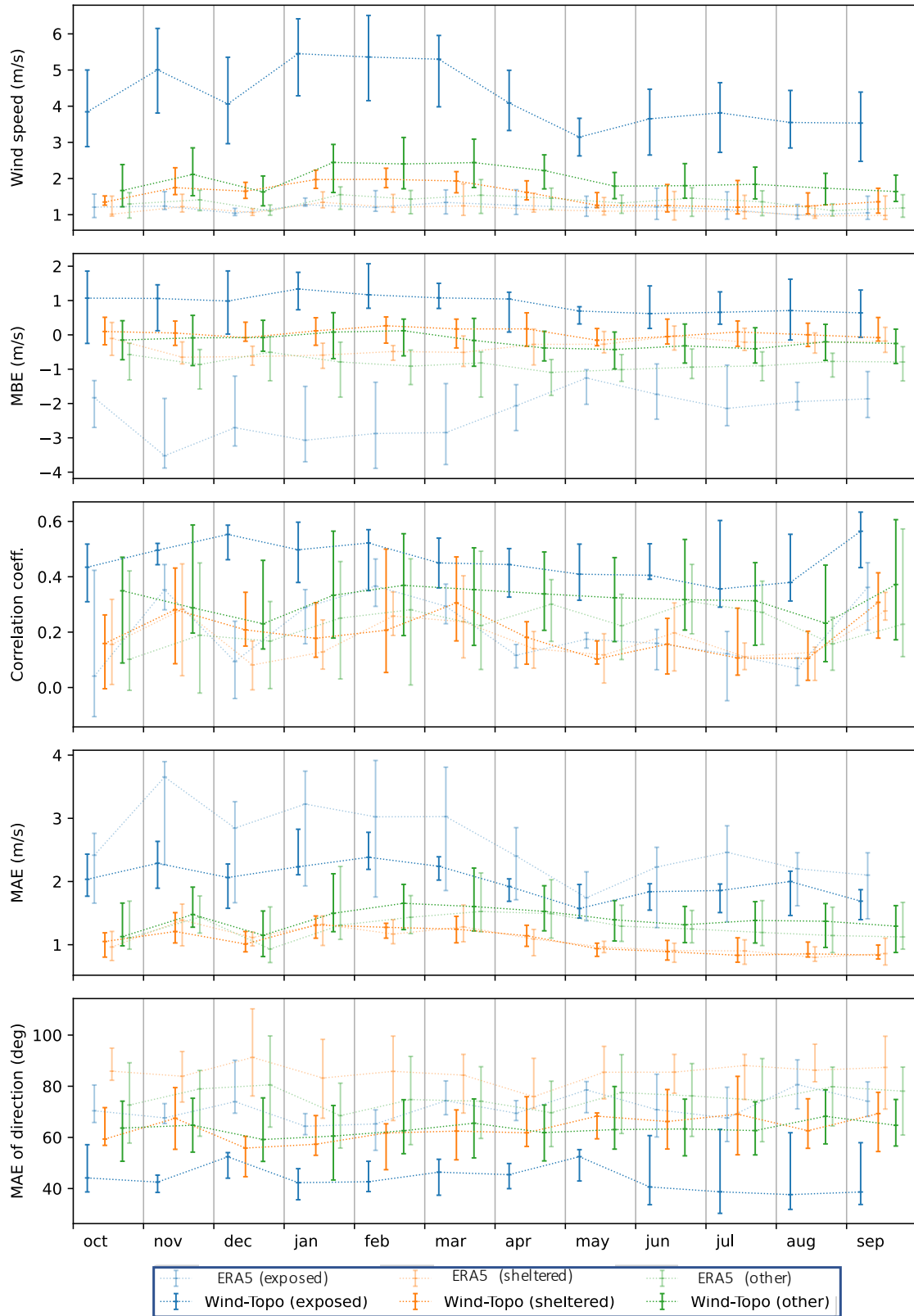
Figure 3.8: Each section illustrates monthly average values for the 3 types of test station along with the inter-quartile and median values. Wind-Topo is presented in bright and ERA5 in dimmed colors.

To better understand the behavior of Wind-Topo, we look at the wind-rose diagrams (Figure 3.9) from the measurements, ERA5 and the new Wind-Topo at three test stations with different expositions, namely ELA-1 (exposed station), ELA-2 (sheltered), and SAM-0 ("other"). Wind-Topo results show a similar pattern to the measurements at the sheltered station, where ERA5 has a larger error in wind speed and direction. At the exposed station (ELA1), the wind direction depicted by ERA5 is wrong, and Wind-Topo is not able to entirely correct the pattern. A similar pattern is observed at SAM-0 where the ERA5 direction is altogether erroneous. At this station, Wind-Topo shifts the direction to resemble the measurements.
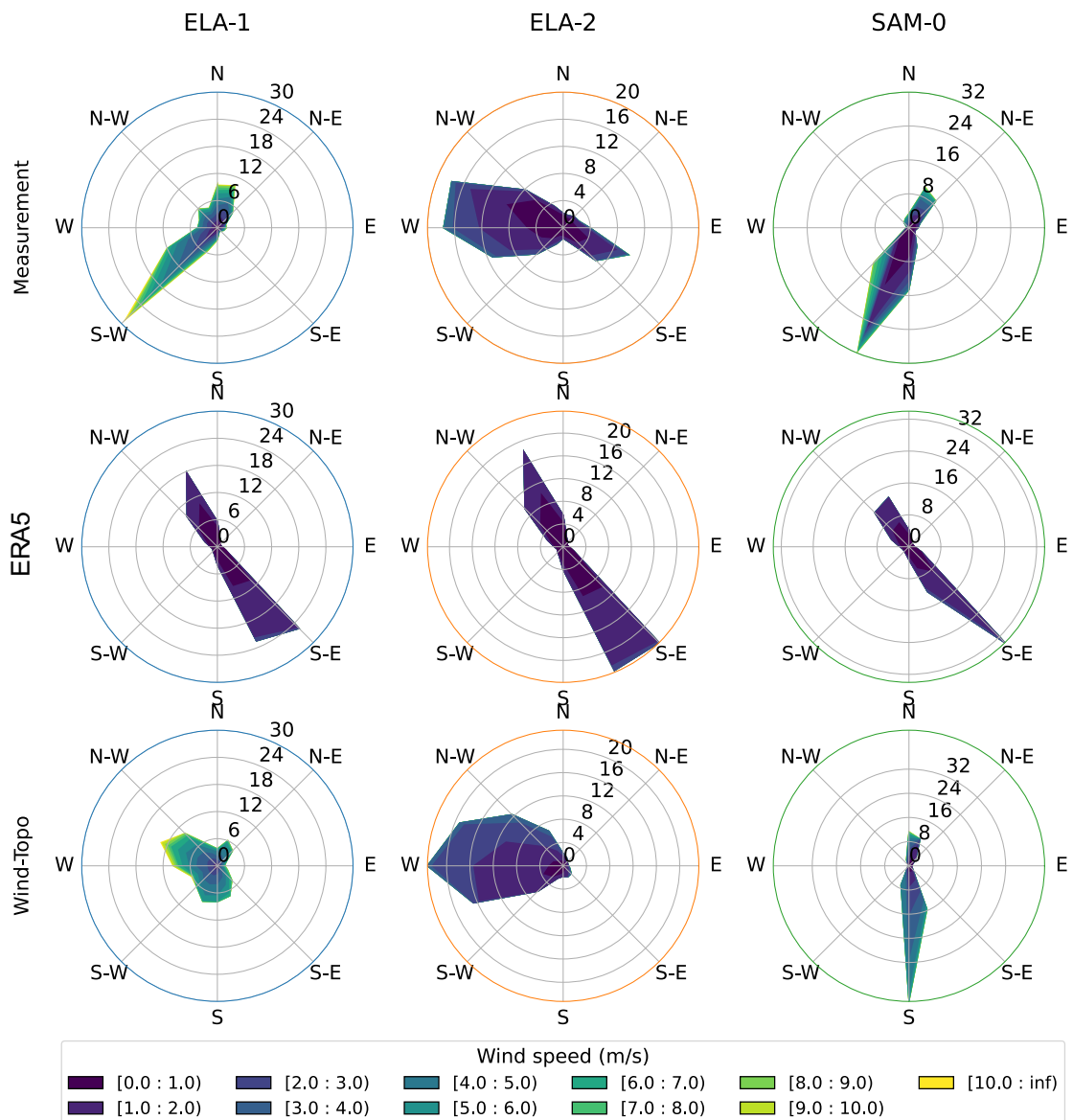
Figure 3.9: Each column represents the wind rose for ELA-1 (exposed station), ELA-2 (sheltered), and SAM-0 (other) for the measurements, ERA5 and Wind-Topo.

A closer look at the probability distribution of the three data sources confirms that ERA5 distribution does not capture the pattern exhibited at the exposed site. The observation of the results at ELA-1 in the top left panel of Figure 3.10 indicates that ERA strongly underestimates and does not get the correct diurnal profile while Wind-Topo does a remarkably good job there. The results found for ELA-2 show that ERA5 does not do too badly in the representation of winds but misses the tail of the distribution. Wind-Topo helps a bit but overestimates because it introduces diurnal fluctuations that are too high. At SAM-0, Wind-Topo increase the diurnal pattern, and can capture the tail of the distribution but at a cost of a strangely shaped distribution.
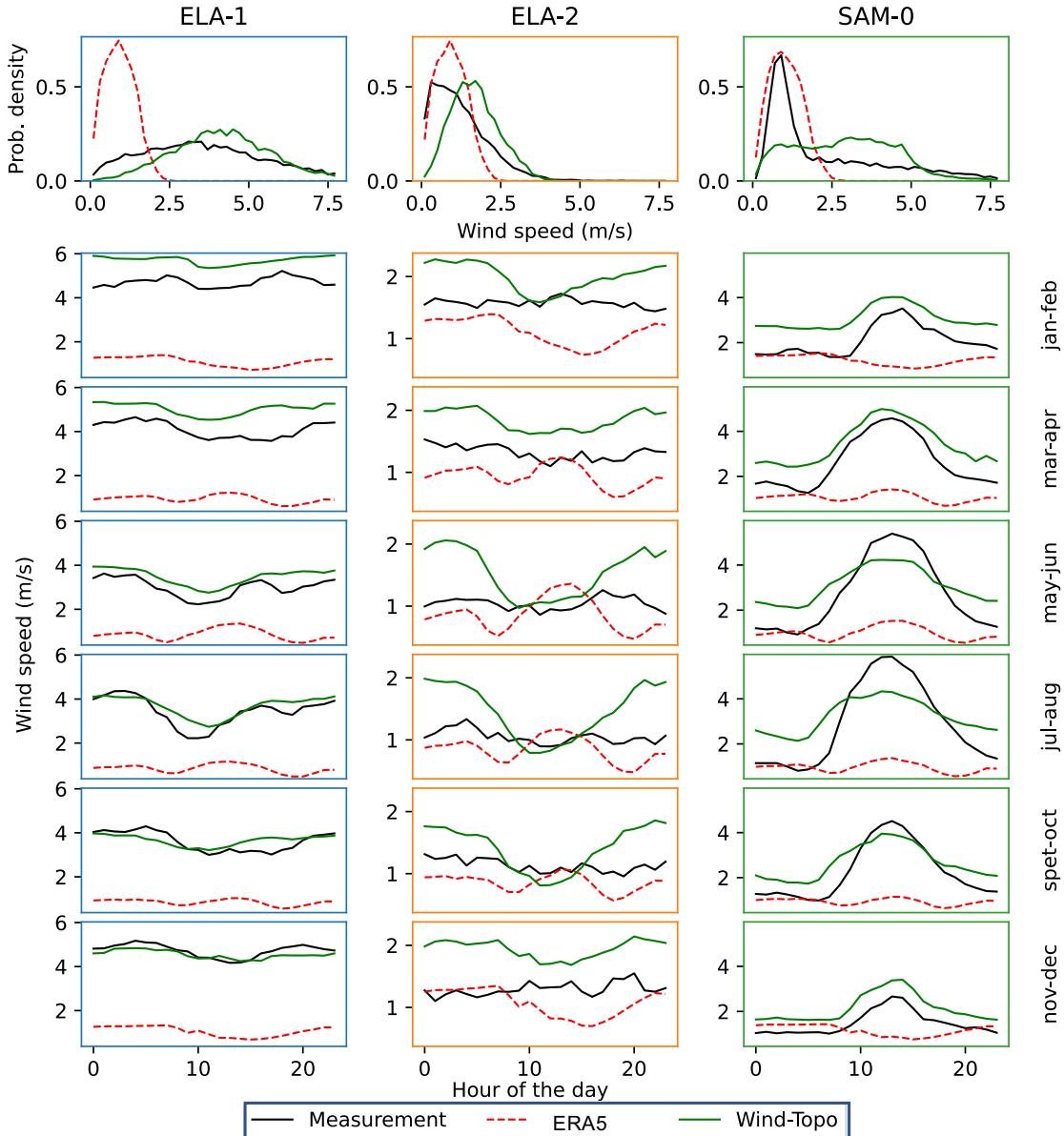
Figure 3.10: Each column represents the probability density function for ELA-1 (exposed station), ELA-2 (sheltered), and SAM-0 (other) for the measurements, ERA5 and Wind-Topo. The other panels indicate the bi-monthly diurnal wind distribution.

3.4.2 Application of the new Wind-Topo in the IN-NP domain

In this section, we present the results obtained with the new Wind-Topo model at the eight sites surveyed in the IN-NP domain. Table 3.2 summarizes the average wind speeds from the measurements, ERA5 and Wind-Topo, and the performance metrics.

Table 3.2: Comparison of the scores for ERA5 and Wind-Topo in Nepal

Stations	Vel_{meas}	Vel_{WT}	Vel_{ERA5}	MBE_{WT}	MBE_{ERA5}	$corr_{WTO}$	$corr_{ERA5}$	MAE_{WT}	MAE_{ERA5}	$rmse_{WT}$	$rmse_{ERA5}$
Nepalgunj	1.90	3.08	1.67	1.19	-0.23	0.28	0.42	1.76	0.85	2.33	1.21
Dang	0.77	1.56	1.57	0.79	0.80	0.36	0.28	0.96	0.90	1.30	1.10
Jumla	1.03	1.30	1.05	0.27	0.02	0.13	0.22	0.84	0.68	1.27	1.06
Surkhet	2.23	1.35	1.05	-0.88	-1.18	0.39	0.33	1.17	1.32	1.50	1.64
Pokhara	1.77	1.28	0.95	-0.49	-0.82	-0.08	-0.07	1.09	1.14	1.35	1.39
Bhairahawa	2.99	2.79	1.74	-0.20	-1.25	0.31	0.55	1.85	1.64	2.45	2.32
Simara	1.43	3.15	1.79	1.72	0.36	0.31	0.39	1.94	0.84	2.47	1.03
Okhaldhunga	1.07	1.04	0.89	-0.04	-0.19	0.26	0.24	0.64	0.53	0.94	0.88

Table 3.2 shows that the MBE value for Wind-Topo is between -0.88 and 1.72 m/s, and -1.25 m/s and 0.80 m/s for ERA5. The MAE for Wind-Topo ranges from 0.64 to 1.93 and from 0.53 to 1.64 for ERA5. The RMSE values range from 0.94 m/s to 2.47 for Wind-Topo, and from 0.88 to 2.32 m/s for ERA5. The average correlation obtained with Wind-Topo 0.25 is slightly lower than the average 0.29 value found for ERA5. A closer look at the sites enables us to detect noticeable improvements realized by Wind-Topo at four mountain locations: Dang, Surkhet, Pokhara, and Okhaldhunga. Overall, the MBE at the four locations is reduced by 0.20 m/s, and the correlation increased by 0.04. At Dang, the MBE is reduced by 0.01 m/s, and the correlation increases by 28%. At Surkhet, the MBE is reduced by 0.30 m/s, MAE by 0.15 m/s, and RMSE by 0.14 m/s. Wind-Topo improves the correlation value with the measurements in Surkhet by 17.4%. At Pokhara, the MAE, MBE, and RMSE are reduced by 0.33, 0.06, and 0.04 m/s. Wind-Topo correlation is also higher than ERA5; however, both correlations at this station are close to zero. At Okhaldhunga, the correlation obtained for Wind-Topo is increased by 7 % compared to ERA5, and the MBE is reduced by 0.15 m/s. At Jumla, the station at the highest altitude, the Wind-Topo model shows no improvement likely because of missing values in the DEM. For stations located in the plains at altitudes lower than 200 meters, Wind-Topo overestimates the wind speeds, as illustrated by the values obtained in Nepalgunj and Simara. We observe a different behavior at Bhairahawa where the average wind measured is 2.98 m/s, Wind-Topo's value is 2.78 m/s, while the estimation given by ERA5 is lower (1.74 m/s). In this station, the bias improvement comes along with a slight deterioration of the Wind-Topo correlation with the measurements. In conclusion, Wind-Topo as it is at the moment is not very useful in India and adds value only at stations where the elevations are high.

3.5   Future improvements and limitations

The limited performance observed for Wind-Topo results in India indicates an over-fitting of Wind-Topo with the Swiss stations. The over-fitting impacts on wind flow estimation in low elevations. The most critical improvement to implement next is training Wind-Topo with data from each one of the domains considered. Therefore, given its relevance and importance, obtaining data collected from high-quality wind sensors from measurement sites in India and Nepal is required. Higher resolution, better model physics, more data assimilated, and more advanced assimilation methods enable ERA5 to improve measurements representation compared to its predecessors [254]. While ERA5 data help estimate weather conditions in areas with no land measurements, some question marks remain regarding its reliability compared to land measurements, and evident discrepancies are still found.

With the default sub-grid scale settings, the bias observed for ERA5 in the CH domain is an explicit limitation for using the reanalysis dataset in regions with complex geographies like the Alps. Regarding the IN-NP domain, ERA5 underestimates wind speeds, particularly during summer. ERA5 bias at the surface can be explained by deficiencies of the sub-grid scale orographic parameterization in the Integrated Forecasting System (IFS) that it uses [255]. Processes that are only partly physically represented in a model have to be parameterized. The shortcomings of the parametrization in IFS can originate from the misrepresentations observed for ERA5 at lower levels. IFS underestimates orographic drag due to gravity wave breaking, notably in the low stratosphere [256]. IFS underestimation of the orographic drag is also found for other models, including COSMO [257]. The orographic drag is parameterized as part of the sub-grid scale orographic (SSO) drag scheme, which also includes a low-level drag component (wake drag) [258]. Studies suggest that a better representation of orographic drag can result in an improved representation of blocking frequency and duration [259]–[261]). The SSO drag scheme in ERA5 represents the gravity wave drag exerted by the breaking of orographically generated vertically propagating gravity waves and flow blocking drag due to the deflection of the flow by the orography at low levels. The underestimation observed in the mountainous areas can be due to the flow being blocked because the current IFS scheme assumes vertical flow deflection when mountain barriers are encountered [256]. The flow is blocked at a certain height as it is assumed not to be able to cross the mountain barrier because it does not have enough energy to cross over it due to weak winds or strong atmospheric stability. The SSO scheme can be altered by adjusting three parameters; decreasing the orographic gravity wave drag constant, altering the low-level wake drag constant (which reduces the near-surface drag), and the critical Froude number (which decreases the orography blocking) [262]. Kohler et al. improve sea level pressure representation, and estimation of the stratospheric westerlies in the NWP model ICOsahedral Nonhydrostatic atmospheric model ICON by altering the parameterizations for the gravity wave drag [262].

More realistic zonal winds representation in the current IFS version is achieved by decreasing the strength of the turbulent orographic form drag while enhancing the low-level flow blocking [256]. Therefore, an adjustment of the SSO drag parameterization can reduce the error by tuning the Froud number, decreasing the strength of the turbulent orographic form drag, and enhancing the

low-level flow blocking.

The bias in wind estimation found for ERA5 at the stations suggests that higher Wind-Topo accuracy can be gained by tuning the SSO in the IFS scheme of ERA5 to correct the inadequacies and then feeding the re-tuned output to re-train Wind-Topo. An alternative to ERA5 re-tuning can be correcting the bias using Swiss station measurements.

Similar to other studies on wind prediction with machine learning algorithms, data preparation is necessary to gain accuracy and avoid porting input dataset errors to the results [263]. For this analysis, ERA5 data have been extrapolated vertically and horizontally to match the requirements of Wind-Topo and provide with high-resolution wind flows. The coarser scale of ERA (compared to COSMO-1) leads to an even larger gap between atmospheric phenomena represented by the NWP model and the ones that Wind-Topo tries to reproduce. Wind-Topo's architecture was designed to extract the most information from COSMO-1, given the scales represented by this NWP model. For ERA-5, an adaptation of the architecture to those new scales would probably lead to better results. Ultimately this would provide with additional data to support decision makers for constructing wind farms in regions where reliable data are scarce and eventually suggest future wind sites in terrains where the geography is complex.

3.6   Conclusion

The availability of high-resolution wind data, including wind speed and direction accounting for the impact of terrain, enables predictions on wind potentials and supports the development of wind farms. Without accurate forecasts, accurate planning for wind generation development is impeded. Leveraging the capabilities of machine learning to provide estimations of local wind data in complex terrain in India and Nepal could provide opportunities for wind developers to estimate wind patterns with a reduced data collection cost.

This chapter investigated methods to improve the availability of wind projection and test the applicability of Wind-Topo in other areas. The motivation was to provide a scientific basis for the availability of more reliable wind flow estimations. In the first steps, we used the formulation of Wind-Topo as it is to a domain selected in India. The unsatisfactory results led to re-training the model with ERA5 in 261 Swiss stations used for calibration and 60 for validation. ERA5 data is used as an alternative to COSMO 1 because of its extensive geographical coverage. After training the model with ERA5, Wind-Topo is applied in the state of Tamil Nadu in India. Furthermore, the limited number of stations to evaluate the results pushes for exploring another domain where altitudes are high and more testing stations are available. The results in Nepal indicate that wind-flow estimations with Wind-Topo have a lower bias than ERA5 in some stations but that overall improvements through the application of Wind-Topo are much smaller than in Switzerland and may even be insufficient for practical application. Wind-Topo is retrained without the w component and climate variables at the lowest level. The results indicate that Wind-Topo performs better than ERA5 at almost all stations in Switzerland and during all seasons. Wind-Topo strongly decreases the MAE at the sheltered sites with high bias values with ERA5. Wind-Topo also lowers the MAE at sheltered sites. It also improves the estimation of wind direction estimation for the Swiss exposed and sheltered sites. The model has a higher correlation coefficient with the measurements than ERA5. The analysis of ERA5 at the Swiss sites indicates its inability to distinguish between sheltered and exposed sites. In the testing domain in IN-CH, Wind-Topo improves the estimation at four mountain locations; namely Dang, Surkhet, Pokhara, and Okhaldhunga. Overall, the MBE at the four locations is reduced by 0.20 m/s, and the correlation increased by 0.04. However, for the stations located in the plains and lower altitudes, Wind-Topo overestimates the wind speeds. Other areas with complex topographies and better measurements like Hong Kong are good candidates for further case studies.

Overall this study adds to the existing literature of studies on wind using machine learning algorithms. Our investigation reveals that machine learning models trained with wind speed data from one location can predict wind speeds effectively in other areas. Still, limitations exist in the geographical scope to offer beneficial results. Furthermore, the analysis of ERA5 in this chapter reveals its limitation in describing the local weather in the closest way to reality. Future work shall consider re-tuning of ERA5 data and re-training Wind-Topo with the output.

Conclusions

This Ph.D. thesis investigates the use of climate information to assess the impacts of climate change on wind and solar energy production and chooses India as a case study. In Chapter 1, the latest CORDEX South Asia RCMs were evaluated to estimate the impact of climate change on future wind resources in the Indian sub-continent. The results indicate increasing annual wind speed trends in the northwest, the center, and the east of the country under the high climate warming scenario until the end of the century, with changes occurring more substantially during the last 30 years. We also find that future perturbations are expected to occur during the pre-monsoon season throughout the Indian sub-continent and that trends with the highest magnitude concentrate during the monsoon season. Regions where wind trends showed an increase should be analyzed further to infer future wind development plans. Our findings on future wind prospects provide energy developers with an overview of wind sensitivity to climate change.

In Chapter 1, we analyzed differences between climate models, measurements, and wind farm data. We calculated trends from climate models without correcting the bias because the length of the measurements available locally was too short to allow their usability. For this reason, we recommend that energy stakeholders invest in installing meteorological stations to measure wind resources and ensure the data is adequately stored and made accessible. Data availability in the future would be beneficial for further climate studies.

A tool to quantify the Spatio-temporal consistency of wind trends based on a structure-function is suggested and applied to two families of CORDEX RCMs. The function quantitatively measures and visualizes trends coherence from climate models. We find that WAS-22 is more consistent than WAS-44. The application of the method to WAS-22 CORDEX and future downscaled CMIP6 GCMs models will allow analyzing the differences in consistency between the trends presented in the results and the new models when available. Such assessment would enable an evaluation of the robustness of the climate change signal considering future modeling improvement.

Chapter 2 further evaluates how the uncertainty regarding the overall trend in changing wind speed and solar radiation due to climate change can be reduced by judiciously combining assets. For India, we demonstrate that the uncertainty about the portfolio of wind and solar assets could be reduced by optimizing the combination of wind and solar assets, thus mitigating the economic impact of climate change. We found a reduction level in uncertainty expressed as return variability for mixed portfolios ranging from 33% to 50% when compared to pure wind portfolios and

from 30% to 96% when compared to pure solar assets. The reductions stem from the negative correlation of wind and solar potential trends, which is stronger in some areas than in others. The work presented in Chapter 2 contributes to the literature on strategies and actions that can be pursued to move towards climate-resilient portfolios.

Overall, our efforts contributed to understanding the strengths and limitations of long-term climate information. We assessed data requirements, timescales, and spatial resolutions to embed in the portfolio framework to consider the long-term impacts of climate variables. The approach to estimating the energy yield of wind and solar assets developed in this thesis can be seen as an attempt to complement existing methods, e.g. deployed by the wind industry, by providing a first estimate of the long-term impacts of climate change. Energy estimations shall be further refined with more sophisticated methods.

Future work shall also consider incorporating other technologies in the portfolio exercise with the inclusion of offshore wind. As rising temperatures are expected in India due to climate change, another critical aspect of supplementing this thesis would be to compare the performance of various PV technologies. A more granular definition of solar technologies in such an exercise could also add value to shaping future climate-proof portfolios by adding diversity and reducing climate change risk. Future investigations shall also include the analysis of the impact of climate change on the evolution of haze conditions.

Another application foreseen for portfolio analysis is assessing the level of resilience of power generation technology options to help determine the energy production mix offering the best collective resilience to climate change, with full consideration of their geographic context and supply chains. Such application would allow the analysis of the risk-benefits of energy infrastructure investments in specific locations and discovery of larger-scale governance mechanisms promoting long-term energy security and resilience to a changing climate.

Research efforts were focused on climate information, and the results presented did not cover the economic aspects of climate change. The question of how climate change uncertainty affects future investments in wind and solar projects remains open. Such investigations would require the inclusion of project data inaccessible at the time of the thesis to formulate investment strategies accounting for climate-induced uncertainties.

The new version of Wind-Topo (Chapter 3) outlines a promising perspective for providing high-resolution surface wind flow predictions. The results indicate that the model performs better than ERA5 at almost all stations and during all seasons in Switzerland's training and testing stations. The analysis of ERA5 in the Swiss Alps indicates its inability to distinguish between sheltered and exposed sites because of its current spatial resolution. The new Wind-Topo model decreases the bias at exposed stations and improves the estimation of wind direction for the Swiss exposed and sheltered sites. Furthermore, the model shows a higher correlation coefficient with these measurements than ERA5. When applied to the domain overlapping with Nepal, Wind-Topo improves the estimation of the wind flow in the mountains. The results obtained at the stations

in the valleys highlight some limitations of the model as the training on the Swiss topography produced a wrong behavior. The investigation in (Chapter 3) features a limitation of machine learning methods applied for downscaling purposes. It shows that while a model can work well in a specific region, its performance is not guaranteed in other locations. Despite the current limitations, Chapter 3 provides a scientific basis for the development and the availability of more reliable and low-cost wind estimations by exploring the use of Wind-Topo in a region where wind measurements are needed. Suppose more station measurements become available or the model is re-trained with a re-tuned ERA5. In that case, it could support the development of wind farms by providing high-resolution wind maps, including wind speed and direction, accounting for the impact of terrain. Further studies must be completed to assess the application of the new Wind-Topo version to other areas and investigate ways to overcome the bias linked to ERA5 as a predictor.

India has been a promising case study because the work conducted in this Ph.D. thesis paves the way to perform similar research in other South-Asian countries. The possibility to upscale the findings and transpose this region-specific case study to other locations has yet to be carried out in future work.

Last but not least, future work shall maintain the efforts dedicated to incorporating climate models in long-term decision-making and bridge the gap between academia and the industry on climate information. Throughout this project, the accuracy of climate model predictions has been a constant challenge. Yet we argue that uncertainty cannot justify inaction.

A Appendices

A.1 Performance of ERA5 in simulating daily and monthly winds

The values of the statistical metrics of ERA5 and ISD data comparison at the monthly and daily resolution are presented on Table A.1.

Table A.1: Analysis of the statistical metrics values of ERA5 and ISD at the monthly and daily resolution.

	RMSE		MAE		fBias		Pearson		R^2	
Stations	**Monthly**	**Daily**	**Monthly**	**Daily**	**Monthly**	**Daily**	**Monthly**	**Daily**	**Monthly**	**Daily**
Jaisalmer	0.87	2.27	0.34	1.35	1.00	2.25	0.90	0.53	0.81	0.28
PBO Anantapure	1.00	1.52	0.53	1.11	1.37	1.96	0.84	0.59	0.70	0.34
Coimbatore	1.06	1.35	0.33	0.40	0.69	0.68	0.87	0.77	0.76	0.59
Belgaum	2.59	2.68	8.6	12.90	9.55	13.90	0.88	0.56	0.77	0.32
Porbandar	0.84	1.48	0.20	0.39	1.09	1.10	0.77	0.45	0.59	0.20
Rajkot	1.02	1.49	0.28	0.38	0.78	0.92	0.84	0.48	0.71	0.23
Chamarajnagar	0.98	2.16	0.78	1.46	1.61	2.20	0.72	-0.04	0.52	0.00
Bangaluru	1.47	2.10	0.30	0.46	0.77	0.85	0.64	0.27	0.41	0.08
Kolhapur	1.22	1.66	0.48	0.52	0.97	1.11	0.54	0.13	0.29	0.02
Bangalore	1.46	1.88	0.80	1.54	1.69	2.46	0.55	0.16	0.31	0.03
Thanjavur	1.53	1.87	1.50	1.84	2.46	2.79	0.47	3.22	0.22	0.01
Ahmadnagar	2.07	2.48	11.8	3.7	12.8	4.7	0.41	-0.02	0.17	0.00
Madurai	1.17	2.00	1.58	3.22	2.50	4.19	0.06	-0.06	0.00	0.00
Coonoor	0.89	1.33	0.92	1.19	1.77	1.95	0.20	0.00	0.04	0.00
Palakkad	1.33	1.60	1.27	1.72	1.90	2.45	-0.08	-0.03	0.01	0.00
Davanger	2.62	2.68	4.2	4.57	5.13	5.56	0.06	0.06	0.00	0.00
Dharwad	2.63	2.71	4.3	4.60	5.23	5.60	-0.10	0.06	0.01	0.00

A.2 Bias and correlation of CORDEX data with local measurements

The results in other ISD sites (Table A.2) show a similar pattern with correlations averaging 0.36 with ISD measurements and 0.60 with ERA5.

The average correlation between ISD and WAS-22 value are low and close to 0 in Conoor, Davangere, and Dharwad, suggesting a potential issue in the ISD data. The fraction bias values found when ERA5 is taken as a reference are smaller than ISD despite values over 2 in 6 sites. For the bias, when ISD data are compared to WAS-22, we found 8 sites where the values do not exceed two and range between 1.08 in Bangaluru and 1.91 in Anantapur. Other sites, including

Table A.2: Summary of the fraction bias (fBias) and Pearson correlation (P.corr) and values of WAS-22 with ISD and ERA5 data.

	Reference datasets	ISD		ERA5	
Metrics	Sites	RCP 2.6	RCP 8.5	RCP 2.6	RCP 8.5
fBias	Jaisalmer	1.25	1.37	1.93	2.05
	Anantapur	1.91	1.83	1.63	1.53
	Coimbatore	1.35	1.26	2.56	2.38
	Belgaum	1.39	1.35	2.40	2.13
	Porbandar	1.31	1.32	1.21	1.23
	Rajkot	1.17	1.15	1.56	1.52
	Chamarajnagar	3.26	3.03	2.29	2.03
	Bangaluru	1.10	1.08	1.65	1.60
	Kolhapur	1.28	1.36	1.80	2.00
	Bangalore	2.43	2.36	1.65	1.59
	Thanjavur	3.60	3.53	1.69	1.61
	Ahmadnagar	17.5	18.2	1.47	1.56
	Madurai	3.83	4.96	2.94	3.68
	Coonoor	3.97	3.61	2.72	2.36
	Palakkad	3.02	2.88	2.47	2.29
	Davangere	6.90	6.75	1.73	1.63
	Dharwad	6.11	5.94	1.69	1.65
	Udhagamandalam	4.19	3.97	2.85	2.56
P.corr	Jaisalmer	0.63	0.65	0.64	0.66
	Anantapur	0.52	0.53	0.61	0.63
	Coimbatore	0.58	0.62	0.68	0.71
	Belgaum	0.58	0.61	0.66	0.70
	Porbandar	0.59	0.57	0.62	0.58
	Rajkot	0.62	0.62	0.71	0.72
	Chamarajnagar	0.37	0.45	0.51	0.63
	Bangaluru	0.41	0.43	0.52	0.53
	Kolhapur	0.34	0.42	0.68	0.68
	Bangalore	0.24	0.29	0.46	0.49
	Thanjavur	0.33	0.30	0.38	0.42
	Ahmadnagar	0.45	0.45	0.73	0.71
	Madurai	0.22	0.23	0.58	0.60
	Coonoor	0.06	0.09	0.40	0.48
	Palakkad	0.10	0.11	0.44	0.49
	Davangere	0.00	0.07	0.53	0.61
	Dharwad	0.05	0.09	0.52	0.58
	Udhagamandalam	0.13	0.17	0.45	0.49

Ahmadnagar, Davangere, and Dharwad, are even more problematic, with values between 6 and 18.

A.3   Area-averaged annual trends in four Indian domains

Table A.3: WAS-22 RegCM4 individual models area-averaged mean annual trends and standard deviation (SD) per sub-domains period 2006 to 2100.

Models	RegCM4-MPI				RegCM4-NCC				RegCM4-MIROC			
Scenarios	RCP 2.6		RCP 8.5		RCP 2.6		RCP 8.5		RCP 2.6		RCP 8.5	
Regions	Mean	SD	Mean	SD	Mean	SD	Mean	SD	Mean	SD	Mean	SD
N-W	-0.01	0.01	0.07	0.03	0.00	0.01	0.02	0.01	0.00	0.01	0.09	0.03
T-N	0.00	0.02	-0.04	0.07	-0.03	0.03	-0.05	0.06	-0.02	0.04	-0.05	0.09
Center	-0.01	9.20×10^{-3}	-0.04	1.76×10^{-2}	0.00	9.20×10^{-3}	0.02	5.00×10^{-3}	0.02	9.60×10^{-3}	0.08	2.12×10^{-2}
East	-0.01	6.10×10^{-3}	0.04	2.82×10^{-2}	-0.01	8.20×10^{-3}	0.02	7.10×10^{-3}	-0.01	7.00×10^{-3}	0.03	1.48×10^{-2}
South	0.00	7.30×10^{-3}	0.02	2.83×10^{-2}	0.00	8.20×10^{-3}	0.02	8.30×10^{-3}	0.00	1.25×10^{-2}	0.01	4.12×10^{-2}

Table A.4: WAS-22 COSMO individual models area-averaged mean annual trends and standard deviation (SD) per sub-domains period 2006 to 2100.

Models	COSMO-MPI				COSMO-NCC				COSMO-ICHEC	
Scenarios	RCP 2.6		RCP 8.5		RCP 2.6		RCP 8.5		RCP 8.5	
Regions	Mean	SD	Mean	SD	Mean	SD	Mean	SD	Mean	SD
N-W	0.09	0.03	0.01	0.01	0.04	0.02	-0.01	0.01	-0.01	0.01
T-N	0.00	0.01	0.00	0.01	0.00	0.01	0.00	0.01	0.00	0.00
Center	0.00	0.01	0.01	1.25×10^{-2}	0.00	0.01	0.01	9.70×10^{-3}	0.00	9.30×10^{-3}
East	0.00	5.10×10^{-3}	0.01	1.08×10^{-2}	-0.01	8.30×10^{-3}	0.00	1.02×10^{-2}	0.02	3.10×10^{-3}
South	0.01	1.22×10^{-2}	-0.01	2.92×10^{-2}	0.00	1.09×10^{-2}	0.01	1.03×10^{-2}	0.00	2.41×10^{-2}

A.4 Performance of ERA5 and Wind-Topo at Swiss stations

Table A.5 provides with an overview of wind speeds measurements, ERA5 and Wind-Topo and their performance for the validation stations in Switzerland.

Table A.5: Overview of wind speeds obtained at the validation stations from the measurements (Vel_{meas}), ERA5 (Vel_{ERA5}) and Wind-Topo (Vel_{WT}). The MBE, corr and MAE scores obtained for ERA5 and Wind-Topo comparison with the calibration stations are also presented.

Vel_{meas}	Vel_{ERA5}	Vel_{WT}	MBE_{ERA5}	MBE_{WT}	$corr_{ERA5}$	$corr_{WT}$	MAE_{ERA5}	MAE_{WT}
1.94	1.84	1.50	-0.09	-0.43	0.01	0.02	1.47	1.31
4.48	0.82	1.35	-3.67	-3.14	-0.04	-0.01	3.84	3.76
1.95	1.64	1.06	-0.31	-0.89	0.01	0.04	1.51	1.27
2.83	1.72	2.80	-1.11	-0.02	0.79	0.73	1.34	1.19
1.35	1.98	1.21	0.62	-0.14	0.01	0.03	1.11	0.66
4.68	1.54	1.94	-3.14	-2.75	0.01	0.01	3.44	3.39
4.29	0.98	1.80	-3.30	-2.49	-0.01	0.00	3.70	3.66
9.99	1.61	5.35	-8.38	-4.64	0.04	0.00	8.46	6.91
1.75	0.93	3.20	-0.82	1.45	0.12	0.15	1.01	2.00
151.05	1.86	1.48	-149.19	-149.57	-0.03	0.03	150.47	150.22
8.68	0.81	2.97	-7.87	-5.70	-0.02	-0.02	8.03	7.79
69.32	1.75	2.27	-67.57	-67.05	0.03	0.02	68.71	68.83
4.31	1.76	1.68	-2.56	-2.63	0.01	0.01	3.31	3.27
5.52	1.25	5.44	-4.26	-0.08	0.15	0.61	4.33	2.34
59.74	1.36	1.66	-58.39	-58.08	-0.10	-0.13	59.15	59.15
4.58	1.62	1.56	-2.97	-3.02	-0.02	-0.02	3.80	3.57
28.26	0.95	3.90	-27.31	-24.36	0.04	0.12	27.33	25.82
4.79	0.96	3.42	-3.83	-1.37	0.03	0.09	3.86	2.89
2.23	0.80	1.34	-1.43	-0.89	0.09	0.36	1.49	1.27
3.31	1.69	3.01	-1.62	-0.30	0.05	0.05	1.80	1.55
6.51	1.59	1.07	-4.91	-5.43	-0.03	0.03	6.02	5.79
29.69	1.48	2.43	-28.21	-27.26	-0.07	-0.08	28.56	28.67
7.29	0.84	5.93	-6.45	-1.36	0.03	0.09	6.46	4.91
13.54	1.23	1.50	-12.31	-12.04	0.03	0.04	12.98	12.98
3.50	1.43	2.83	-2.07	-0.67	0.05	0.07	2.17	1.66
5.48	0.79	6.04	-4.69	0.55	0.29	0.77	4.70	2.08
3.89	2.16	2.92	-1.73	-0.96	0.06	0.05	2.16	1.96
3.73	1.95	1.50	-1.79	-2.23	-0.02	-0.02	2.80	2.71
4.31	0.88	1.50	-3.43	-2.81	-0.02	-0.01	3.67	3.62
3.29	0.93	2.40	-2.36	-0.89	0.06	0.08	2.43	1.71
59.84	0.93	1.54	-58.91	-58.30	0.00	-0.18	59.31	59.10
14.27	1.16	1.93	-13.11	-12.34	-0.02	-0.03	13.57	13.36

10.81	1.23	2.26	-9.58	-8.55	-0.03	-0.03	10.10	10.07
5.92	0.71	1.96	-5.22	-3.96	-0.01	-0.01	5.27	4.82
21.83	0.97	7.42	-20.86	-14.40	0.01	0.02	20.93	18.58
2.19	0.95	1.58	-1.23	-0.60	0.05	0.24	1.34	1.02
3.09	1.05	2.93	-2.03	-0.15	-0.01	0.02	2.40	2.30
26.69	1.01	2.63	-25.68	-24.05	0.03	-0.08	26.08	25.47
8.39	1.02	1.31	-7.37	-7.07	0.07	0.00	7.65	7.67
5.52	0.96	1.49	-4.56	-4.04	-0.03	0.00	4.83	4.96
4.77	1.01	1.95	-3.77	-2.82	0.01	0.03	3.88	3.30
44.39	1.56	2.45	-42.84	-41.94	-0.01	-0.05	43.16	42.74
2.77	1.78	2.33	-0.99	-0.44	0.01	0.05	2.08	1.83
8.67	0.98	1.72	-7.69	-6.95	0.02	0.02	8.00	7.93
5.49	0.91	1.54	-4.58	-3.95	-0.01	-0.02	4.80	4.56
3.63	0.95	1.71	-2.68	-1.91	-0.01	0.01	2.85	2.52
4.11	0.99	1.48	-3.11	-2.62	0.04	0.00	3.35	3.52
15.39	0.74	1.80	-14.65	-13.58	0.02	-0.05	14.75	14.36
3.24	1.05	2.99	-2.19	-0.25	0.00	0.05	2.38	2.11
6.81	0.80	1.54	-6.01	-5.27	0.01	-0.01	6.30	6.20
2.23	1.18	1.06	-1.05	-1.17	0.01	0.01	1.47	1.45
30.30	1.00	8.93	-29.30	-21.36	0.02	0.06	29.32	26.50
30.43	1.18	1.91	-29.25	-28.53	-0.02	-0.04	29.89	29.73
3.38	0.86	2.99	-2.52	-0.39	0.41	0.62	2.52	1.25
23.25	0.95	1.95	-22.30	-21.30	-0.04	-0.06	22.54	22.40
4.85	1.81	1.52	-3.03	-3.33	0.06	0.06	3.70	3.71
22.92	1.01	1.75	-21.91	-21.18	-0.02	-0.07	22.34	22.31
3.64	1.57	2.78	-2.07	-0.85	0.03	0.06	2.80	2.54
8.40	1.77	3.01	-6.63	-5.39	0.01	0.04	6.73	6.11
1.51	0.86	0.99	-0.65	-0.52	0.31	0.37	0.93	0.89
3.64	1.09	1.41	-2.55	-2.22	0.04	0.07	2.93	2.76

Bibliography

[1] D. Archer and S. Rahmstorf, *The climate crisis: An introductory guide to climate change.* Cambridge University Press, 2010.

[2] R. Pierrehumbert, "There is no plan b for dealing with the climate crisis", *Bulletin of the Atomic Scientists*, vol. 75, no. 5, pp. 215–221, 2019. DOI: 10.1080/00963402.2019. 1654255. [Online]. Available: https://doi.org/10.1080/00963402.2019.1654255.

[3] M. J. Bush, "How to End the Climate Crisis", in *Climate Change and Renewable Energy: How to End the Climate Crisis*, Cham: Springer International Publishing, 2020, pp. 421–475, ISBN: 978-3-030-15424-0. DOI: 10.1007/978-3-030-15424-0_9. [Online]. Available: https://doi.org/10.1007/978-3-030-15424-0_9.

[4] M. M. Halmann and M. Steinberg, *Greenhouse gas carbon dioxide mitigation: science and technology*. CRC press, 1998.

[5] M. L. Khandekar, T. S. Murty, and P. Chittibabu, "The Global Warming Debate: A Review of the State of Science", *pure and applied geophysics*, vol. 162, no. 8, pp. 1557–1586, Aug. 2005, ISSN: 1420-9136. DOI: 10.1007/s00024-005-2683-x. [Online]. Available: https://doi.org/10.1007/s00024-005-2683-x.

[6] P. release: The Nobel Prize in Physics 2021. "Nobelprize.org. nobel prize outreach ab 2022". (Mar. 12, 2022), [Online]. Available: https://www.nobelprize.org/prizes/physics/2021/press-release/.

[7] IPCC. "The intergovernmental panel on climate change (ipcc)". (), [Online]. Available: https://www.ipcc.ch/about/ (visited on 09/30/2022).

[8] ——, *Climate Change 2021: The Physical Science Basis. Contribution of Working Group I to the Sixth Assessment Report of the Intergovernmental Panel on Climate Change*. Cambridge, UK and New York, NY, USA: Cambridge University Press, 2021.

[9] ——, *Climate Change 2022: Impacts, Adaptation and Vulnerability Working Group II Contribution to the IPCC Sixth Assessment Report*. Cambridge, UK and New York, NY, USA: Cambridge University Press, 2022.

[10] K. K. Rao, S. K. Patwardhan, A. Kulkarni, K. Kamala, S. S. Sabade, and K. K. Kumar, "Projected changes in mean and extreme precipitation indices over India using PRECIS", *Global and Planetary Change*, vol. 113, pp. 77–90, 2014, ISSN: 0921-8181. DOI: https: //doi.org/10.1016/j.gloplacha.2013.12.006. [Online]. Available: https://www. sciencedirect.com/science/article/pii/S0921818113002774.

[11] K. C. Armour, I. Eisenman, E. Blanchard-Wrigglesworth, K. E. McCusker, and C. M. Bitz, "The reversibility of sea ice loss in a state-of-the-art climate model", *Geophysical Research Letters*, vol. 38, no. 16, 2011. DOI: https://doi.org/10.1029/2011GL048739. eprint: https://agupubs.onlinelibrary.wiley.com/doi/pdf/10.1029/2011GL048739. [Online]. Available: https://agupubs.onlinelibrary.wiley.com/doi/abs/10.1029/ 2011GL048739.

[12] S. K. Srivastava, "New challenges on natural resources and their impact on climate change in the indian context", in *India: Climate Change Impacts, Mitigation and Adaptation in Developing Countries*, M. N. Islam and A. van Amstel, Eds. Cham: Springer International Publishing, 2021, pp. 1–15, ISBN: 978-3-030-67865-4. DOI: 10.1007/978-3-030-67865-4_1. [Online]. Available: https://doi.org/10.1007/978-3-030-67865-4_1.

[13] J. Zscheischler, S. Westra, B. J. J. M. van den Hurk, *et al.*, "Future climate risk from compound events", *Nature Climate Change*, vol. 8, no. 6, pp. 469–477, Jun. 1, 2018, ISSN: 1758-6798. DOI: 10.1038/s41558-018-0156-3. [Online]. Available: https: //doi.org/10.1038/s41558-018-0156-3.

[14] N. N. Ridder, A. M. Ukkola, A. J. Pitman, and S. E. Perkins-Kirkpatrick, "Increased occurrence of high impact compound events under climate change", *npj Climate and Atmospheric Science*, vol. 5, no. 1, p. 3, Jan. 12, 2022, ISSN: 2397-3722. DOI: 10.1038/ s41612-021-00224-4. [Online]. Available: https://doi.org/10.1038/s41612-021-00224-4.

[15] T. Ming, R. deRichter, W. Liu, and S. Caillol, "Fighting global warming by climate engineering: is the earth radiation management and the solar radiation management any option for fighting climate change?", *Renewable and Sustainable Energy Reviews*, vol. 31, pp. 792–834, Mar. 2014, ISSN: 13640321. DOI: 10.1016/j.rser.2013.12.032. [Online]. Available: https://linkinghub.elsevier.com/retrieve/pii/S1364032113008460 (visited on 08/10/2022).

[16] IPCC, *Climate Change 2022: Mitigation of Climate Change. Contribution of Working Group III to the Sixth Assessment Report of the Intergovernmental Panel on Climate Change*, P. Shukla, J. Skea, R. Slade, *et al.*, Eds. Cambridge, UK and New York, NY, USA: Cambridge University Press, 2022. DOI: 10.1017/9781009157926.

[17] P. R. Shukla and V. Chaturvedi, "Sustainable energy transformations in india under climate policy", *Sustainable Development*, vol. 21, no. 1, pp. 48–59, 2013. DOI: https: //doi.org/10.1002/sd.516. eprint: https://onlinelibrary.wiley.com/doi/pdf/10.1002/sd.516. [Online]. Available: https://onlinelibrary.wiley.com/doi/abs/10.1002/sd.516.

[18] C. H. News. "Climate home news". (Mar. 12, 2022), [Online]. Available: https://www.climatechangenews.com/2020/10/07/eu-parliament-votes-favour-cutting-emissions-60-2030/.

[19] S. T. N. Y. T. Sengupta. "China, in pointed message to the u.s., tightens its climate targets". (Mar. 12, 2022), [Online]. Available: https://www.nytimes.com/2020/09/22/climate/china-emissions.html/.

[20] F. Wang, J. D. Harindintwali, Z. Yuan, *et al.*, "Technologies and perspectives for achieving carbon neutrality", *The Innovation*, vol. 2, no. 4, p. 100 180, 2021, ISSN: 2666-6758. DOI: https://doi.org/10.1016/j.xinn.2021.100180. [Online]. Available: https://www.sciencedirect.com/science/article/pii/S2666675821001053.

[21] M. Fripp, "Switch: a planning tool for power systems with large shares of intermittent renewable energy", *Environmental Science & Technology*, vol. 46, no. 11, pp. 6371–6378, Jun. 5, 2012, ISSN: 0013-936X, 1520-5851. DOI: 10.1021/es204645c. [Online]. Available: https://pubs.acs.org/doi/10.1021/es204645c (visited on 07/19/2022).

[22] J. L. Holechek, H. M. E. Geli, M. N. Sawalhah, and R. Valdez, "A global assessment: can renewable energy replace fossil fuels by 2050?", *Sustainability*, vol. 14, no. 8, p. 4792, Apr. 16, 2022, ISSN: 2071-1050. DOI: 10.3390/su14084792. [Online]. Available: https://www.mdpi.com/2071-1050/14/8/4792 (visited on 07/19/2022).

[23] W. Leal Filho and D. Surroop, Eds., *The Nexus: Energy, Environment and Climate Change*, Green Energy and Technology, Cham: Springer International Publishing, 2018, ISBN: 978-3-319-63611-5 978-3-319-63612-2. DOI: 10.1007/978-3-319-63612-2. [Online]. Available: http://link.springer.com/10.1007/978-3-319-63612-2 (visited on 07/19/2022).

[24] E. Goodale, C. Mammides, W. Mtemi, *et al.*, "Increasing collaboration between china and india in the environmental sciences to foster global sustainability", *Ambio*, vol. 51, no. 6, pp. 1474–1484, Jun. 1, 2022, ISSN: 1654-7209. DOI: 10.1007/s13280-021-01681-0. [Online]. Available: https://doi.org/10.1007/s13280-021-01681-0.

[25] D. E. H. J. Gernaat, H. S. de Boer, V. Daioglou, S. G. Yalew, C. Müller, and D. P. van Vuuren, "Climate change impacts on renewable energy supply", en, *Nature Climate Change*, vol. 11, no. 2, pp. 119–125, Feb. 2021, ISSN: 1758-678X, 1758-6798. DOI: 10.1038/s41558-020-00949-9. [Online]. Available: http://www.nature.com/articles/s41558-020-00949-9 (visited on 08/13/2021).

[26] S. C. Pryor, R. J. Barthelmie, M. S. Bukovsky, L. R. Leung, and K. Sakaguchi, "Climate change impacts on wind power generation", *Nature Reviews Earth & Environment*, vol. 1, no. 12, pp. 627–643, Dec. 1, 2020, ISSN: 2662-138X. DOI: 10.1038/s43017-020-0101-7. [Online]. Available: https://doi.org/10.1038/s43017-020-0101-7.

[27] R. J. Barthelmie and S. C. Pryor, "Climate change mitigation potential of wind energy", *Climate*, vol. 9, no. 9, 2021, ISSN: 2225-1154. DOI: 10.3390/cli9090136. [Online]. Available: https://www.mdpi.com/2225-1154/9/9/136.

[28]   Duta Wacana Christian University, Indonesia and P. B. Titalessy, "Renewable energy consumption and economic growth in asia pacific", *Journal of Economics and Business*, vol. 4, no. 2, Jun. 30, 2021, ISSN: 26153726. DOI: 10.31014/aior.1992.04.02.362. [Online]. Available: https://www.asianinstituteofresearch.org/JEBarchives/Renewable-Energy-Consumption-and-Economic-Growth-in-Asia-Pacific- (visited on 07/19/2022).

[29]   T. V. Ramachandra, "Energy footprint of india: scope for improvements in end-use energy efficiency and renewable energy", in *Energy Footprints of the Energy Sector*, S. S. Muthu, Ed., Singapore: Springer Singapore, 2019, pp. 77–107, ISBN: 978-981-13-2457-4. DOI: 10.1007/978-981-13-2457-4_3. [Online]. Available: https://doi.org/10.1007/978-981-13-2457-4_3.

[30]   S. Chakravarty and E. Somanathan, "There is no economic case for new coal plants in india", *World Development Perspectives*, vol. 24, p. 100 373, 2021, ISSN: 2452-2929. DOI: https://doi.org/10.1016/j.wdp.2021.100373. [Online]. Available: https://www.sciencedirect.com/science/article/pii/S2452292921000898.

[31]   International Energy Agency, *India Energy Outlook 2021*, en. OECD, Mar. 2021, ISBN: 978-92-64-97691-7. DOI: 10.1787/ec2fd78d-en. [Online]. Available: https://www.oecd-ilibrary.org/energy/india-energy-outlook-2021_ec2fd78d-en (visited on 11/09/2021).

[32]   G. Anandarajah and A. Gambhir, "India's CO2 emission pathways to 2050: what role can renewables play?", *Applied Energy*, vol. 131, pp. 79–86, 2014, ISSN: 0306-2619. DOI: https://doi.org/10.1016/j.apenergy.2014.06.026. [Online]. Available: https://www.sciencedirect.com/science/article/pii/S0306261914006084.

[33]   A. Pandey, P. Pandey, and J. S. Tumuluru, "Solar energy production in india and commonly used technologies—an overview", *Energies (Basel)*, vol. 15, no. 2, pp. 500–, 2022, Place: Basel Publisher: MDPI AG, ISSN: 1996-1073.

[34]   ——, "Solar energy production in india and commonly used technologies—an overview", eng, *Energies (Basel)*, vol. 15, no. 2, pp. 500–, 2022, ISSN: 1996-1073.

[35]   S. Sharma and S. Sinha, "Indian wind energy & its development-policies-barriers: an overview", *Environmental and Sustainability Indicators*, vol. 1-2, p. 100 003, 2019, ISSN: 2665-9727. DOI: https://doi.org/10.1016/j.indic.2019.100003. [Online]. Available: https://www.sciencedirect.com/science/article/pii/S2665972719300030.

[36]   S. Lal S R, J. Herbert G M, P. Arjunan, and A. Suryan, "Advancements in renewable energy transition in india: a review", *Energy Sources, Part A: Recovery, Utilization and Environmental Effects*, 2022, cited By 1. DOI: 10.1080/15567036.2021.2024921.

[37]   S. Dawn, P. K. Tiwari, A. K. Goswami, A. K. Singh, and R. Panda, "Wind power: existing status, achievements and government's initiative towards renewable power dominating india", *Energy Strategy Reviews*, vol. 23, pp. 178–199, 2019, ISSN: 2211-467X. DOI: https://doi.org/10.1016/j.esr.2019.01.002. [Online]. Available: https://www.sciencedirect.com/science/article/pii/S2211467X19300033.

[38] M. R and M. M, "Principal component analysis of climatological impact on rooftop solar power plant installed in western india", *International Journal of Ambient Energy*, 2020. DOI: 10.1080/01430750.2020.1845239.

[39] K. Tibrewal and C. Venkataraman, "Climate co-benefits of air quality and clean energy policy in india", *Nature Sustainability*, vol. 4, no. 4, pp. 305–313, Apr. 2021, ISSN: 2398-9629. DOI: 10.1038/s41893-020-00666-3. [Online]. Available: http://www.nature. com/articles/s41893-020-00666-3 (visited on 07/19/2022).

[40] R. Neal, J. Robbins, R. Dankers, A. Mitra, A. Jayakumar, E. N. Rajagopal, and G. Adamson, "Deriving optimal weather pattern definitions for the representation of precipitation variability over India", *International Journal of Climatology*, vol. 40, no. 1, pp. 342– 360, 2020, _eprint: https://rmets.onlinelibrary.wiley.com/doi/pdf/10.1002/joc.6215. DOI: https://doi.org/10.1002/joc.6215. [Online]. Available: https://rmets.onlinelibrary.wiley. com/doi/abs/10.1002/joc.6215.

[41] Y. Jang and D. M. Straus, "The indian monsoon circulation response to el niño diabatic heating", *Journal of Climate*, vol. 25, no. 21, pp. 7487–7508, 2012. DOI: 10.1175/JCLI-D-11-00637.1. [Online]. Available: https://journals.ametsoc.org/view/journals/clim/25/ 21/jcli-d-11-00637.1.xml.

[42] R. K. Yadav, "Emerging role of indian ocean on indian northeast monsoon", *Climate dynamics*, vol. 41, no. 1, pp. 105–116, 2013.

[43] J. S. Chowdary, H. S. Harsha, C. Gnanaseelan, G. Srinivas, A. Parekh, P. Pillai, and C. V. Naidu, "Indian summer monsoon rainfall variability in response to differences in the decay phase of el niño", *Climate Dynamics*, vol. 48, no. 7, pp. 2707–2727, Apr. 1, 2017, ISSN: 1432-0894. DOI: 10.1007/s00382-016-3233-1.

[44] R. Kripalani, K.-J. Ha, C.-H. Ho, J.-H. Oh, B. Preethi, M. Mujumdar, and A. Prabhu, "Erratic asian summer monsoon 2020: COVID-19 lockdown initiatives possible cause for these episodes?", *Climate Dynamics*, Jan. 24, 2022, ISSN: 0930-7575, 1432-0894. DOI: 10.1007/s00382-021-06042-x. [Online]. Available: https://link.springer.com/10.1007/ s00382-021-06042-x (visited on 06/05/2022).

[45] J.-Y. Hong, J.-B. Ahn, and J.-G. Jhun, "Winter climate changes over east asian region under RCP scenarios using east asian winter monsoon indices", *Climate Dynamics*, vol. 48, no. 1, pp. 577–595, Jan. 1, 2017, ISSN: 1432-0894. DOI: 10.1007/s00382-016-3096-5. [Online]. Available: https://doi.org/10.1007/s00382-016-3096-5.

[46] C. Zhang and Y. Wang, "Projected future changes of tropical cyclone activity over the western north and south pacific in a 20-km-mesh regional climate model", *Journal of Climate*, vol. 30, no. 15, pp. 5923–5941, 2017. DOI: 10.1175/JCLI-D-16-0597.1. [Online]. Available: https://journals.ametsoc.org/view/journals/clim/30/15/jcli-d-16-0597.1.xml.

[47] A. Katzenberger, J. Schewe, J. Pongratz, and A. Levermann, "Robust increase of Indian monsoon rainfall and its variability under future warming in CMIP6 models", *Earth System Dynamics*, vol. 12, no. 2, pp. 367–386, 2021. DOI: 10.5194/esd-12-367-2021. [Online]. Available: https://esd.copernicus.org/articles/12/367/2021/.

[48] R. T. Konduru and H. G. Takahashi, "Effects of convection representation and model resolution on diurnal precipitation cycle over the indian monsoon region: toward a convection-permitting regional climate simulation", *Journal of Geophysical Research: Atmospheres*, vol. 125, no. 16, Aug. 27, 2020, ISSN: 2169-897X, 2169-8996. DOI: 10.1029/2019JD032150. [Online]. Available: https://onlinelibrary.wiley.com/doi/10.1029/2019JD032150 (visited on 06/06/2022).

[49] A. Mitra, "A Comparative Study on the Skill of CMIP6 Models to Preserve Daily Spatial Patterns of Monsoon Rainfall Over India", *Frontiers in Climate*, vol. 3, p. 37, 2021, ISSN: 2624-9553. DOI: 10.3389/fclim.2021.654763. [Online]. Available: https://www.frontiersin.org/article/10.3389/fclim.2021.654763.

[50] M. D. Zelinka, T. A. Myers, D. T. McCoy, S. Po-Chedley, P. M. Caldwell, P. Ceppi, S. A. Klein, and K. E. Taylor, "Causes of higher climate sensitivity in cmip6 models", *Geophysical Research Letters*, vol. 47, no. 1, e2019GL085782, 2020, e2019GL085782 10.1029/2019GL085782. DOI: https://doi.org/10.1029/2019GL085782. eprint: https://agupubs.onlinelibrary.wiley.com/doi/pdf/10.1029/2019GL085782. [Online]. Available: https://agupubs.onlinelibrary.wiley.com/doi/abs/10.1029/2019GL085782.

[51] A. Gusain, S. Ghosh, and S. Karmakar, "Added value of CMIP6 over CMIP5 models in simulating indian summer monsoon rainfall", *Atmospheric Research*, vol. 232, p. 104 680, 2020, ISSN: 0169-8095. DOI: https://doi.org/10.1016/j.atmosres.2019.104680. [Online]. Available: https://www.sciencedirect.com/science/article/pii/S0169809519307665.

[52] Y. Yang, K. Javanroodi, and V. M. Nik, "Climate change and renewable energy generation in europe—long-term impact assessment on solar and wind energy using high-resolution future climate data and considering climate uncertainties", *Energies*, vol. 15, no. 1, 2022, ISSN: 1996-1073. DOI: 10.3390/en15010302. [Online]. Available: https://www.mdpi.com/1996-1073/15/1/302.

[53] V. Zapata, D. E. H. J. Gernaat, S. G. Yalew, S. R. Santos da Silva, G. Iyer, M. Hejazi, and D. P. van Vuuren, "Climate change impacts on the energy system: a model comparison", *Environmental Research Letters*, vol. 17, no. 3, p. 034 036, Mar. 1, 2022, ISSN: 1748-9326. DOI: 10.1088/1748-9326/ac5141. [Online]. Available: https://iopscience.iop.org/article/10.1088/1748-9326/ac5141 (visited on 07/10/2022).

[54] S. C. Lewis and A. D. King, "Evolution of mean, variance and extremes in 21st century temperatures", *Weather and climate extremes*, vol. 15, pp. 1–10, 2017.

[55] L. O. Mearns, R. W. Katz, and S. H. Schneider, "Extreme high-temperature events: changes in their probabilities with changes in mean temperature", *Journal of Applied Meteorology and Climatology*, vol. 23, no. 12, pp. 1601–1613, 1984. DOI: 10.1175/1520-0450(1984)023<1601:EHTECI>2.0.CO;2. [Online]. Available: https://journals.ametsoc.org/view/journals/apme/23/12/1520-0450_1984_023_1601_ehteci_2_0_co_2.xml.

[56] L. O. Mearns, C. Rosenzweig, and R. Goldberg, "Mean and variance change in climate scenarios: methods, agricultural applications, and measures of uncertainty", *Climatic Change*, vol. 35, no. 4, pp. 367–396, 1997.

[57] M. A. D. Larsen, S. Petrović, A. M. Radoszynski, R. McKenna, and O. Balyk, "Climate change impacts on trends and extremes in future heating and cooling demands over europe", *Energy and Buildings*, vol. 226, p. 110 397, 2020, ISSN: 0378-7788. DOI: https://doi.org/10.1016/j.enbuild.2020.110397. [Online]. Available: https://www.sciencedirect.com/science/article/pii/S0378778820309737.

[58] C. Shen, J. Zha, J. Wu, D. Zhao, C. Azorin-Molina, W. Fan, and Y. Yu, "Does CRA-40 outperform other reanalysis products in evaluating near-surface wind speed changes over china?", *Atmospheric Research*, vol. 266, p. 105 948, 2022, ISSN: 0169-8095. DOI: https://doi.org/10.1016/j.atmosres.2021.105948. [Online]. Available: https://www.sciencedirect.com/science/article/pii/S0169809521005044.

[59] M. Chattopadhyay and D. Chattopadhyay, "Renewable energy contingencies in power systems: concept and case study", *Energy for Sustainable Development*, vol. 54, pp. 25–35, 2020, ISSN: 0973-0826. DOI: https://doi.org/10.1016/j.esd.2019.10.006. [Online]. Available: https://www.sciencedirect.com/science/article/pii/S0973082619312797.

[60] A. Martinez and G. Iglesias, "Climate change impacts on wind energy resources in north america based on the cmip6 projections", *Science of The Total Environment*, vol. 806, p. 150 580, 2022, ISSN: 0048-9697. DOI: https://doi.org/10.1016/j.scitotenv.2021.150580. [Online]. Available: https://www.sciencedirect.com/science/article/pii/S0048969721056576.

[61] X. Zhao, G. Huang, C. Lu, X. Zhou, and Y. Li, "Impacts of climate change on photovoltaic energy potential: a case study of china", *Applied Energy*, vol. 280, p. 115 888, 2020, ISSN: 0306-2619. DOI: https://doi.org/10.1016/j.apenergy.2020.115888. [Online]. Available: https://www.sciencedirect.com/science/article/pii/S0306261920313581.

[62] W. D. Soto, S. A. Klein, and W. A. Beckman, "Improvement and validation of a model for photovoltaic array performance", *Solar Energy*, vol. 80, no. 1, pp. 78–88, 2006, ISSN: 0038-092X. DOI: https://doi.org/10.1016/j.solener.2005.06.010. [Online]. Available: https://www.sciencedirect.com/science/article/pii/S0038092X05002410.

[63] S. Wang, J. Zhu, G. Huang, B. Baetz, G. Cheng, X. Zeng, and X. Wang, "Assessment of climate change impacts on energy capacity planning in ontario, canada using high-resolution regional climate model", *Journal of Cleaner Production*, vol. 274, p. 123 026, 2020, ISSN: 0959-6526. DOI: https://doi.org/10.1016/j.jclepro.2020.123026. [Online]. Available: https://www.sciencedirect.com/science/article/pii/S0959652620330717.

[64] S. Feron, R. R. Cordero, A. Damiani, and R. B. Jackson, "Climate change extremes and photovoltaic power output", en, *Nature Sustainability*, vol. 4, no. 3, pp. 270–276, Mar. 2021, ISSN: 2398-9629. DOI: 10.1038/s41893-020-00643-w. [Online]. Available: http://www.nature.com/articles/s41893-020-00643-w (visited on 08/13/2021).

[65] F. Kreienkamp, H. Huebener, C. Linke, and A. Spekat, "Good practice for the usage of climate model simulation results - a discussion paper", *Environmental Systems Research*, vol. 1, no. 1, p. 9, 2012, ISSN: 2193-2697. DOI: 10.1186/2193-2697-1-9. [Online].

Available: http://environmentalsystemsresearch.springeropen.com/articles/10.1186/2193-2697-1-9 (visited on 06/05/2022).

[66] A. S. Randall and K. Taylor, "Climate models and their evaluation", Contribution of Working Group I to the Fourth Assessment Report of the Intergovernmental Panel on Climate Change, 2007.

[67] Z. Hausfather, H. Drake, T. Abbott, and G. Schmidt, "Evaluating the performance of past climate model projections", *Geophysical Research Letters*, vol. 47, Jan. 2020. DOI: 10.1029/2019GL085378.

[68] M. Collins, R. E. Chandler, P. M. Cox, J. M. Huthnance, J. Rougier, and D. B. Stephenson, "Quantifying future climate change", *Nature Climate Change*, vol. 2, no. 6, pp. 403–409, Jun. 1, 2012, ISSN: 1758-6798. DOI: 10.1038/nclimate1414. [Online]. Available: https://doi.org/10.1038/nclimate1414.

[69] E. Winsberg, "Communicating uncertainty to policymakers: the ineliminable role of values", in *Climate Modelling: Philosophical and Conceptual Issues*, E. A. Lloyd and E. Winsberg, Eds., Cham: Springer International Publishing, 2018, pp. 381–412, ISBN: 978-3-319-65058-6. DOI: 10.1007/978-3-319-65058-6_13. [Online]. Available: https://doi.org/10.1007/978-3-319-65058-6_13.

[70] S. I. Seneviratne and M. Hauser, "Regional climate sensitivity of climate extremes in cmip6 versus cmip5 multimodel ensembles", *Earth's Future*, vol. 8, no. 9, e2019EF001474, 2020, e2019EF001474 2019EF001474. DOI: https://doi.org/10.1029/2019EF001474. eprint: https://agupubs.onlinelibrary.wiley.com/doi/pdf/10.1029/2019EF001474. [Online]. Available: https://agupubs.onlinelibrary.wiley.com/doi/abs/10.1029/2019EF001474.

[71] C. Jung and D. Schindler, "A review of recent studies on wind resource projections under climate change", *Renewable and Sustainable Energy Reviews*, vol. 165, p. 112 596, 2022, ISSN: 1364-0321. DOI: https://doi.org/10.1016/j.rser.2022.112596. [Online]. Available: https://www.sciencedirect.com/science/article/pii/S1364032122004920.

[72] A. A. Akinsanola, K. O. Ogunjobi, A. T. Abolude, and S. Salack, "Projected changes in wind speed and wind energy potential over west africa in CMIP6 models", *Environmental Research Letters*, vol. 16, no. 4, p. 044 033, Mar. 2021. DOI: 10.1088/1748-9326/abed7a. [Online]. Available: https://doi.org/10.1088/1748-9326/abed7a.

[73] T. Katopodis, I. Markantonis, D. Vlachogiannis, N. Politi, and A. Sfetsos, "Assessing climate change impacts on wind characteristics in greece through high resolution regional climate modelling", *Renewable Energy*, vol. 179, pp. 427–444, 2021, ISSN: 0960-1481. DOI: https://doi.org/10.1016/j.renene.2021.07.061. [Online]. Available: https://www.sciencedirect.com/science/article/pii/S0960148121010661.

[74] V. V. Klimenko and E. V. Fedotova, "Long-term development prospects of russia's wind energy in the conditions of expected climate changes", *Thermal Engineering*, vol. 67, no. 6, pp. 331–342, Jun. 1, 2020, ISSN: 1555-6301. DOI: 10.1134/S0040601520060051. [Online]. Available: https://doi.org/10.1134/S0040601520060051.

[75] S. S. Band, S. M. Bateni, M. Almazroui, S. Sajjadi, K.-w. Chau, and A. Mosavi, "Evaluating the potential of offshore wind energy in the gulf of oman using the mena-cordex wind speed data simulations", *Engineering Applications of Computational Fluid Mechanics*, vol. 15, no. 1, pp. 613–626, 2021. DOI: 10.1080/19942060.2021.1893225. eprint: https://doi.org/10.1080/19942060.2021.1893225. [Online]. Available: https://doi.org/10.1080/19942060.2021.1893225.

[76] R. Vautard, F. Thais, I. Tobin, F.-M. Bréon, J.-G. de Lavergne, A. Colette, P. Yiou, and P. Ruti, "Regional climate model simulations indicate limited climatic impacts by operational and planned European wind farms", *Nature communications*, vol. 5, p. 3196, Feb. 2014. DOI: 10.1038/ncomms4196.

[77] K. Solaun and E. Cerdá, "Impacts of climate change on wind energy power – Four wind farms in Spain", *Renewable Energy*, vol. 145, pp. 1306–1316, 2020, ISSN: 0960-1481. DOI: https://doi.org/10.1016/j.renene.2019.06.129. [Online]. Available: https://www.sciencedirect.com/science/article/pii/S0960148119309632.

[78] C. Jung and D. Schindler, "Introducing a new approach for wind energy potential assessment under climate change at the wind turbine scale", *Energy Conversion and Management*, vol. 225, p. 113 425, 2020, ISSN: 0196-8904. DOI: https://doi.org/10.1016/j.enconman.2020.113425. [Online]. Available: https://www.sciencedirect.com/science/article/pii/S0196890420309602.

[79] M. Wild, D. Folini, F. Henschel, N. Fischer, and B. Müller, "Projections of long-term changes in solar radiation based on CMIP5 climate models and their influence on energy yields of photovoltaic systems", en, *Solar Energy*, vol. 116, pp. 12–24, Jun. 2015, ISSN: 0038092X. DOI: 10.1016/j.solener.2015.03.039. [Online]. Available: https://linkinghub.elsevier.com/retrieve/pii/S0038092X15001668 (visited on 08/13/2021).

[80] S. Jerez, I. Tobin, R. Vautard, *et al.*, "The impact of climate change on photovoltaic power generation in Europe", en, *Nature Communications*, vol. 6, no. 1, p. 10 014, Dec. 2015, ISSN: 2041-1723. DOI: 10.1038/ncomms10014. [Online]. Available: http://www.nature.com/articles/ncomms10014 (visited on 08/13/2021).

[81] J. A. Crook, L. A. Jones, P. M. Forster, and R. Crook, "Climate change impacts on future photovoltaic and concentrated solar power energy output", *Energy Environ. Sci.*, vol. 4, pp. 3101–3109, 9 2011. DOI: 10.1039/C1EE01495A. [Online]. Available: http://dx.doi.org/10.1039/C1EE01495A.

[82] A. Bichet, B. Hingray, G. Evin, A. Diedhiou, C. M. F. Kebe, and S. Anquetin, "Potential impact of climate change on solar resource in Africa for photovoltaic energy: analyses from CORDEX-AFRICA climate experiments", *Environmental Research Letters*, vol. 14, no. 12, p. 124 039, Dec. 2019, Publisher: IOP Publishing. DOI: 10.1088/1748-9326/ab500a. [Online]. Available: https://doi.org/10.1088/1748-9326/ab500a.

[83] T. E. Patchali, O. O. Ajide, O. J. Matthew, T. A. O. Salau, and O. M. Oyewola, "Examination of potential impacts of future climate change on solar radiation in togo, west africa", *SN Applied Sciences*, vol. 2, no. 12, p. 1941, Nov. 3, 2020, ISSN: 2523-3971. DOI: 10.1007/s42452-020-03738-3. [Online]. Available: https://doi.org/10.1007/s42452-020-03738-3.

[84] M. Niyongendako, A. E. Lawin, C. Manirakiza, S. D. Y. B. Bazyomo, and B. Lamboni, "CLIMATE CHANGE IMPACTS ON PROJECTED PV POWER POTENTIAL UNDER RCP 8.5 SCENARIO IN BURUNDI", *International Journal of Research - GRANTHAALAYAH*, vol. 8, no. 5, pp. 1–14, May 31, 2020, ISSN: 2350-0530, 2394-3629. DOI: 10.29121/granthaalayah.v8.i5.2020.37. [Online]. Available: https://www.granthaalayahpublication.org/journals/index.php/granthaalayah/article/view/IJRG20_B04_3306 (visited on 06/06/2022).

[85] S. Poddar, J. P. Evans, M. Kay, A. Prasad, and S. Bremner, "Estimation of future changes in photovoltaic potential in australia due to climate change", *Environmental Research Letters*, vol. 16, no. 11, p. 114 034, Nov. 2021. DOI: 10.1088/1748-9326/ac2a64. [Online]. Available: https://doi.org/10.1088/1748-9326/ac2a64.

[86] N. K. Sharma, P. K. Tiwari, and Y. R. Sood, "Solar energy in india: strategies, policies, perspectives and future potential", *Renewable and Sustainable Energy Reviews*, vol. 16, no. 1, pp. 933–941, Jan. 2012, ISSN: 13640321. DOI: 10.1016/j.rser.2011.09.014. [Online]. Available: https://linkinghub.elsevier.com/retrieve/pii/S1364032111004643 (visited on 08/17/2021).

[87] K. Kapoor, K. K. Pandey, A. K. Jain, and A. Nandan, "Evolution of solar energy in India: A review", *Renewable and Sustainable Energy Reviews*, vol. 40, pp. 475–487, 2014, ISSN: 1364-0321. DOI: https://doi.org/10.1016/j.rser.2014.07.118. [Online]. Available: https://www.sciencedirect.com/science/article/pii/S136403211400570X.

[88] M. K. Hairat and S. Ghosh, "100GW solar power in India by 2022 – A critical review", *Renewable and Sustainable Energy Reviews*, vol. 73, pp. 1041–1050, 2017, ISSN: 1364-0321. DOI: https://doi.org/10.1016/j.rser.2017.02.012. [Online]. Available: https://www.sciencedirect.com/science/article/pii/S1364032117302149.

[89] S. Mohanty, P. K. Patra, S. S. Sahoo, and A. Mohanty, "Forecasting of solar energy with application for a growing economy like India: Survey and implication", *Renewable and Sustainable Energy Reviews*, vol. 78, pp. 539–553, 2017, ISSN: 1364-0321. DOI: https://doi.org/10.1016/j.rser.2017.04.107. [Online]. Available: https://www.sciencedirect.com/science/article/pii/S1364032117305853.

[90] P. K. S. Rathore, S. Rathore, R. P. Singh, and S. Agnihotri, "Solar power utility sector in india: challenges and opportunities", *Renewable and Sustainable Energy Reviews*, vol. 81, pp. 2703–2713, 2018, ISSN: 1364-0321. DOI: https://doi.org/10.1016/j.rser.2017.06.077. [Online]. Available: https://www.sciencedirect.com/science/article/pii/S1364032117310171.

[91] C. L. Archer and M. Z. Jacobson, "Supplying Baseload Power and Reducing Transmission Requirements by Interconnecting Wind Farms", en, *Journal of Applied Meteorology and Climatology*, vol. 46, no. 11, pp. 1701–1717, Nov. 2007, ISSN: 1558-8432, 1558-8424. DOI: 10.1175/2007JAMC1538.1. [Online]. Available: https://journals.ametsoc.org/doi/10.1175/2007JAMC1538.1 (visited on 08/17/2021).

[92] N. Kannan and D. Vakeesan, "Solar energy for future world: - A review", *Renewable and Sustainable Energy Reviews*, vol. 62, pp. 1092–1105, 2016, ISSN: 1364-0321. DOI: https://doi.org/10.1016/j.rser.2016.05.022. [Online]. Available: https://www.sciencedirect.com/science/article/pii/S1364032116301320.

[93] P. E. Bett and H. E. Thornton, "The climatological relationships between wind and solar energy supply in Britain", *Renewable Energy*, vol. 87, pp. 96–110, 2016, ISSN: 0960-1481. DOI: https://doi.org/10.1016/j.renene.2015.10.006. [Online]. Available: https://www.sciencedirect.com/science/article/pii/S0960148115303591.

[94] C. M. Grams, R. Beerli, S. Pfenninger, I. Staffell, and H. Wernli, "Balancing Europe's wind-power output through spatial deployment informed by weather regimes", en, *Nature Climate Change*, vol. 7, no. 8, pp. 557–562, Aug. 2017, ISSN: 1758-678X, 1758-6798. DOI: 10.1038/nclimate3338. [Online]. Available: http://www.nature.com/articles/nclimate3338 (visited on 08/17/2021).

[95] J. Weber, J. Wohland, M. Reyers, J. Moemken, C. Hoppe, J. G. Pinto, and D. Witthaut, "Impact of climate change on backup energy and storage needs in wind-dominated power systems in europe", *PLOS ONE*, vol. 13, no. 8, pp. 1–20, Aug. 2018, Publisher: Public Library of Science. DOI: 10.1371/journal.pone.0201457. [Online]. Available: https://doi.org/10.1371/journal.pone.0201457.

[96] M. T. Craig, S. Cohen, J. Macknick, C. Draxl, O. J. Guerra, M. Sengupta, S. E. Haupt, B.-M. Hodge, and C. Brancucci, "A review of the potential impacts of climate change on bulk power system planning and operations in the united states", *Renewable and Sustainable Energy Reviews*, vol. 98, pp. 255–267, 2018, ISSN: 1364-0321. DOI: https://doi.org/10.1016/j.rser.2018.09.022. [Online]. Available: https://www.sciencedirect.com/science/article/pii/S1364032118306701.

[97] T. Lu, P. Sherman, X. Chen, S. Chen, X. Lu, and M. McElroy, "India's potential for integrating solar and on- and offshore wind power into its energy system", en, *Nature Communications*, vol. 11, no. 1, p. 4750, Dec. 2020, ISSN: 2041-1723. DOI: 10.1038/s41467-020-18318-7. [Online]. Available: http://www.nature.com/articles/s41467-020-18318-7 (visited on 08/17/2021).

[98] Z. Wang, X. Wen, Q. Tan, G. Fang, X. Lei, H. Wang, and J. Yan, "Potential assessment of large-scale hydro-photovoltaic-wind hybrid systems on a global scale", *Renewable and Sustainable Energy Reviews*, vol. 146, p. 111 154, 2021, ISSN: 1364-0321. DOI: https://doi.org/10.1016/j.rser.2021.111154. [Online]. Available: https://www.sciencedirect.com/science/article/pii/S1364032121004433.

[99]   H. M. Markowitz, "Foundations of portfolio theory", *The journal of finance*, vol. 46, no. 2, pp. 469–477, 1991.

[100] F. deLlano-Paz, A. Calvo-Silvosa, S. I. Antelo, and I. Soares, "Energy planning and modern portfolio theory: a review", *Renewable and Sustainable Energy Reviews*, vol. 77, pp. 636–651, 2017, ISSN: 1364-0321. DOI: https://doi.org/10.1016/j.rser.2017.04.045. [Online]. Available: https://www.sciencedirect.com/science/article/pii/S136403211730552X.

[101] A. W. Ando, J. Fraterrigo, G. Guntenspergen, A. Howlader, M. Mallory, J. H. Olker, and S. Stickley, "When portfolio theory can help environmental investment planning to reduce climate risk to future environmental outcomes—and when it cannot", *Conservation Letters*, vol. 11, no. 6, e12596, 2018. DOI: https://doi.org/10.1111/conl.12596. [Online]. Available: https://conbio.onlinelibrary.wiley.com/doi/abs/10.1111/conl.12596.

[102] A. Tantet, M. Stéfanon, P. Drobinski, J. Badosa, S. Concettini, A. Cretì, C. D'Ambrosio, D. Thomopulos, and P. Tankov, "E4clim 1.0: The Energy for a Climate Integrated Model: Description and Application to Italy", *Energies*, vol. 12, no. 22, 2019, ISSN: 1996-1073. DOI: 10.3390/en12224299. [Online]. Available: https://www.mdpi.com/1996-1073/12/22/4299.

[103] J. Hu, R. Harmsen, W. Crijns-Graus, and E. Worrell, "Geographical optimization of variable renewable energy capacity in china using modern portfolio theory", *Applied Energy*, vol. 253, p. 113 614, 2019, ISSN: 0306-2619. DOI: https://doi.org/10.1016/j.apenergy.2019.113614. [Online]. Available: https://www.sciencedirect.com/science/article/pii/S0306261919312887.

[104] S. Scher and G. Messori, "Approximating simple general circulation models with deep learning", in *EGU General Assembly Conference Abstracts*, ser. EGU General Assembly Conference Abstracts, Apr. 2019, 8028, p. 8028.

[105] S. Dewitte, J. P. Cornelis, R. Müller, and A. Munteanu, "Artificial intelligence revolutionises weather forecast, climate monitoring and decadal prediction", *Remote Sensing*, vol. 13, no. 16, p. 3209, Aug. 13, 2021, ISSN: 2072-4292. DOI: 10.3390/rs13163209. [Online]. Available: https://www.mdpi.com/2072-4292/13/16/3209 (visited on 06/01/2022).

[106] B. Bochenek and Z. Ustrnul, "Machine learning in weather prediction and climate analyses—applications and perspectives", *Atmosphere*, vol. 13, no. 2, p. 180, Jan. 23, 2022, ISSN: 2073-4433. DOI: 10.3390/atmos13020180. [Online]. Available: https://www.mdpi.com/2073-4433/13/2/180 (visited on 06/01/2022).

[107] T. Wu and R. Snaiki, "Applications of machine learning to wind engineering", *Frontiers in Built Environment*, vol. 8, 2022, ISSN: 2297-3362. DOI: 10.3389/fbuil.2022.811460. [Online]. Available: https://www.frontiersin.org/article/10.3389/fbuil.2022.811460.

[108] N. Nabipour, A. Mosavi, E. Hajnal, L. Nadai, S. Shamshirband, and K.-W. Chau, "Modeling climate change impact on wind power resources using adaptive neuro-fuzzy inference system", *Engineering Applications of Computational Fluid Mechanics*, vol. 14, no. 1, pp. 491–506, 2020. DOI: 10.1080/19942060.2020.1722241. [Online]. Available: https://doi.org/10.1080/19942060.2020.1722241.

[109] K. Ahmed, D. A. Sachindra, S. Shahid, Z. Iqbal, N. Nawaz, and N. Khan, "Multi-model ensemble predictions of precipitation and temperature using machine learning algorithms", *Atmospheric Research*, vol. 236, p. 104 806, 2020, ISSN: 0169-8095. DOI: https://doi.org/10.1016/j.atmosres.2019.104806. [Online]. Available: https://www.sciencedirect.com/science/article/pii/S0169809519309858.

[110] D. M. Jose, A. M. Vincent, and G. S. Dwarakish, "Improving multiple model ensemble predictions of daily precipitation and temperature through machine learning techniques", *Scientific Reports*, vol. 12, no. 1, p. 4678, Mar. 18, 2022, ISSN: 2045-2322. DOI: 10.1038/s41598-022-08786-w. [Online]. Available: https://doi.org/10.1038/s41598-022-08786-w.

[111] M. Graf, S. C. Scherrer, C. Schwierz, M. Begert, O. Martius, C. C. Raible, and S. Brönnimann, "Near-surface mean wind in switzerland: climatology, climate model evaluation and future scenarios", *International Journal of Climatology*, vol. 39, no. 12, pp. 4798–4810, Oct. 2019, ISSN: 0899-8418, 1097-0088. DOI: 10.1002/joc.6108. [Online]. Available: https://onlinelibrary.wiley.com/doi/10.1002/joc.6108 (visited on 06/01/2022).

[112] J. Zhang, M. Zhang, Y. Li, J. Qin, K. Wei, and L. Song, "Analysis of wind characteristics and wind energy potential in complex mountainous region in southwest china", *Journal of Cleaner Production*, vol. 274, p. 123 036, 2020, ISSN: 0959-6526. DOI: https://doi.org/10.1016/j.jclepro.2020.123036. [Online]. Available: https://www.sciencedirect.com/science/article/pii/S095965262033081X.

[113] M. Mortezazadeh, J. Zou, M. Hosseini, S. Yang, and L. Wang, "Estimating urban wind speeds and wind power potentials based on machine learning with city fast fluid dynamics training data", *Atmosphere*, vol. 13, no. 2, p. 214, Jan. 28, 2022, ISSN: 2073-4433. DOI: 10.3390/atmos13020214. [Online]. Available: https://www.mdpi.com/2073-4433/13/2/214 (visited on 07/01/2022).

[114] S. Biswas and M. Sinha, "Performances of deep learning models for indian ocean wind speed prediction", *Modeling Earth Systems and Environment*, vol. 7, no. 2, pp. 809–831, Jun. 1, 2021, ISSN: 2363-6211. DOI: 10.1007/s40808-020-00974-9. [Online]. Available: https://doi.org/10.1007/s40808-020-00974-9.

[115] J. Dujardin and M. Lehning, "Wind-topo: downscaling near-surface wind fields to high-resolution topography in highly complex terrain with deep learning", *Quarterly Journal of the Royal Meteorological Society*, vol. 148, no. 744, pp. 1368–1388, 2022. DOI: https://doi.org/10.1002/qj.4265. eprint: https://rmets.onlinelibrary.wiley.com/doi/pdf/10.1002/qj.4265. [Online]. Available: https://rmets.onlinelibrary.wiley.com/doi/abs/10.1002/qj.4265.

[116] C. Teutschbein and J. Seibert, "Bias correction of regional climate model simulations for hydrological climate-change impact studies: review and evaluation of different methods", *Journal of hydrology*, vol. 456, pp. 12–29, 2012.

[117] N. Peleg, P. Molnar, P. Burlando, and S. Fatichi, "Exploring stochastic climate uncertainty in space and time using a gridded hourly weather generator", *Journal of Hydrology*, vol. 571, pp. 627–641, 2019.

[118] M. Meliho, M. Braun, A. Khattabi, and C. A. Orlando, "Methodological approach for climate simulations selection for climate change impact studies", 2022.

[119] M. Collins, K. Ashok, M. Barreiro, M. K. Roxy, S. M. Kang, T. L. Frölicher, G. Wang, and R. G. Tedeschi, "Editorial: new techniques for improving climate models, predictions and projections", *Frontiers in Climate*, vol. 3, 2021, ISSN: 2624-9553. DOI: 10.3389/fclim.2021.811205. [Online]. Available: https://www.frontiersin.org/article/10.3389/fclim.2021.811205.

[120] N. Haughton, G. Abramowitz, A. Pitman, and S. J. Phipps, "Weighting climate model ensembles for mean and variance estimates", *Climate Dynamics*, vol. 45, no. 11, pp. 3169–3181, Dec. 1, 2015, ISSN: 1432-0894. DOI: 10.1007/s00382-015-2531-3. [Online]. Available: https://doi.org/10.1007/s00382-015-2531-3.

[121] A. S. Elshall, M. Ye, S. A. Kranz, J. Harrington, X. Yang, Y. Wan, and M. Maltrud, "Prescreening-based subset selection for improving predictions of earth system models with application to regional prediction of red tide", *Frontiers in Earth Science*, vol. 10, 2022, ISSN: 2296-6463. DOI: 10.3389/feart.2022.786223. [Online]. Available: https://www.frontiersin.org/article/10.3389/feart.2022.786223.

[122] D. P. Dee, S. M. Uppala, A. J. Simmons, *et al.*, "The era-interim reanalysis: configuration and performance of the data assimilation system", *Quarterly Journal of the Royal Meteorological Society*, vol. 137, no. 656, pp. 553–597, 2011. DOI: https://doi.org/10.1002/qj.828. [Online]. Available: https://rmets.onlinelibrary.wiley.com/doi/abs/10.1002/qj.828.

[123] R. Knutti, J. Sedláček, B. M. Sanderson, R. Lorenz, E. M. Fischer, and V. Eyring, "A climate model projection weighting scheme accounting for performance and interdependence: model projection weighting scheme", *Geophysical Research Letters*, 2017, ISSN: 00948276. DOI: 10.1002/2016GL072012. [Online]. Available: http://doi.wiley.com/10.1002/2016GL072012 (visited on 06/17/2022).

[124] T. DelSole, X. Yang, and M. K. Tippett, "Is unequal weighting significantly better than equal weighting for multi-model forecasting?", *Quarterly Journal of the Royal Meteorological Society*, vol. 139, no. 670, pp. 176–183, 2013. DOI: https://doi.org/10.1002/qj.1961. eprint: https://rmets.onlinelibrary.wiley.com/doi/pdf/10.1002/qj.1961. [Online]. Available: https://rmets.onlinelibrary.wiley.com/doi/abs/10.1002/qj.1961.

[125] N. Herger, G. Abramowitz, R. Knutti, O. Angélil, K. Lehmann, and B. M. Sanderson, "Selecting a climate model subset to optimise key ensemble properties", *Earth System Dynamics*, vol. 9, no. 1, pp. 135–151, 2018. DOI: 10.5194/esd-9-135-2018. [Online]. Available: https://esd.copernicus.org/articles/9/135/2018/.

[126] D. W. Pierce, T. P. Barnett, B. D. Santer, and P. J. Gleckler, "Selecting global climate models for regional climate change studies", *Proceedings of the National Academy of Sciences*, vol. 106, no. 21, pp. 8441–8446, 2009. DOI: 10.1073/pnas.0900094106. eprint: https://www.pnas.org/doi/pdf/10.1073/pnas.0900094106. [Online]. Available: https://www.pnas.org/doi/abs/10.1073/pnas.0900094106.

[127] K. M. Parding, A. Dobler, C. F. McSweeney, *et al.*, "GCMeval – an interactive tool for evaluation and selection of climate model ensembles", *Climate Services*, vol. 18, p. 100 167, 2020, ISSN: 2405-8807. DOI: https://doi.org/10.1016/j.cliser.2020.100167. [Online]. Available: https://www.sciencedirect.com/science/article/pii/S2405880720300194.

[128] Y. Zakari, F. Vuille, and M. Lehning, "Climate change impact assessment for future wind and solar energy installations in india", *Frontiers in Energy Research*, vol. 10, 2022, ISSN: 2296-598X. DOI: 10.3389/fenrg.2022.859321. [Online]. Available: https://www.frontiersin.org/articles/10.3389/fenrg.2022.859321.

[129] Y. Zakari, A. Michel, and M. Lehning, "Future trends in wind resources and their consistency in the indian sub-continent", *Sustainable Energy Technologies and Assessments*, vol. 53, p. 102 460, 2022, ISSN: 2213-1388. DOI: https://doi.org/10.1016/j.seta.2022.102460.

[130] O. Hoegh-Guldberg, D. Jacob, M. Taylor, *et al.*, "Impacts of 1.5°c global warming on natural and human systems", English, in *Global warming of 1.5°C. An IPCC Special Report on the impacts of global warming of 1.5°C above pre-industrial levels and related global greenhouse gas emission pathways, in the context of strengthening the global response to the threat of climate change*, V. Masson-Delmotte, P. Zhai, H. Pörtner, *et al.*, Eds. World Meteorological Organization Technical Document, 2018.

[131] O. Edenhofer, I. P. on Climate Change, and W. G. 3, *Renewable energy sources and climate change mitigation: summary for policymakers and technical summary: special report of the intergovernmental panel on climate change.* New York: Cambridge University Press, 2011.

[132] M. Gross and V. Magar, "Offshore Wind Energy Climate Projection Using UPSCALE Climate Data under the RCP8.5 Emission Scenario", *PLOS ONE*, vol. 11, no. 10, J. A. Añel, Ed., e0165423, Oct. 2016, https://doi.org/10.1371/journal.pone.0165423.

[133] REN21, *Renewables 2017: Global Status Report*, https://www.ren21.net/wp-content/uploads/2019/05/GSR2017_Full-Report_English.pdf, Accessed 29 January 2020, 2017.

[134] S. Sinha, *Why India is the new hotspot for renewable energy investors*, https://www.weforum.org/agenda/2020/01/india-new-hotspot-renewable-energy-investors/, accessed 28 September 2020, Jan. 2020.

[135] V. Prakash, S. Ghosh, and K. Kanjilal, "Costs of avoided carbon emission from thermal and renewable sources of power in india and policy implications", *Energy*, vol. 200, p. 117 522, 2020, https://doi.org/10.1016/j.energy.2020.117522, ISSN: 0360-5442.

[136] S. C. Pryor, R. J. Barthelmie, and J. T. Schoof, "Inter-annual variability of wind indices across Europe", *Wind Energy*, vol. 9, no. 1-2, pp. 27–38, Jan. 2006, https://doi.org/10.1002/we.178.

[137] R. J. Barthelmie and L. E. Jensen, "Evaluation of wind farm efficiency and wind turbine wakes at the Nysted offshore wind farm", *Wind Energy*, vol. 13, no. 6, pp. 573–586, May 2010, https://doi.org/10.1002/we.408.

[138] S. C. Pryor, T. J. Shepherd, and R. J. Barthelmie, "Inter-annual variability of wind climates and wind turbine annual energy production", *Wind Energy Science Discussions*, pp. 1–23, Jul. 2018, https://doi.org/10.5194/wes-3-651-2018.

[139] K. B. Karnauskas, J. K. Lundquist, and L. Zhang, "Southward shift of the global wind energy resource under high carbon dioxide emissions", *Nature Geoscience*, vol. 11, no. 1, pp. 38–43, Jan. 2018, https://doi.org/10.1038/s41561-017-0029-9.

[140] B. C. O'Neill, C. Tebaldi, D. P. van Vuuren, *et al.*, "The Scenario Model Intercomparison Project (ScenarioMIP) for CMIP6", *Geoscientific Model Development*, vol. 9, no. 9, pp. 3461–3482, 2016, https://doi.org/10.5194/gmd-9-3461-2016.

[141] J. Moemken, M. Reyers, H. Feldmann, and J. G. Pinto, "Future changes of wind speed and wind energy potentials in euro-cordex ensemble simulations", *Journal of Geophysical Research: Atmospheres*, vol. 123, no. 12, pp. 6373–6389, 2018. DOI: https://doi.org/10.1029/2018JD028473. eprint: https://agupubs.onlinelibrary.wiley.com/doi/pdf/10.1029/2018JD028473. [Online]. Available: https://agupubs.onlinelibrary.wiley.com/doi/abs/10.1029/2018JD028473.

[142] M. Meinshausen, Z. R. J. Nicholls, J. Lewis, *et al.*, "The shared socio-economic pathway (ssp) greenhouse gas concentrations and their extensions to 2500", *Geoscientific Model Development*, vol. 13, no. 8, pp. 3571–3605, 2020. DOI: 10.5194/gmd-13-3571-2020. [Online]. Available: https://gmd.copernicus.org/articles/13/3571/2020/.

[143] E. Rusu, "A 30-year projection of the future wind energy resources in the coastal environment of the black sea", *Renewable Energy*, vol. 139, pp. 228–234, 2019, ISSN: 0960-1481. DOI: https://doi.org/10.1016/j.renene.2019.02.082. [Online]. Available: https://www.sciencedirect.com/science/article/pii/S0960148119302368.

[144] D. Carvalho, A. Rocha, X. Costoya, M. deCastro, and M. Gómez-Gesteira, "Wind energy resource over europe under cmip6 future climate projections: what changes from cmip5 to cmip6", *Renewable and Sustainable Energy Reviews*, vol. 151, p. 111 594, 2021, ISSN: 1364-0321. DOI: https://doi.org/10.1016/j.rser.2021.111594. [Online]. Available: https://www.sciencedirect.com/science/article/pii/S1364032121008716.

[145] K. Kim, B. Kim, and H. Kim, "A decision-making model for the analysis of offshore wind farm projects under climate uncertainties: a case study of south korea", *Renewable and Sustainable Energy Reviews*, vol. 94, pp. 853–860, 2018, https://doi.org/10.1016/j.rser.2018.06.061, ISSN: 1364-0321.

[146] K. Solaun and E. Cerdá, "Impacts of climate change on wind energy power – four wind farms in spain", *Renewable Energy*, vol. 145, pp. 1306–1316, 2020, https://doi.org/10.1016/j.renene.2019.06.129, ISSN: 0960-1481.

[147] Cordex, *CORDEX CORE*, https://cordex.org/experiment-guidelines/cordex-core/, accessed 20 May 2020, 2020.

[148] S. Kulkarni, M. C. Deo, and S. Ghosh, "Performance of the CORDEX regional climate models in simulating offshore wind and wind potential", *Theoretical and Applied Climatology*, vol. 135, no. 3-4, pp. 1449–1464, Feb. 2019, https://doi.org/10.1007/s00704-018-2401-0.

[149] F. Giorgi, "Thirty Years of Regional Climate Modeling: Where Are We and Where Are We Going next?", *Journal of Geophysical Research: Atmospheres*, pp. 2018–030 094, Jun. 2019, https://doi.org/10.1029/2018JD030094.

[150] S. Kulkarni, M. Deo, and S. Ghosh, "Impact of climate change on local wind conditions", https://doi.org/10.13140/RG.2.1.1882.2240, Dec. 2013.

[151] Y. Shi, G. Wang, and X. Gao, "Role of resolution in regional climate change projections over China", *Climate Dynamics*, vol. 51, no. 5-6, pp. 2375–2396, Sep. 2018, https://doi.org/10.1007/s00382-017-4018-x.

[152] A. Smith, N. Lott, and R. Vose, "The Integrated Surface Database: Recent Developments and Partnerships", *Bulletin of the American Meteorological Society*, vol. 92, no. 6, pp. 704–708, Jun. 2011, https://doi.org/10.1175/2011BAMS3015.1.

[153] R Core Team, *R: a language and environment for statistical computing*, R Foundation for Statistical Computing, Vienna, Austria, 2017. [Online]. Available: https://www.R-project.org/.

[154] K. E. Taylor, R. J. Stouffer, and G. A. Meehl, "An Overview of CMIP5 and the Experiment Design", *Bulletin of the American Meteorological Society*, vol. 93, no. 4, pp. 485–498, Apr. 2012, https://doi.org/10.1175/BAMS-D-11-00094.1.

[155] J. Evans, "CORDEX - An international climate downscaling initiative", Jan. 2011, pp. 2705–2711.

[156] C. G. Jones, P. Samuelsson, and E. Kjellström, "Regional climate modelling at the rossby centre", *Tellus A*, vol. 63, no. 1, pp. 1–3, 2011, https://doi.org/10.1111/j.1600-0870.2010.00491.x.

[157] R. Gelaro, W. McCarty, M. J. Suárez, *et al.*, "The Modern-Era Retrospective Analysis for Research and Applications, Version 2 (MERRA-2)", *Journal of Climate*, vol. 30, no. 14, pp. 5419–5454, Jul. 2017, https://doi.org/10.1175/JCLI-D-16-0758.1.

[158] H. Hersbach, B. Bell, P. Berrisford, *et al.*, "The ERA5 global reanalysis", *Quarterly Journal of the Royal Meteorological Society*, qj–3803, Jun. 2020, https://doi.org/10.1002/qj.3803.

[159]   J. Ramon, L. Lledó, V. Torralba, A. Soret, and F. J. Doblas-Reyes, "What global reanalysis best represents near-surface winds?", *Quarterly Journal of the Royal Meteorological Society*, vol. 145, no. 724, pp. 3236–3251, 2019, https://doi.org/10.1002/qj.3616.

[160]   D. Spera and T. Richards, "Modified power law equations for vertical wind profiles", Feb. 1979.

[161]   E. W. Peterson and J. P. Hennessey, "On the use of power laws for estimates of wind power potential", *Journal of Applied Meteorology and Climatology*, vol. 17, no. 3, pp. 390–394, 1978. DOI: 10.1175/1520-0450(1978)017<0390:OTUOPL>2.0.CO;2. [Online]. Available: https://journals.ametsoc.org/view/journals/apme/17/3/1520-0450_1978_017_0390_otuopl_2_0_co_2.xml.

[162]   D. Sisterson, B. Hicks, R. Coulter, and M. Wesely, "Difficulties in using power laws for wind energy assessment", *Solar Energy*, vol. 31, no. 2, pp. 201–204, 1983, ISSN: 0038-092X. DOI: https://doi.org/10.1016/0038-092X(83)90082-8. [Online]. Available: https://www.sciencedirect.com/science/article/pii/0038092X83900828.

[163]   R. B. Cleveland, W. S. Cleveland, J. E. McRae, and I. Terpenning, "Stl: a seasonal-trend decomposition procedure based on loess (with discussion)", *Journal of Official Statistics*, vol. 6, pp. 3–73, 1990.

[164]   P. K. Sen, "Estimates of the regression coefficient based on kendall's tau", *Journal of the American Statistical Association*, vol. 63, no. 324, pp. 1379–1389, 1968, http://dx.doi.org/10.1080/01621459.1968.10480934.

[165]   R. Mahmood, S. Jia, and W. Zhu, "Analysis of climate variability, trends, and prediction in the most active parts of the Lake Chad basin, Africa", *Scientific Reports*, vol. 9, no. 1, p. 6317, Dec. 2019, https://doi.org/10.1038/s41598-019-42811-9.

[166]   M. Taszarek, N. Pilguj, J. T. Allen, V. Gensini, H. E. Brooks, and P. Szuster, "Comparison of convective parameters derived from ERA5 and MERRA2 with rawinsonde data over europe and north america", *Journal of Climate*, pp. 1–55, Dec. 28, 2020, ISSN: 0894-8755, 1520-0442. DOI: 10.1175/JCLI-D-20-0484.1. [Online]. Available: https://journals.ametsoc.org/view/journals/clim/aop/JCLI-D-20-0484.1/JCLI-D-20-0484.1.xml (visited on 04/13/2022).

[167]   M. Hofer, B. Marzeion, and T. Mölg, "Comparing the skill of different reanalyses and their ensembles as predictors for daily air temperature on a glaciated mountain (peru)", *Climate Dynamics*, vol. 39, no. 7, pp. 1969–1980, Oct. 2012, ISSN: 0930-7575, 1432-0894. DOI: 10.1007/s00382-012-1501-2. [Online]. Available: http://link.springer.com/10.1007/s00382-012-1501-2 (visited on 04/13/2022).

[168]   J. Santos, Y. Sakagami, R. Haas, J. Passos, M. Machuca, W. Radünz, E. Dias, and M. Lima, "Wind speed evaluation of MERRA-2, ERA-interim and ERA-5 reanalysis data at a wind farm located in brazil", in *Proceedings of the ISES Solar World Congress 2019*, Santiago, Chile: International Solar Energy Society, 2019, pp. 1–10, ISBN: 978-3-9820408-1-3. DOI: 10.18086/swc.2019.45.10. [Online]. Available: http://proceedings.ises.org/citation?doi=swc.2019.45.10 (visited on 04/13/2022).

[169] M. Taszarek, N. Pilguj, J. T. Allen, V. Gensini, H. E. Brooks, and P. Szuster, "Comparison of convective parameters derived from era5 and merra2 with rawinsonde data over europe and north america", *Journal of Climate*, pp. 1–55, 2020. DOI: 10.1175/JCLI-D-20-0484.1. [Online]. Available: https://journals.ametsoc.org/view/journals/clim/aop/JCLI-D-20-0484.1/JCLI-D-20-0484.1.xml.

[170] H. Zandler, T. Senftl, and K. A. Vanselow, "Reanalysis datasets outperform other gridded climate products in vegetation change analysis in peripheral conservation areas of central asia", *Scientific Reports*, vol. 10, no. 1, p. 22 446, Dec. 31, 2020, ISSN: 2045-2322. DOI: 10.1038/s41598-020-79480-y. [Online]. Available: https://doi.org/10.1038/s41598-020-79480-y.

[171] E. Doddy Clarke, S. Griffin, F. McDermott, J. Monteiro Correia, and C. Sweeney, "Which reanalysis dataset should we use for renewable energy analysis in ireland?", *Atmosphere*, vol. 12, no. 5, p. 624, May 13, 2021, ISSN: 2073-4433. DOI: 10.3390/atmos12050624. [Online]. Available: https://www.mdpi.com/2073-4433/12/5/624 (visited on 04/13/2022).

[172] M. L. Roderick, L. D. Rotstayn, G. D. Farquhar, and M. T. Hobbins, "On the attribution of changing pan evaporation", *Geophysical Research Letters*, vol. 34, no. 17, 2007, https://doi.org/10.1029/2007GL031166.

[173] Z. Zeng, S. Piao, L. Li, P. Ciais, Y. Li, X. Cai, L. Yang, M. Liu, and E. Wood, "Global terrestrial stilling: does earth's greening play a role?", *Environmental Research Letters*, vol. 13, Oct. 2018, https://doi.org/10.1088/1748-9326/aaea84.

[174] L. Zhang, T. L. Delworth, W. Cooke, and X. Yang, "Natural variability of Southern Ocean convection as a driver of observed climate trends", *Nature Climate Change*, vol. 9, no. 1, pp. 59–65, Jan. 2019, https://doi.org/10.1038/s41558-018-0350-3.

[175] A. Michel, T. Brauchli, M. Lehning, B. Schaefli, and H. Huwald, "Stream temperature and discharge evolution in switzerland over the last 50 years: annual and seasonal behaviour", *Hydrology and Earth System Sciences*, vol. 24, pp. 115–142, Jan. 2020, https://doi.org/10.5194/hess-24-115-2020.

[176] C. Mauritzen, T. Zivkovic, and V. Veldore, "On the relationship between climate sensitivity and modelling uncertainty", *Tellus A: Dynamic Meteorology and Oceanography*, vol. 69, no. 1, p. 1 327 765, Jan. 2017, https://doi.org/10.1080/16000870.2017.1327765.

[177] M. Suman and R. Maity, "Southward shift of precipitation extremes over south Asia: Evidences from CORDEX data", *Scientific Reports*, vol. 10, no. 1, p. 6452, Dec. 2020, https://doi.org/10.1038/s41598-020-63571-x.

[178] S. Hasson, J. Böhner, and F. Chishtie, "Low fidelity of CORDEX and their driving experiments indicates future climatic uncertainty over Himalayan watersheds of Indus basin", *Climate Dynamics*, Mar. 2018, https://doi.org/10.1007/s00382-018-4160-0.

[179] P. Ajay, B. Pathak, F. Solmon, P. K. Bhuyan, and F. Giorgi, "Obtaining best parameterization scheme of RegCM 4.4 for aerosols and chemistry simulations over the CORDEX South Asia", *Climate Dynamics*, vol. 53, no. 1-2, pp. 329–352, Jul. 2019, https://doi.org/10.1007/s00382-018-4587-3.

Bibliography

[180]   I. Tobin, S. Jerez, R. Vautard, *et al.*, "Climate change impacts on the power generation potential of a european mid-century wind farms scenario", *Environmental Research Letters*, vol. 11, no. 3, p. 034 013, Mar. 2016, http://dx.doi.org/10.1088/1748-9326/11/3/034013.

[181]   C. M. Dunning, A. G. Turner, and D. J. Brayshaw, "The impact of monsoon intraseasonal variability on renewable power generation in India", *Environmental Research Letters*, vol. 10, no. 6, p. 064 002, Jun. 2015, http://dx.doi.org/10.1088/1748-9326/10/6/064002.

[182]   P. Sherman, S. Song, X. Chen, and M. McElroy, "Projected changes in wind power potential over china and india in high resolution climate models", *Environmental Research Letters*, vol. 16, no. 3, p. 034 057, Mar. 2021, ISSN: 1748-9326. DOI: 10.1088/1748-9326/abe57c. [Online]. Available: https://iopscience.iop.org/article/10.1088/1748-9326/abe57c.

[183]   D. Kumar, "Spatial variability analysis of the solar energy resources for future urban energy applications using Meteosat satellite-derived datasets", *Remote Sensing Applications: Society and Environment*, vol. 22, p. 100 481, 2021, ISSN: 2352-9385. DOI: https://doi.org/10.1016/j.rsase.2021.100481. [Online]. Available: https://www.sciencedirect.com/science/article/pii/S2352938521000173.

[184]   J. Dujardin, A. Kahl, and M. Lehning, "Synergistic optimization of renewable energy installations through evolution strategy", *Environmental Research Letters*, vol. 16, no. 6, p. 064 016, May 2021, Publisher: IOP Publishing. DOI: 10.1088/1748-9326/abfc75. [Online]. Available: https://doi.org/10.1088/1748-9326/abfc75.

[185]   R. Krishnan, J. Sanjay, C. Gnanaseelan, M. Mujumdar, A. Kulkarni, and S. Chakraborty, Eds., *Assessment of Climate Change over the Indian Region: A Report of the Ministry of Earth Sciences (MoES), Government of India*, en. Singapore: Springer Singapore, 2020, ISBN: 9789811543265 9789811543272. DOI: 10.1007/978-981-15-4327-2. [Online]. Available: https://link.springer.com/10.1007/978-981-15-4327-2 (visited on 08/17/2021).

[186]   A. Sharma, "Assessing the Labor Impact of Clean Energy Transitions in India", in *AGU Fall Meeting Abstracts*, vol. 2019, Dec. 2019, GC31O-1281, GC31O–1281.

[187]   A. Kumar, D. Pal, S. K. Kar, S. K. Mishra, and R. Bansal, "An overview of wind energy development and policy initiatives in India", *Clean Technologies and Environmental Policy*, Jan. 2022, ISSN: 1618-9558. DOI: 10.1007/s10098-021-02248-z. [Online]. Available: https://doi.org/10.1007/s10098-021-02248-z.

[188]   A. G. Turner and H. Annamalai, "Climate change and the South Asian summer monsoon", en, *Nature Climate Change*, vol. 2, no. 8, pp. 587–595, Aug. 2012, ISSN: 1758-678X, 1758-6798. DOI: 10.1038/nclimate1495. [Online]. Available: http://www.nature.com/articles/nclimate1495 (visited on 08/17/2021).

[189]   S. C. Pryor and R. J. Barthelmie, "Assessing climate change impacts on the near-term stability of the wind energy resource over the United States", *Proceedings of the National Academy of Sciences*, vol. 108, no. 20, pp. 8167–8171, 2011, ISSN: 0027-8424. DOI: 10.1073/pnas.1019388108. [Online]. Available: https://www.pnas.org/content/108/20/8167.

[190] K. Solaun and E. Cerdá, "Climate change impacts on renewable energy generation. A review of quantitative projections", *Renewable and Sustainable Energy Reviews*, vol. 116, p. 109 415, 2019, ISSN: 1364-0321. DOI: https://doi.org/10.1016/j.rser.2019.109415. [Online]. Available: https://www.sciencedirect.com/science/article/pii/S1364032119306239.

[191] J. Wu, J. Zha, D. Zhao, and Q. Yang, "Changes in terrestrial near-surface wind speed and their possible causes: an overview", en, *Climate Dynamics*, vol. 51, no. 5-6, pp. 2039–2078, Sep. 2018, ISSN: 0930-7575, 1432-0894. DOI: 10.1007/s00382-017-3997-y. [Online]. Available: http://link.springer.com/10.1007/s00382-017-3997-y (visited on 11/24/2021).

[192] B. Wang, M. Biasutti, M. P. Byrne, *et al.*, "Monsoons climate change assessment", *Bulletin of the American Meteorological Society*, vol. 102, no. 1, E1–E19, 2021. DOI: 10.1175/BAMS-D-19-0335.1.

[193] R. K and C. T, *Impacts of Climate Change on the Indian Summer Monsoon*, ser. Climate Change and Water Resources in India. Ministry of Environment, Forest and Climate Change (MoEF CC), Government of India, 2018, ISBN: 9788193313169. [Online]. Available: https://books.google.ch/books?id=uex%5C_DwAAQBAJ.

[194] Z. Zeng, S. Piao, L. Z. X. Li, P. Ciais, Y. Li, X. Cai, L. Yang, M. Liu, and E. F. Wood, "Global terrestrial stilling: does Earth's greening play a role?", en, *Environmental Research Letters*, vol. 13, no. 12, p. 124 013, Dec. 2018, ISSN: 1748-9326. DOI: 10.1088/1748-9326/aaea84. [Online]. Available: https://iopscience.iop.org/article/10.1088/1748-9326/aaea84 (visited on 09/29/2021).

[195] M. Gao, Y. Ding, S. Song, X. Lu, X. Chen, and M. B. McElroy, "Secular decrease of wind power potential in India associated with warming in the Indian Ocean", *Science Advances*, vol. 4, no. 12, 2018. DOI: 10.1126/sciadv.aat5256. [Online]. Available: https://advances.sciencemag.org/content/4/12/eaat5256.

[196] C. Sabeerali and R. Ajayamohan, "On the shortening of indian summer monsoon season in a warming scenario", *Climate Dyn*, vol. 50, pp. 1609–1624, 2017.

[197] S. Solomon, M. Manning, M. Marquis, D. Qin, *et al.*, *Climate change 2007-the physical science basis: Working group I contribution to the fourth assessment report of the IPCC*. Cambridge university press, 2007, vol. 4.

[198] A. Patt, S. Pfenninger, and J. Lilliestam, "Vulnerability of solar energy infrastructure and output to climate change", en, *Climatic Change*, vol. 121, no. 1, pp. 93–102, Nov. 2013, ISSN: 0165-0009, 1573-1480. DOI: 10.1007/s10584-013-0887-0. [Online]. Available: http://link.springer.com/10.1007/s10584-013-0887-0 (visited on 08/13/2021).

[199] A. Zhisheng, W. Guoxiong, L. Jianping, *et al.*, "Global monsoon dynamics and climate change", *Annual Review of Earth and Planetary Sciences*, vol. 43, no. 1, pp. 29–77, 2015. DOI: 10.1146/annurev-earth-060313-054623. eprint: https://doi.org/10.1146/annurev-earth-060313-054623. [Online]. Available: https://doi.org/10.1146/annurev-earth-060313-054623.

Bibliography

[200] V. Soni, G. Pandithurai, and D. Pai, "Evaluation of long-term changes of solar radiation in india", *International Journal of Climatology*, vol. 32, pp. 540–551, Mar. 2012. DOI: 10.1002/joc.2294.

[201] J. Singh and M. Kumar, "Solar Radiation over Four Cities of India: Trend Analysis using Mann-Kendall Test", *International Journal of Renewable Energy Research*, vol. 6, Dec. 2016.

[202] I. M. Peters and T. Buonassisi, "The Impact of Global Warming on Silicon PV Energy Yield in 2100", en, in *2019 IEEE 46th Photovoltaic Specialists Conference (PVSC)*, Chicago, IL, USA: IEEE, Jun. 2019, pp. 3179–3181, ISBN: 978-1-72810-494-2. DOI: 10.1109/PVSC40753.2019.8980515. [Online]. Available: https://ieeexplore.ieee.org/document/8980515/ (visited on 11/15/2021).

[203] M. Schlott, A. Kies, T. Brown, S. Schramm, and M. Greiner, "The Impact of Climate Change on a Cost-Optimal Highly Renewable European Electricity Network", en, *Applied Energy*, vol. 230, pp. 1645–1659, Nov. 2018, arXiv: 1805.11673, ISSN: 03062619. DOI: 10.1016/j.apenergy.2018.09.084. [Online]. Available: http://arxiv.org/abs/1805.11673 (visited on 08/17/2021).

[204] S. Stefanidis, S. Dafis, and D. Stathis, "Evaluation of regional climate models (rcms) performance in simulating seasonal precipitation over mountainous central pindus (greece)", *Water*, vol. 12, no. 10, 2020, ISSN: 2073-4441. DOI: 10.3390/w12102750. [Online]. Available: https://www.mdpi.com/2073-4441/12/10/2750.

[205] G. Evin, S. Somot, and B. Hingray, "Balanced estimate and uncertainty assessment of european climate change using the large euro-cordex regional climate model ensemble", *Earth System Dynamics Discussions*, vol. 2021, pp. 1–40, 2021. DOI: 10.5194/esd-2021-8. [Online]. Available: https://esd.copernicus.org/preprints/esd-2021-8/.

[206] IPCC, "Annex i: atlas of global and regional climate projections", in *Climate Change 2013: The Physical Science Basis. Contribution of Working Group I to the Fifth Assessment Report of the Intergovernmental Panel on Climate Change*, T. Stocker, D. Qin, G.-K. Plattner, M. Tignor, S. Allen, J. Boschung, A. Nauels, Y. Xia, V. Bex, and P. Midgley, Eds. Cambridge, United Kingdom and New York, NY, USA: Cambridge University Press, 2013, ch. AI, pp. 1311–1394, ISBN: ISBN 978-1-107-66182-0. DOI: 10.1017/CBO9781107415324.029. [Online]. Available: www.climatechange2013.org.

[207] Intergovernmental Panel on Climate Change, *Climate Change 2014 Mitigation of Climate Change: Working Group III Contribution to the Fifth Assessment Report of the Intergovernmental Panel on Climate Change*, en. Cambridge: Cambridge University Press, 2014, ISBN: 978-1-107-41541-6. DOI: 10.1017/CBO9781107415416. [Online]. Available: http://ebooks.cambridge.org/ref/id/CBO9781107415416 (visited on 11/23/2021).

[208] G. Evin, B. Hingray, J. Blanchet, N. Eckert, S. Morin, and D. Verfaillie, "Partitioning uncertainty components of an incomplete ensemble of climate projections using data augmentation", *Journal of Climate*, vol. 32, no. 8, pp. 2423–2440, 2019. DOI: 10.1175/

JCLI-D-18-0606.1. [Online]. Available: https://journals.ametsoc.org/view/journals/clim/32/8/jcli-d-18-0606.1.xml.

[209]   A. Bichet, A. Diedhiou, B. Hingray, G. Evin, N. E. Touré, K. N. A. Browne, and K. Kouadio, "Assessing uncertainties in the regional projections of precipitation in cordex-africa", en, *Climatic Change*, vol. 162, no. 2, pp. 583–601, Sep. 2020, ISSN: 0165-0009, 1573-1480. DOI: 10.1007/s10584-020-02833-z. (visited on 11/23/2021).

[210]   A. W. Ando, J. Fraterrigo, G. Guntenspergen, A. Howlader, M. Mallory, J. H. Olker, and S. Stickley, "When portfolio theory can help environmental investment planning to reduce climate risk to future environmental outcomes—and when it cannot", *Conservation Letters*, vol. 11, no. 6, e12596, 2018. DOI: https://doi.org/10.1111/conl.12596. eprint: https://conbio.onlinelibrary.wiley.com/doi/pdf/10.1111/conl.12596. [Online]. Available: https://conbio.onlinelibrary.wiley.com/doi/abs/10.1111/conl.12596.

[211]   S. Lolla, S. B. Roy, and S. Chowdhury, "Wind and Solar Energy Resources in India", *Energy Procedia*, vol. 76, pp. 187–192, 2015, ISSN: 1876-6102. DOI: https://doi.org/10.1016/j.egypro.2015.07.895. [Online]. Available: https://www.sciencedirect.com/science/article/pii/S1876610215016719.

[212]   S. Pachar, R. Singh, and M. A. Wahid, "Implication of renewable energy in sustainable development in india: future strategy", vol. 1149, no. 1, p. 012 020, May 2021. DOI: 10.1088/1757-899x/1149/1/012020. [Online]. Available: https://doi.org/10.1088/1757-899x/1149/1/012020.

[213]   Q. Jin, J. Wei, W. K. M. Lau, B. Pu, and C. Wang, "Interactions of Asian mineral dust with Indian summer monsoon: Recent advances and challenges", *Earth-Science Reviews*, vol. 215, p. 103 562, 2021, ISSN: 0012-8252. DOI: https://doi.org/10.1016/j.earscirev.2021.103562. [Online]. Available: https://www.sciencedirect.com/science/article/pii/S0012825221000611.

[214]   K. Riahi, S. Rao, V. Krey, C. Cho, V. Chirkov, G. Fischer, G. Kindermann, N. Nakicenovic, and P. Rafaj, "Rcp 8.5—a scenario of comparatively high greenhouse gas emissions", *Climatic change*, vol. 109, no. 1, pp. 33–57, 2011.

[215]   F. Giorgi, E. Coppola, F. Solmon, L. Mariotti, M. Sylla, X. Bi, N. Elguindi, G. Diro, V. Nair, G. Giuliani, *et al.*, "Regcm4: model description and preliminary tests over multiple cordex domains", *Climate Research*, vol. 52, pp. 7–29, 2012.

[216]   S. Sorland, R. Brogli, P. k. Pothapakula, *et al.*, "Cosmo-clm regional climate simulations in the cordex framework: a review", Feb. 2021. DOI: 10.5194/gmd-2020-443.

[217]   D. Jacob, A. Elizalde, A. Haensler, S. Hagemann, P. Kumar, R. Podzun, D. Rechid, A. R. Remedio, F. Saeed, K. Sieck, *et al.*, "Assessing the transferability of the regional climate model remo to different coordinated regional climate downscaling experiment (cordex) regions", *Atmosphere*, vol. 3, no. 1, pp. 181–199, 2012.

[218]   M. Sabater and J., "Era5-land hourly data from 1981 to present", *Copernicus Climate Change Service (C3S) Climate Data Store (CDS)*, 2019. DOI: https://doi.org/10.24381/cds.e2161bac.

[219] H. Theil, "A rank-invariant method of linear and polynomial regression analysis, 1-2; confidence regions for the parameters of linear regression equations in two, three and more variables", *Indagationes Mathematicae*, vol. XII, no. SP 5/49/R, Jan. 1950.

[220] P. K. Sen, "Estimates of the regression coefficient based on kendall's tau", *Journal of the American Statistical Association*, vol. 63, no. 324, pp. 1379–1389, 1968. DOI: 10.1080/01621459.1968.10480934. [Online]. Available: https://www.tandfonline.com/doi/abs/10.1080/01621459.1968.10480934.

[221] H. B. Mann, "Nonparametric tests against trend", *Econometrica: Journal of the econometric society*, pp. 245–259, 1945.

[222] M. G. Kendall, "Rank correlation methods", 1948.

[223] C. L. Archer and M. Z. Jacobson, "Evaluation of global wind power", *Journal of Geophysical Research: Atmospheres*, vol. 110, no. D12, 2005. DOI: https://doi.org/10.1029/2004JD005462. [Online]. Available: https://agupubs.onlinelibrary.wiley.com/doi/abs/10.1029/2004JD005462.

[224] S. Jerez, I. Tobin, R. Vautard, *et al.*, "The impact of climate change on photovoltaic power generation in europe", *Nature Communications*, vol. 6, p. 10 014, Dec. 2015. DOI: 10.1038/ncomms10014.

[225] S. L. Sørland, R. Brogli, P. K. Pothapakula, *et al.*, "Cosmo-clm regional climate simulations in the cordexframework: a review", Feb. 2021. DOI: 10.5194/gmd-2020-443. [Online]. Available: https://gmd.copernicus.org/preprints/gmd-2020-443/gmd-2020-443.pdf.

[226] S. Dubey, J. N. Sarvaiya, and B. Seshadri, "Temperature Dependent Photovoltaic (PV) Efficiency and Its Effect on PV Production in the World – A Review", *Energy Procedia*, vol. 33, pp. 311–321, 2013, ISSN: 1876-6102. DOI: https://doi.org/10.1016/j.egypro.2013.05.072. [Online]. Available: https://www.sciencedirect.com/science/article/pii/S1876610213000829.

[227] A. Michel, V. Sharma, M. Lehning, and H. Huwald, "Climate change scenarios at hourly time-step over switzerland from an enhanced temporal downscaling approach", *International Journal of Climatology*, vol. 41, no. 6, pp. 3503–3522, 2021. DOI: https://doi.org/10.1002/joc.7032. eprint: https://rmets.onlinelibrary.wiley.com/doi/pdf/10.1002/joc.7032. [Online]. Available: https://rmets.onlinelibrary.wiley.com/doi/abs/10.1002/joc.7032.

[228] A. Smith, N. Lott, and R. Vose, "The integrated surface database: recent developments and partnerships", *Bulletin of the American Meteorological Society*, vol. 92, no. 6, pp. 704–708, 2011. DOI: 10.1175/2011BAMS3015.1. [Online]. Available: https://journals.ametsoc.org/view/journals/bams/92/6/2011bams3015_1.xml.

[229] L. Ziegler, E. Gonzalez, T. Rubert, U. Smolka, and J. J. Melero, "Lifetime extension of onshore wind turbines: a review covering germany, spain, denmark, and the uk", *Renewable and Sustainable Energy Reviews*, vol. 82, pp. 1261–1271, 2018, ISSN: 1364-0321. DOI: https://doi.org/10.1016/j.rser.2017.09.100. [Online]. Available: https://www.sciencedirect.com/science/article/pii/S1364032117313503.

[230] COSMO. "Cosmo 1". (), [Online]. Available: http://www.cosmo-model.org/ (visited on 09/30/2022).

[231] S. Hanifi, X. Liu, Z. Lin, and S. Lotfian, "A critical review of wind power forecasting methods—past, present and future", *Energies*, vol. 13, no. 15, p. 3764, Jul. 22, 2020, ISSN: 1996-1073. DOI: 10.3390/en13153764. [Online]. Available: https://www.mdpi.com/1996-1073/13/15/3764 (visited on 08/12/2022).

[232] Y. Wang, R. Zou, F. Liu, L. Zhang, and Q. Liu, "A review of wind speed and wind power forecasting with deep neural networks", *Applied Energy*, vol. 304, p. 117 766, 2021, ISSN: 0306-2619. DOI: https://doi.org/10.1016/j.apenergy.2021.117766. [Online]. Available: https://www.sciencedirect.com/science/article/pii/S0306261921011053.

[233] M. Santhosh, C. Venkaiah, and D. M. Vinod Kumar, "Current advances and approaches in wind speed and wind power forecasting for improved renewable energy integration: a review", *Engineering Reports*, vol. 2, no. 6, e12178, 2020. DOI: https://doi.org/10.1002/eng2.12178. eprint: https://onlinelibrary.wiley.com/doi/pdf/10.1002/eng2.12178. [Online]. Available: https://onlinelibrary.wiley.com/doi/abs/10.1002/eng2.12178.

[234] H.-G. Kim, Y.-H. Kang, and J.-Y. Kim, "Evaluation of wind resource potential in mountainous region considering morphometric terrain characteristics", *Wind Engineering*, vol. 41, no. 2, pp. 114–123, 2017, ISSN: 0309524X, 2048402X. [Online]. Available: https://www.jstor.org/stable/90007202 (visited on 07/16/2022).

[235] B. Kruyt, J. Dujardin, and M. Lehning, "Improvement of wind power assessment in complex terrain: the case of COSMO-1 in the swiss alps", *Frontiers in Energy Research*, vol. 6, p. 102, Oct. 16, 2018, ISSN: 2296-598X. DOI: 10.3389/fenrg.2018.00102. [Online]. Available: https://www.frontiersin.org/article/10.3389/fenrg.2018.00102/full (visited on 08/10/2022).

[236] H. Schulz and S. Behnke, "Deep Learning", *KI - Künstliche Intelligenz*, vol. 26, no. 4, pp. 357–363, Nov. 2012, ISSN: 1610-1987. DOI: 10.1007/s13218-012-0198-z. [Online]. Available: https://doi.org/10.1007/s13218-012-0198-z.

[237] Y. LeCun, Y. Bengio, and G. Hinton, "Deep learning", *Nature*, vol. 521, no. 7553, pp. 436–444, May 2015, ISSN: 1476-4687. DOI: 10.1038/nature14539. [Online]. Available: https://doi.org/10.1038/nature14539.

[238] S. S. Mousavi, M. Schukat, and E. Howley, "Deep reinforcement learning: an overview", in *Proceedings of SAI Intelligent Systems Conference (IntelliSys) 2016*, Springer International Publishing, Aug. 2017, pp. 426–440. DOI: 10.1007/978-3-319-56991-8_32.

[239] I. H. Sarker, "Deep Learning: A Comprehensive Overview on Techniques, Taxonomy, Applications and Research Directions", en, *SN Computer Science*, vol. 2, no. 6, p. 420, Nov. 2021, ISSN: 2662-995X, 2661-8907. DOI: 10.1007/s42979-021-00815-1. (visited on 11/02/2022).

[240] S. Gao and D. Lima, "A review of the application of deep learning in the detection of Alzheimer's disease", *International Journal of Cognitive Computing in Engineering*, vol. 3, pp. 1–8, 2022, ISSN: 2666-3074. DOI: https://doi.org/10.1016/j.ijcce.2021.12.002.

[241] K. P. Wai, M. Y. Chia, C. H. Koo, Y. F. Huang, and W. C. Chong, "Applications of deep learning in water quality management: A state-of-the-art review", *Journal of Hydrology*, vol. 613, p. 128 332, 2022, ISSN: 0022-1694. DOI: https://doi.org/10.1016/j.jhydrol.2022.128332.

[242] K. B. Dang, V. B. Dang, V. L. Ngo, *et al.*, "Application of deep learning models to detect coastlines and shorelines", *Journal of Environmental Management*, vol. 320, p. 115 732, 2022, ISSN: 0301-4797. DOI: https://doi.org/10.1016/j.jenvman.2022.115732.

[243] B. Zhang, Y. Rong, R. Yong, D. Qin, M. Li, G. Zou, and J. Pan, "Deep learning for air pollutant concentration prediction: A review", *Atmospheric Environment*, vol. 290, p. 119 347, 2022, ISSN: 1352-2310. DOI: https://doi.org/10.1016/j.atmosenv.2022.119347.

[244] W. Khan, S. Walker, and W. Zeiler, "Improved solar photovoltaic energy generation forecast using deep learning-based ensemble stacking approach", *Energy*, vol. 240, p. 122 812, 2022, ISSN: 0360-5442. DOI: https://doi.org/10.1016/j.energy.2021.122812.

[245] L. Cheng, H. Zang, Z. Wei, F. Zhang, and G. Sun, "Evaluation of opaque deep-learning solar power forecast models towards power-grid applications", *Renewable Energy*, vol. 198, pp. 960–972, 2022, ISSN: 0960-1481. DOI: https://doi.org/10.1016/j.renene.2022.08.054.

[246] O. F. Eikeland, F. D. Hovem, T. E. Olsen, M. Chiesa, and F. M. Bianchi, "Probabilistic forecasts of wind power generation in regions with complex topography using deep learning methods: An Arctic case", *Energy Conversion and Management: X*, vol. 15, p. 100 239, 2022, ISSN: 2590-1745. DOI: https://doi.org/10.1016/j.ecmx.2022.100239.

[247] B. Knüsel, M. Zumwald, C. Baumberger, G. Hirsch Hadorn, E. M. Fischer, D. N. Bresch, and R. Knutti, "Applying big data beyond small problems in climate research", *Nature Climate Change*, vol. 9, no. 3, pp. 196–202, Mar. 2019, ISSN: 1758-6798. DOI: 10.1038/s41558-019-0404-1.

[248] P. Valsaraj, D. A. Thumba, and K. S. Kumar, "Spatio-temporal independent applicability of one time trained machine learning wind forecast models: a promising case study from the wind energy perspective", *International Journal of Sustainable Energy*, vol. 0, no. 0, pp. 1–19, 2022. DOI: 10.1080/14786451.2022.2032060.

[249] R. K. Samal, "Assessment of wind energy potential using reanalysis data: a comparison with mast measurements", *Journal of Cleaner Production*, vol. 313, p. 127 933, 2021, ISSN: 0959-6526. DOI: https://doi.org/10.1016/j.jclepro.2021.127933. [Online]. Available: https://www.sciencedirect.com/science/article/pii/S095965262102151X.

[250] R. Laudari, "Assessment of economic viability of wind energy in nepal: a case study of ten sites", Jun. 2016. DOI: 10.13140/RG.2.1.1982.1682.

[251] J. Teuwen and N. Moriakov, "Chapter 20 - convolutional neural networks", in *Handbook of Medical Image Computing and Computer Assisted Intervention*, ser. The Elsevier and MICCAI Society Book Series, S. K. Zhou, D. Rueckert, and G. Fichtinger, Eds., Academic Press, 2020, pp. 481–501, ISBN: 978-0-12-816176-0. DOI: https://doi.org/10.1016/B978-0-12-816176-0.00025-9. [Online]. Available: https://www.sciencedirect.com/science/article/pii/B9780128161760000259.

[252] L. Hoffmann and R. Spang, "An assessment of tropopause characteristics of the ERA5 and ERA-interim meteorological reanalyses", Dynamics/Atmospheric Modelling/Troposphere/Physics (physical properties and processes), preprint, Nov. 29, 2021. DOI: 10.5194/acp-2021-961. [Online]. Available: https://acp.copernicus.org/preprints/acp-2021-961/acp-2021-961.pdf (visited on 08/08/2022).

[253] L. Kornblueh, U. Schulzweida, D. Kleberg, T. Jahns, and I. Fast, "Cdo - data processing (and production)", p. 12,

[254] L. Minola, F. Zhang, C. Azorin-Molina, A. A. S. Pirooz, R. G. J. Flay, H. Hersbach, and D. Chen, "Near-surface mean and gust wind speeds in ERA5 across sweden: towards an improved gust parametrization", *Climate Dynamics*, vol. 55, no. 3, pp. 887–907, Aug. 1, 2020, ISSN: 1432-0894. DOI: 10.1007/s00382-020-05302-6. [Online]. Available: https://doi.org/10.1007/s00382-020-05302-6.

[255] "Ifs documentation cy47r3 - part iv physical processes", in *IFS Documentation CY47R3*, ser. IFS Documentation 4. ECMWF, Sep. 2021. DOI: 10.21957/eyrpir4vj. [Online]. Available: https://www.ecmwf.int/node/20198.

[256] T. Kanehama, I. Sandu, A. Beljaars, A. van Niekerk, N. Wedi, S. Boussetta, S. Lang, S. Johnson, and L. Magnusson, "Evaluation and optimizaton of orographic drag in the ifs", no. 893, Mar. 2022. DOI: 10.21957/fps6gngqe. [Online]. Available: https://www.ecmwf.int/node/20333.

[257] J.-P. Schulz, "Introducing sub-grid scale orographic effects in the COSMO model", no. 9, p. 8, 2008.

[258] M. J. Miller, "Subgrid-scale orographic drag", p. 9, 2004.

[259] F. Pithan, A. Ackerman, W. M. Angevine, *et al.*, "Select strengths and biases of models in representing the arctic winter boundary layer over sea ice: the larcform 1 single column model intercomparison", *Journal of Advances in Modeling Earth Systems*, vol. 8, no. 3, pp. 1345–1357, 2016. DOI: https://doi.org/10.1002/2016MS000630. eprint: https://agupubs.onlinelibrary.wiley.com/doi/pdf/10.1002/2016MS000630. [Online]. Available: https://agupubs.onlinelibrary.wiley.com/doi/abs/10.1002/2016MS000630.

[260] I. Sandu, A. van Niekerk, T. G. Shepherd, *et al.*, "Impacts of orography on large-scale atmospheric circulation", *npj Climate and Atmospheric Science*, vol. 2, no. 1, p. 10, Dec. 2019, ISSN: 2397-3722. DOI: 10.1038/s41612-019-0065-9. [Online]. Available: http://www.nature.com/articles/s41612-019-0065-9 (visited on 08/11/2022).

[261] P. Davini, A. Weisheimer, M. Balmaseda, S. J. Johnson, F. Molteni, C. D. Roberts, R. Senan, and T. N. Stockdale, "The representation of winter northern hemisphere atmospheric blocking in ecmwf seasonal prediction systems", *Quarterly Journal of the Royal Meteorological Society*, vol. 147, no. 735, pp. 1344–1363, 2021. DOI: https://doi.org/10.1002/qj.3974. eprint: https://rmets.onlinelibrary.wiley.com/doi/pdf/10.1002/qj.3974. [Online]. Available: https://rmets.onlinelibrary.wiley.com/doi/abs/10.1002/qj.3974.

[262] R. Köhler, D. Handorf, R. Jaiser, K. Dethloff, G. Zängl, D. Majewski, and M. Rex, "Improved circulation in the northern hemisphere by adjusting gravity wave drag parameterizations in seasonal experiments with icon-nwp", *Earth and Space Science*, vol. 8, no. 3, e2021EA001676, 2021, e2021EA001676 2021EA001676. DOI: https://doi.org/10.1029/2021EA001676. eprint: https://agupubs.onlinelibrary.wiley.com/doi/pdf/10.1029/2021EA001676. [Online]. Available: https://agupubs.onlinelibrary.wiley.com/doi/abs/10.1029/2021EA001676.

[263] M. Barque, S. Martin, J. E. N. Vianin, D. Genoud, and D. Wannier, "Improving wind power prediction with retraining machine learning algorithms", in *2018 International Workshop on Big Data and Information Security (IWBIS)*, Jakarta: IEEE, May 2018, pp. 43–48, ISBN: 978-1-5386-5525-2. DOI: 10.1109/IWBIS.2018.8471713. [Online]. Available: https://ieeexplore.ieee.org/document/8471713/ (visited on 08/09/2022).

YASMINE ZAKARI

E-mail : yasminezakari3007@gmail.com

LinkedIn: https://www.linkedin.com/in/yasmine-zakari/

GitHub: https://github.com/yasminezakari

EDUCATION

École Polytechnique Fédérale de Lausanne, Switzerland | PhD
Doctoral school of civil and environmental engineering, *February 2018 - September 2022*
- Thesis title: "Addressing the risk of climate change on wind and solar energy: The case of India"

University of California, Berkeley - Berkeley, California, United States | Master Thesis (6/6)
Energy and Resources, *January-September 2016*
- Thesis title: "Addressing the cost-risk of climate change on the Chinese power sector"

École Polytechnique Fédérale de Lausanne, Switzerland | Master of Science (5.2/6)
Environmental Sciences and Engineering, *September 2014 - October 2016*
- Minored in Management of Technology

École Polytechnique Fédérale de Lausanne, Switzerland | Bachelor of Science (4.6/6)
Environmental Sciences and Engineering, *September 2010 - July 2014*

WORK HISTORY

SUSTAINABILITY AND ENVIRONMENTAL ENGINEER | 01/2022 to Current

Schindler Management ltd. - Ebikon, Switzerland

- Project planning for the implementation of circular economy strategies
- Green product strategy definition and planning
- Lead on market survey initiatives and competitive benchmarking
- Lead on full material declaration for elevators related to the European Waste Framework directive
- Supervision of a research project in collaboration with Schindler's EPFL laboratory

DOCTORAL ASSISTANT | 02/2018 to 12/2021

CRYOS Laboratory and Energy Center (EPFL) - Lausanne, Switzerland

- Research project in collaboration with China Light & Power on climate change impacts and energy

SMART ENERGY CONSULTANT | 02/2017 to 02/2018

DNV GL - Dubai, United Arab Emirates

- Developed business cases and implementation plans for Al Ain Distribution Company (AADC) Demand Side Management (DSM) Program in collaboration with Abu Dhabi Water & Electricity Authority (ADWEC)
- Negotiated budget approval for quick-start programs with Abu Dhabi's Regulatory & Supervisory Bureau
- Lead on consumer-behavior initiatives, marketing & advertising awareness campaigns
- Management of stakeholders and project reporting

ENVIRONMENTAL ENGINEER | 12/2016 to 02/2017

CSD Engineer - Milano, Italy

- Environmental impact assessment
- Technical consulting on environmental regulations and compliance specifications

ENGINEERING INTERN | 07/2015 to 12/2015

PHILIA S.A - Geneva, Switzerland

- Formulated and guided the implementation of the Health, Safety and Environment Policy for Oil & Gas
- Coordination and supervision of environmental impact assessment studies in Congo

PUBLICATIONS

- Yasmine Zakari, Adrien Michel, Michael Lehning, Future trends in wind resources and their consistency in the Indian sub-continent, Sustainable Energy Technologies and Assessments, Volume 53, Part A, 2022,102460, ISSN 2213-1388, doi/10.1016/j.seta.2022.102460
- Yasmine Zakari, François Vuille, Michael Lehning, Climate Change Impact Assessment for Future Wind and Solar Energy Installations in India, Frontiers in Energy Research, Volume 10, 2022, doi/10.3389/fenrg.2022.859321